Fuzzy Logic Control of Hydraulic Robots with Flow-Deadband Nonlinearities

by

Todd Corbet

A thesis
presented to the University of Manitoba
in fulfilment of the
thesis requirement for the degree of
Master of Science
in
Mechanical Engineering

Winnipeg, Manitoba, Canada 1995

ISBN 0-315-99103-8

Name TODD CORBET

Dissertation Abstracts International is arranged by broad, general subject categories. Please select the one subject which most nearly describes the content of your dissertation. Enter the corresponding four-digit code in the spaces provided.

Mechanical Engineering
SUBJECT TERM

0548
SUBJECT CODE

U·M·I

Subject Categories

THE HUMANITIES AND SOCIAL SCIENCES

COMMUNICATIONS AND THE ARTS
Architecture 0729
Art History 0377
Cinema 0900
Dance 0378
Fine Arts 0357
Information Science 0723
Journalism 0391
Library Science 0399
Mass Communications 0708
Music 0413
Speech Communication 0459
Theater 0465

EDUCATION
General 0515
Administration 0514
Adult and Continuing 0516
Agricultural 0517
Art 0273
Bilingual and Multicultural 0282
Business 0688
Community College 0275
Curriculum and Instruction 0727
Early Childhood 0518
Elementary 0524
Finance 0277
Guidance and Counseling 0519
Health 0680
Higher 0745
History of 0520
Home Economics 0278
Industrial 0521
Language and Literature 0279
Mathematics 0280
Music 0522
Philosophy of 0998
Physical 0523
Psychology 0525
Reading 0535
Religious 0527
Sciences 0714
Secondary 0533
Social Sciences 0534
Sociology of 0340
Special 0529
Teacher Training 0530
Technology 0710
Tests and Measurements 0288
Vocational 0747

LANGUAGE, LITERATURE AND LINGUISTICS
Language
- General 0679
- Ancient 0289
- Linguistics 0290
- Modern 0291

Literature
- General 0401
- Classical 0294
- Comparative 0295
- Medieval 0297
- Modern 0298
- African 0316
- American 0591
- Asian 0305
- Canadian (English) 0352
- Canadian (French) 0355
- English 0593
- Germanic 0311
- Latin American 0312
- Middle Eastern 0315
- Romance 0313
- Slavic and East European 0314

PHILOSOPHY, RELIGION AND THEOLOGY
Philosophy 0422
Religion
- General 0318
- Biblical Studies 0321
- Clergy 0319
- History of 0320
- Philosophy of 0322

Theology 0469

SOCIAL SCIENCES
American Studies 0323
Anthropology
- Archaeology 0324
- Cultural 0326
- Physical 0327

Business Administration
- General 0310
- Accounting 0272
- Banking 0770
- Management 0454
- Marketing 0338

Canadian Studies 0385
Economics
- General 0501
- Agricultural 0503
- Commerce-Business 0505
- Finance 0508
- History 0509
- Labor 0510
- Theory 0511

Folklore 0358
Geography 0366
Gerontology 0351
History
- General 0578
- Ancient 0579
- Medieval 0581
- Modern 0582
- Black 0328
- African 0331
- Asia, Australia and Oceania 0332
- Canadian 0334
- European 0335
- Latin American 0336
- Middle Eastern 0333
- United States 0337

History of Science 0585
Law 0398
Political Science
- General 0615
- International Law and Relations 0616
- Public Administration 0617

Recreation 0814
Social Work 0452
Sociology
- General 0626
- Criminology and Penology 0627
- Demography 0938
- Ethnic and Racial Studies 0631
- Individual and Family Studies 0628
- Industrial and Labor Relations 0629
- Public and Social Welfare 0630
- Social Structure and Development 0700
- Theory and Methods 0344

Transportation 0709
Urban and Regional Planning 0999
Women's Studies 0453

THE SCIENCES AND ENGINEERING

BIOLOGICAL SCIENCES
Agriculture
- General 0473
- Agronomy 0285
- Animal Culture and Nutrition 0475
- Animal Pathology 0476
- Food Science and Technology 0359
- Forestry and Wildlife 0478
- Plant Culture 0479
- Plant Pathology 0480
- Plant Physiology 0817
- Range Management 0777
- Wood Technology 0746

Biology
- General 0306
- Anatomy 0287
- Biostatistics 0308
- Botany 0309
- Cell 0379
- Ecology 0329
- Entomology 0353
- Genetics 0369
- Limnology 0793
- Microbiology 0410
- Molecular 0307
- Neuroscience 0317
- Oceanography 0416
- Physiology 0433
- Radiation 0821
- Veterinary Science 0778
- Zoology 0472

Biophysics
- General 0786
- Medical 0760

EARTH SCIENCES
Biogeochemistry 0425
Geochemistry 0996
Geodesy 0370
Geology 0372
Geophysics 0373
Hydrology 0388
Mineralogy 0411
Paleobotany 0345
Paleoecology 0426
Paleontology 0418
Paleozoology 0985
Palynology 0427
Physical Geography 0368
Physical Oceanography 0415

HEALTH AND ENVIRONMENTAL SCIENCES
Environmental Sciences 0768
Health Sciences
- General 0566
- Audiology 0300
- Chemotherapy 0992
- Dentistry 0567
- Education 0350
- Hospital Management 0769
- Human Development 0758
- Immunology 0982
- Medicine and Surgery 0564
- Mental Health 0347
- Nursing 0569
- Nutrition 0570
- Obstetrics and Gynecology 0380
- Occupational Health and Therapy 0354
- Ophthalmology 0381
- Pathology 0571
- Pharmacology 0419
- Pharmacy 0572
- Physical Therapy 0382
- Public Health 0573
- Radiology 0574
- Recreation 0575
- Speech Pathology 0460
- Toxicology 0383

Home Economics 0386

PHYSICAL SCIENCES
Pure Sciences
Chemistry
- General 0485
- Agricultural 0749
- Analytical 0486
- Biochemistry 0487
- Inorganic 0488
- Nuclear 0738
- Organic 0490
- Pharmaceutical 0491
- Physical 0494
- Polymer 0495
- Radiation 0754

Mathematics 0405
Physics
- General 0605
- Acoustics 0986
- Astronomy and Astrophysics 0606
- Atmospheric Science 0608
- Atomic 0748
- Electronics and Electricity 0607
- Elementary Particles and High Energy 0798
- Fluid and Plasma 0759
- Molecular 0609
- Nuclear 0610
- Optics 0752
- Radiation 0756
- Solid State 0611

Statistics 0463

Applied Sciences
Applied Mechanics 0346
Computer Science 0984
Engineering
- General 0537
- Aerospace 0538
- Agricultural 0539
- Automotive 0540
- Biomedical 0541
- Chemical 0542
- Civil 0543
- Electronics and Electrical 0544
- Heat and Thermodynamics 0348
- Hydraulic 0545
- Industrial 0546
- Marine 0547
- Materials Science 0794
- Mechanical 0548
- Metallurgy 0743
- Mining 0551
- Nuclear 0552
- Packaging 0549
- Petroleum 0765
- Sanitary and Municipal 0554
- System Science 0790

Geotechnology 0428
Operations Research 0796
Plastics Technology 0795
Textile Technology 0994

PSYCHOLOGY
General 0621
Behavioral 0384
Clinical 0622
Developmental 0620
Experimental 0623
Industrial 0624
Personality 0625
Physiological 0989
Psychobiology 0349
Psychometrics 0632
Social 0451

FUZZY LOGIC CONTROL OF HYDRAULIC ROBOTS WITH FLOW-DEADBAND NONLINEARITIES

BY

TODD CORBET

A Thesis submitted to the Faculty of Graduate Studies of the University of Manitoba in partial fulfillment of the requirements of the degree of

MASTER OF SCIENCE

Abstract

Application of a fuzzy logic controller to a class of hydraulically actuated industrial robots is investigated in this thesis. A simple, yet effective, set of membership functions and rules are developed to meet the control requirements of such robots. The proposed PD-type fuzzy controller is first examined through simulation of a two-link hydraulic robot. The robot has the same hydraulic configuration as many existing industrial manipulators. It is shown that the controller exhibits positive aspects which cannot be easily achieved by conventional control techniques, such as a PD controller. These aspects include a short rise-time and a well maintained dampened response.

The fuzzy controller is then utilized on an instrumented Unimate MK-II robot which has been retrofitted as a research robot. An off-line routine based on the simplex method is applied to find the best performing control gains for different links. This is accomplished by minimizing the summation of errors over step input responses. The controller, although effective, is shown to produce steady-state errors. The steady-state error in a step input response is mainly due to the hydraulic valve deadband in which the control action is not effective. The steady-state position error in a ramp input response is shown to be due to both valve deadband and the nature of the PD-type fuzzy controller.

In order to eliminate the steady-state errors, conceptually simple methods are developed and applied in parallel with the PD-type fuzzy controller. In particular, two methods are proposed. In the first method, a control term proportional to the integral of error is calculated and added to the output from the main controller. In the second method, the control measure of the steady-state error obtained from the PD-type fuzzy controller is used as an offset. Both actions are activated only in a region of fuzzy zero velocity error.

Acknowledgments

I would like to thank Dr. N. Sepehri for his support during the course of this study. I would also like to thank A. Al-Zaher for providing me with the hydraulic robot simulator that he has developed during the course of his M.Sc studies. The software allowed me to study the performance of my algorithms before actually implementing them. Finally I would like to acknowledge the support of the Natural Science and Engineering Research Council of Canada, the Institute for Robotics and Intelligent Systems (IRIS) and Precarn Associates Inc.

Contents

List of Figures

Chapter 1

Introduction

1.1 Background

Fuzzy logic has become one of the most successful fields of research in developing control systems. A fuzzy logic controller is a nonlinear controller [2]. It can provide robust control and accuracy [2–3], and is ideally suited for systems with unknown or complex models [4–7]. Fuzzy controllers have been identified as promising alternatives to conventional controllers and have been proven to achieve better performance (i.e., shorter rise-time and smaller overshoot) when compared to linear PD controllers [8–9].

Fuzzy logic control is based on fuzzy logic which is close in spirit to human thinking and natural language [5]. It is best suited to a process which is analog in nature, must be controlled on a digital control system, and to which the modeling of the process is difficult [1]. One example would be temperature which could have ranges of cold, medium, warm and hot, where the separation between states is not well defined.

A fuzzy logic controller applies a series of rules to system variables which are first converted to linguistic notions. It then outputs a control action based on a weighted result of rule evaluations. Rules are normally written based on experience,

observation and the attributes to which system response must contain. Conventional PID controllers, on the other hand, are based on exact mathematical models. The sensors read precise values and specific outputs are produced. A PID controller, with fixed gains, is difficult to tune for both stability and responsiveness. To some extent this is not the case with a fuzzy logic controller [8]. Fuzzy logic controllers can cover a wide range of operating conditions and possess robust control characteristics [9].

In the last few years, research devoted to fuzzy logic and it's application has significantly increased as attested to by the existence of several conferences and publications on the topic. One example is the annual IEEE International Conference on Fuzzy Systems. Many articles on the successful application of fuzzy logic control to electrically-actuated robots have been presented, ranging from the application of a fuzzy logic control matrix (similar to a lookup table) to the implementation of actual fuzzy rules and membership functions. To name a few, Kumbla et al. [2] incorporated all the aspects of a fuzzy logic controller including fuzzification, rule evaluation and defuzzification and applied it to an industrial Rhino robot. The fuzzy logic controller, being an adaptive technique, performed better than the linear PD controller. Ken et al. [10] used a fuzzy lookup table in parallel with a position feedback controller and showed that both dynamic performance and static behavior were improved as compared to a conventional PID controller with fixed gains. Fuzzy logic was also implemented by Tzafestas et al. [11] in order to enhance the performance of a conventional PID controller; the gains of the PID controller were incrementally changed using a fuzzy lookup table. Wakileh and Gill [14] proposed a self-organizing fuzzy logic and implemented it on the Stanford manipulator. General issues in tuning and validation of fuzzy systems were outlined by Boscolo [12] and the need for a systematic methodology for developing and tuning fuzzy rules and gains was addressed by Daugherity [9] and, Smith and Comer [13].

The application of fuzzy logic control to hydraulically actuated robots, however,

is sparse and can only be found in a few research papers. Zhao and Virvalo [15] combined a linear state controller with fuzzy rule evaluation to produce what they named a fuzzy state controller. The method indirectly detects the presence of a load, based on fuzzy rule evaluation of actuator's velocity, and decides on the gains of a state controller accordingly in order to make the controller insensitive to load variations. Chou and Lu [16] developed a fuzzy logic controller for a class of hydraulic servo systems. The robustness and tracking ability of the controller was demonstrated through extensive simulations and some experimental studies.

Hydraulically actuated robots are, in general, different from electrically actuated robots. The difference is not only in the way the actuating force is created but also in the way it is transmitted to the links. In a hydraulic robot, the application of force is based on a pressure differential which, in the process of equalization, applies a force to the link some distance from the joint. The pressure differential is achieved by means of a spool displacement in a valve that controls the fluid flow into and out of the actuator. Compared with electric drives, hydraulic ones are much stiffer when handling large payloads. Hydraulic actuators have found there largest use on manipulators handling large payloads, requiring positioning accuracy, rapid dynamics and quick starts and stops [17]. In spite of the above advantages, hydraulic systems are complex, nonlinear and difficult to analyze for control purposes [25,26].

When applying a fuzzy logic controller, one should not expect to implement similar control strategies to both electric and hydraulic robots. Each class has different control requirements and characteristics which must be accounted for when designing the rules. For example, in hydraulic robots, given a zero spool displacement (i.e., valve closed) the arm can be kept in place due to the oil trapped on both sides of the cylinder. Also, the hydraulic robot can come to rest quickly when the valve spool returns to its neutral position. In electric robots, the link may pass the target point with a zero motor voltage. The amount of the overshoot depends on the inertia and

the velocity. Negative motor voltage is usually applied before the arm reaches the desired position to prevent excessive overshoot. Also, a constant control input (motor voltage) is required in order to keep the arm in place in the presence of gravity. This is normally achieved either in the presence of a steady-state error or with the addition of a control value equivalent to an integral action.

1.2 Thesis Scope

This thesis investigates the implementation of a fuzzy logic controller on a class of hydraulically actuated manipulators. A PD-type fuzzy logic controller is initially developed. The controller has few rules, uses simple membership functions, is computationally efficient and is easy to implement. Furthermore, the fuzzy controller incorporates an off-line tuning algorithm based on a simplex optimization method in order to find appropriate gains for each axis.

Simulation studies are first performed leading to the construction of suitable fuzzy membership functions and control plans. The experiments are performed on an instrumented Unimate MK-II hydraulic robot. Experimental studies however result in steady-state errors in both step and ramp input responses. The deadband in the hydraulic valve is identified as the primary source of steady-state error in the step input response. Other nonideal characteristics of the system components such as dry friction in the servo valves, also contribute to the steady-state error. The steady-state position error observed in the ramp input is shown to be primarily due to the nature of the PD-type fuzzy logic controller. The inclusion of a scheme which can measure the steady-state error and translate it to an added control action is then discussed.

Eliminating the steady-state error is normally done by adding an integral control action. Zheng [8] utilized a summation of control actions from a PD-type fuzzy logic controller to produce a fuzzy PI controller. PI controllers, however, are known to give

poor performance in transient response due to the internal integrating operation. In order to improve the performance of PI-type controllers, Lee [18] proposed two methods which take out appropriate amounts of the accumulated control inputs according to a set of rules based on fuzzily described states on errors, error rates and control inputs. Chen and Yen [19] suggested the use of PID-type fuzzy logic controllers to avoid some of the shortcomings when only PD or PI controllers are used. Mizumoto [20] constructed a PID controller based on the product-sum-gravity method and a simplified fuzzy reasoning method. To improve the transient and steady-state performance of control systems containing deadzones, Kim et al. [21] used a precompensator which magnified, according to a fuzzy rule table, the position error input to a linear PD controller. Only simulation results for step inputs of a control system with a second order plant were shown. None of the above techniques were implemented in experiments. In particular, no report was found regarding application to hydraulic manipulators with valve deadbands or systems dealing with ramp input responses.

Towards eliminating the steady-state error, we first examine a method which is basically a fuzzy PID-type control; the actions from the PD-type fuzzy controller are summed to produce a PI-type fuzzy control action, which is then added to the output from the PD-type fuzzy controller. Based on the examination of this technique, two methods are developed. In the first method, a control term proportional to the integral of error is calculated in parallel, and is added to the fuzzy PD controller. In the second method, the control measure of the steady-state error obtained from the fuzzy PD control part is used as an offset to be added to the current control action. Further study is then performed on the reset offset integral method due to its speed of calculation, stability and ease of application. The results shown in this thesis indicate that a fuzzy controller displays valuable control characteristics and the steady-state error elimination methods developed are novel and valuable in application.

1.3 Thesis Organization

The remaining chapters of this thesis are organized as follows. Chapter 2 describes the hydraulic actuation system model used in simulations, followed by an overview of fuzzy logic control. Chapter 3 describes the development of the PD-type fuzzy controller for a hydraulically actuated manipulator. Simulation results are presented in this chapter to substantiate the approach. Chapter 4 examines the experimental application of the PD-type fuzzy controller. Chapter 5 details the development of the steady-state error elimination methods, and Chapter 6 describes further experimental evaluation of the reset offset integral method. The thesis is concluded with Chapter 7 which outlines the contributions of this work and future work.

Chapter 2

Background

2.1 Hydraulic Actuation Systems

Figure 2.1 shows a typical hydraulic drive unit. The linear piston actuator is connected to a closed-center spool valve through hoses. The valve meters the flow to and from the actuator. The pressure compensated pump provides a flow at sufficiently constant pressure to provide the motion. The use of a closed-center valve along with a constant supply pressure system, in a multi-link manipulator, allows each valve to function independently. Most indoor hydraulic robots use the above configuration. Valves, connecting hoses, motors and pumps are the main components. Other components such as check valves and relief valves are for the machine safety.

The inputs required to model a valve are the spool displacement (x), the supply pressure (P_s), the return pressure (P_r) and the line pressures (P_i and P_o). The governing nonlinear equations are written using the continuous equations for orifices [24]:

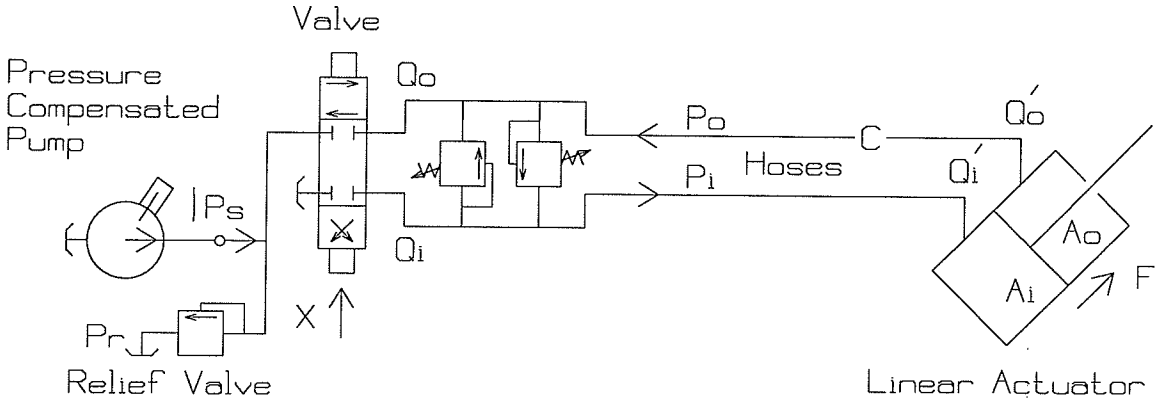

Figure 2.1: Schematic of a hydraulic drive unit

$$
\begin{aligned}
x > 0 \quad & (positive \ \ direction) \\
& Q_i = kwx\sqrt{P_s - P_i} \\
& Q_o = kwx\sqrt{P_o - P_r} \qquad (2.1) \\
x < 0 \quad & (negative \ \ direction) \\
& Q_i = kwx\sqrt{P_i - P_r} \\
& Q_o = kwx\sqrt{P_s - P_o} \qquad (2.2)
\end{aligned}
$$

where k is the orifice coefficient and w is the area gradient. Q_i and Q_o are the flow into and out of the valve, respectively.

The nonlinear equations of fluid flow for the valves can be linearized using a Taylor series expansion about an operating point and neglecting the higher order terms [24],

$$
\begin{aligned}
Q_i &= \mathcal{K}_x x - \mathcal{K}_p P_i \\
Q_o &= \mathcal{K}_x x + \mathcal{K}_p P_o \qquad (2.3)
\end{aligned}
$$

where

$$\begin{aligned} \mathcal{K}_x &= kw\sqrt{\frac{P_s - P_l}{2}} = \textit{flow gain} \\ \mathcal{K}_p &= \frac{kwx}{2\sqrt{2(P_s - P_l)}} = \textit{flow pressure gain} \\ P_l &= P_i - P_o = \textit{load pressure} \end{aligned}$$

$\mathcal{K}_p$ contributes to the damping ratio. Therefore for critical center valves it makes sense to carry out the analysis around the center point where damping is minimum.

The inputs required to model the actuator are the line pressures (P_i and P_o) and the cylinder linear acceleration ($\ddot{X}$):

$$F = (P_i A_i - P_o A_o) = J\ddot{X} + f_d\dot{X} \tag{2.4}$$

Where f_d is the equivalent damping coefficient and J is the inertia driven by the actuator. A_i and A_o are the piston areas.

Valves and the actuators are connected through pipes or flexible hoses. Using lumped parameter theory, the first order pipe model is (refer to Figure 2.1):

$$\begin{aligned} \dot{P}_i\frac{V_i}{\beta} &= Q_i - \acute{Q}_i \\ \dot{P}_o\frac{V_o}{\beta} &= \acute{Q}_o - Q_o \\ \acute{Q}_i &= A_i\dot{X} \\ \acute{Q}_o &= A_o\dot{X} \end{aligned} \tag{2.5}$$

$\acute{Q}_i$ and $\acute{Q}_o$ are the flow into and out of the cylinder, respectively. V_i and V_o are the volume of fluid trapped at the sides of the actuator, respectively. β is the effective bulk modulus of the combined hydraulic fluid and connecting hoses.

Linear analysis can be performed in frequency domain using a Laplace transformation to obtain the input-output relationship in an explicit form:

$$\frac{X(s)}{x(s)} = \frac{\mathcal{K}_x(A_i + A_o)}{(JC)s^3 + (J\mathcal{K}_p + f_d C)s^2 + (f_d\mathcal{K}_p + A_i^2 + A_o^2)s} \tag{2.6}$$

where $C = \frac{V_i}{\beta} \approx \frac{V_o}{\beta}$ is called the hydraulic compliance [24]. The above equation is a third order system and has the following form:

$$\frac{X(s)}{x(s)} = \frac{\kappa}{s\left[\frac{s^2}{\omega_n^2} + (\frac{2\zeta}{\omega_n})s + 1\right]} \tag{2.7}$$

where,

$$\begin{aligned} \kappa &= \frac{\mathcal{K}_x(A_i + A_o)}{\mathcal{K}_p f_d + (A_i^2 + A_o^2)} \\ \omega_n &= \sqrt{\frac{\mathcal{K}_p f_d + (A_i^2 + A_o^2)}{JC}} \\ \zeta &= \frac{\mathcal{K}_p J + f_d C}{2\sqrt{JC(\mathcal{K}_p f_d + (A_i^2 + A_o^2))}} \end{aligned}$$

The inclusion of $\frac{1}{s}$ in Eq. (2.7), basically means that the actuator is pushed by fluid flow. The oscillatory roots are lying in the second order part and they are functions of ζ (damping) and ω_n (hydraulic natural frequency). The increase in compliance also decreases damping which together with low natural frequency may cause an undesirable response. The effect of damping in stability is quite important. The sources of damping excluding J, C, A_i and A_o are; load damping which appears in the form of $\mathcal{K}_p$ in the equations, linkage (structural) damping included in f_d, dry friction and leakage. Leakage effect can be included in the linearized model by changing $\mathcal{K}_p$ to $(\mathcal{K}_p + \mathcal{K}_l)$, where $\mathcal{K}_l$ is the leakage coefficient.

In the above analysis, the dynamics of the valve has been ignored. For most indoor industrial manipulators the response of the servovalve is quite fast. So, the response

of the whole system is dominated by the dynamics of the linkages and the hoses which deliver fluid to the actuators. Therefore, a third order system can describe these manipulators quite well [26].

2.2 Fuzzy Logic Controllers

2.2.1 General Overview

To model a system using fuzzy logic, the response of the system in terms of the input-process-output must be known and the designer should be aware of how the inputs and outputs are related. Each input or output variable has its own control surface which consists of fuzzy regions. These regions overlap each other to give a smooth control response. This is seen in Figure 2.2. The area in which membership functions are dense is where accurate control is crucial. The input and output regions are related by a set of rules. A typical rule table is shown in Figure 2.2. This rule table, which is referred to in this thesis as a conventional rule table, is similar to the rule table in [8] except for the number of rules, and the maximum control value which is applied at large error for all values of velocity error. Once the fuzzy controller is activated, rule evaluation is done and all the rules which are true are fired. The true output membership functions are then summed and a centroid is found. This is called defuzzification which results in a crisp control action. The fuzzy reasoning method used in this thesis is based on Mamdani's 'Minimum Operation Rule (MOR)' and the 'Center of Area (COA)' defuzzification technique (see [6] for details).

As a demonstration, consider the case depicted in Figure 2.3. The position error of 0.75 (after being scaled) falls into two regions of its fuzzy set – zero (ZR) and positive small (PS). The degree of truth in each statement is determined by membership functions. For example the degree of truth in the statement of *'position error being a*

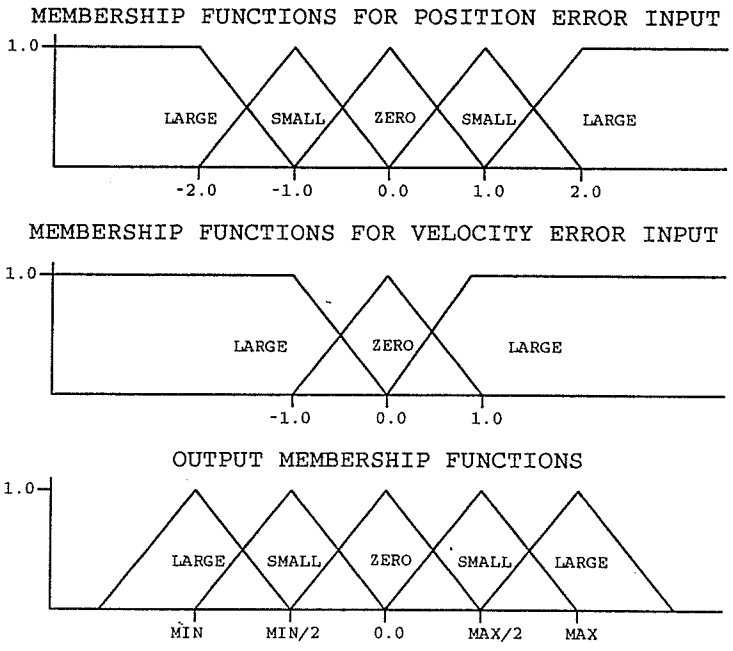

Velocity Error \ Position Error	NL	NS	ZR	PS	PL
NL	NL	NL	NS	ZR	PL
ZR	NL	NS	ZR	PS	PL
PL	NL	ZR	PS	PL	PL

PL positive large.
PS positive small.
ZR zero.
NS negative small.
NL negative large.

Figure 2.2: Typical membership functions and rule table

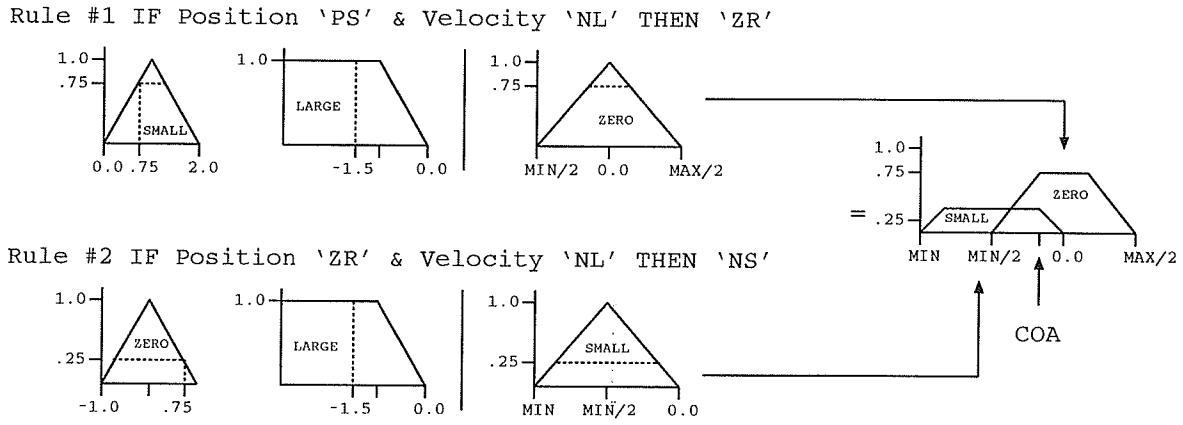

Figure 2.3: Example of fuzzy reasoning and rule defuzzification

small error' is %75 which is graphically displayed in Figure 2.3. The velocity error of -1.5, on the other hand, falls within one single region, i.e., negative large (NL). This combination causes two rules to fire. Referring to the table shown in Figure 2.2, the first rule implies sending a zero (ZR) control signal, for a small positive position error and a large negative velocity error. The second rule demands a negative small (NS) control output, for a zero position error and a large negative velocity error. These two rules have, somehow, to be combined to form a single output. A logical AND is first applied to each rule which is equivalent to taking the lowest of the two membership functions ('MOR'). The output control areas for both rules are then combined, and the center of the resultant control area ('COA') provides a crisp control action.

2.2.2 Fuzzy Logic Parameters and Controller Gains

A conventional PD controller has only two gains to set. A fuzzy controller has similar proportional and derivative gains (can also be called scaling factors) as well as parameters governing membership functions and rules. A fuzzy controller can be designed to produce a specific output for a prescribed input by means of these additional parameters. Figure 2.2 depicts a typical fuzzy controller with inputs of position and

velocity errors. The universe of discourse for these inputs can be scaled with gains much like a conventional PD controller. The input gains are P_e for position error and V_e for velocity error.

Referring to Figure 2.2 and the rule table, positive large position and velocity errors result in the application of a positive large (PL) control output. From this corner of the rule table, the controller then makes its way to the center of the table, where both position and velocity errors are zero. The route that it takes in getting there is a measure of the stability and responsiveness of the fuzzy controller [18]. A direct movement to the center would indicate a well designed controller. If firing of the rules has a rotation around the center, then the controller is oscillatory and must be tuned. These oscillations could be reduced by tuning the peak values, width or rules of the fuzzy controller without altering P_e and V_e gains [8].

This section describes how changes in the controller gains affect the response. It also discusses the effect of other fuzzy logic parameters such as width and peak values of the membership functions. The definitions in the following sections have been adapted from reference [8].

P_e and V_e Controller Gains

The position error (P_e) and the velocity error (V_e) gains are the values to which the input errors are multiplied before they are tested to see which membership functions they are contained within. Changing these gains puts the inputs within different membership functions and subsequently alters the control action. For example, a certain position error input may fall within a membership function range. After an increase in the gain, this same error will fall outside that membership function. Referring to Figure 2.2, any value outside the range of 2.0 to -2.0 position error is assigned a maximum control action, as defined by the rule table. The higher the P_e

gain, the smaller this range is when the position error is applied. Therefore, changing P_e and V_e gains alters the control calculation for the entire universe of discourse of each input.

Peak Values

The peak value fuzzy logic parameter is the point at which the membership function has a level of truth equal to one. The value is therefore the distance from the origin to the peak, as shown in Figure 2.4(a). All peak values are relative to the origin.

When altering the peak value of a membership function, the effect on the control calculation is different depending upon whether it is an input or an output membership function. For example, when the peak value of the PL (positive large) velocity error input membership function is changed, this affects all the rules which contain the PL velocity error (i.e., all 5 rules on the top row of the table in Figure 2.2). On the other hand, if PS output membership function is altered then all the rules with a PS output would be affected (2 rules). An increase in the small voltage output membership function can be seen in Figure 2.4(b).

Peak value changes for input membership functions will not be examined here due to the nonlinear characteristics which are present. Input membership functions must overlap by 1/2. When the functions do not have correct overlapping, the control becomes more of a 2-level logic controller [8]. This is seen in Figure 2.5. The same characteristic is also present if the width of a membership function is reduced.

In a PD controller, tuning for stability is usually done to the detriment of the system responsiveness. Because of the nonlinear characteristics of a fuzzy controller, tuning is possible for both responsiveness and stability. Different areas of the fuzzy control table can be tuned in different ways without affecting the control output of another area. If the output membership function peak value of NS and PS are altered

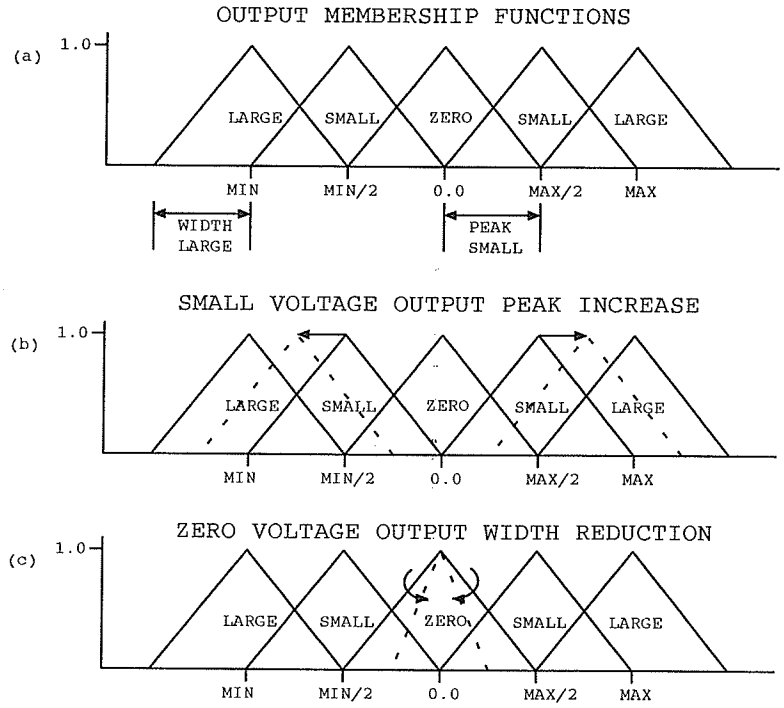

Figure 2.4: Width and peak tuning [8]

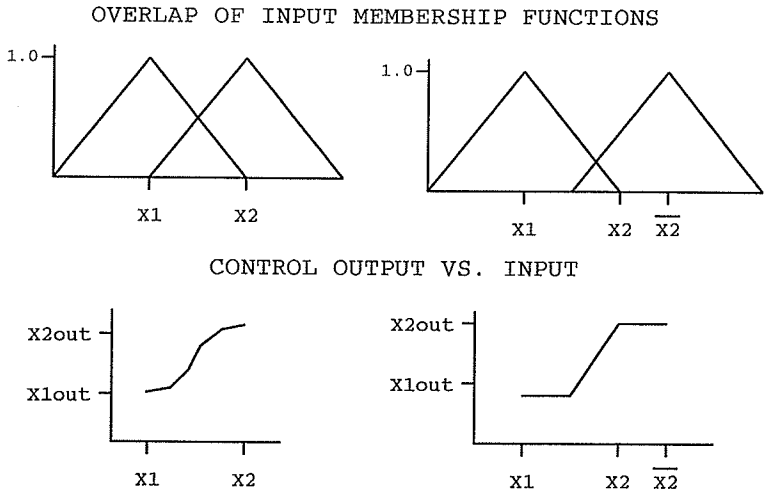

Figure 2.5: Membership function overlap [8]

in the control table in Figure 2.2 (i.e., the area surrounding the center of the control table), this would affect slightly the control calculation at the center of the control table, and affect greatly the control calculation around it. Therefore, while creating a fast response, one can still tune for no oscillations at the set point. A peak value change, which affects only specific areas of the rule table, can be referred to as a local scaling factor [8].

Width Values

Referring to Figure 2.4(a), the width fuzzy logic parameter is the length between the peak of the membership function and the point at which it has a zero value. When altering the width value of a membership function, its affect on the control calculation is different depending upon whether it is an input or an output membership function. Responsiveness and stability can be controlled more readily with output functions, and smooth control (as mentioned in the previous section) is affected by input functions. If the width of the output membership function is large, it then has a dominant effect over the other membership functions in terms of a larger area in the 'Center of Area' calculation. This becomes evident when two rules are fired with a different degree of truth. The weight of an output membership function with a large width, but low level of truth, may have the same weight as a small width output function with a much higher level of truth. Referring to Figure 2.4(c), a width reduction of the zero control output decreases its weight, or dominance, relative to the adjacent output membership functions.

Rules

Fuzzy rules relate the input membership functions to the output membership functions. Tuning the rules is a powerful way of obtaining certain responses for a particular

set of inputs. Altering, the fuzzy logic parameters of a membership function can affect multiple rules containing the altered membership function. On the other hand, a single rule change may not even be noticeable if it is a rule which is not crucial to stability or responsiveness. If there are very few rules to tune, as there is in the 15-rule controller shown in Figure 2.2, there may not be many tuning options. It is believed that a rule table with 50 rules would better demonstrate the power of rule tuning.

Tuning of fuzzy logic parameters, such as peak, width and rules, changes the response for a certain range of inputs. By altering these parameters, any number of responses can be achieved. This is done while maintaining a consistent set of P_e and V_e gains, or range of non-maximum control actions. This illustrates the benefits of a fuzzy controller as a nonlinear controller as opposed to a conventional PD controller [2].

In this thesis the input gains will be referred to as controller gains, and values which describe a membership function, such as width and peak values but not rules will be referred to as fuzzy logic parameters.

Chapter 3

Controller Design and Simulations

3.1 PD-type Fuzzy Controller

The basic fuzzy controller used in this thesis is a simple two-input controller. The inputs are the angular position error (*Desired Angle* − *Actual Angle*), and the angular velocity error (*Desired Velocity* − *Actual Velocity*). The universe of discourse of position and velocity error are fuzzily partitioned into 5 and 3 sets, respectively, as shown in Figure 3.1. These regions cover the entire range of possible inputs. Figure 3.1 also shows the 5 output regions, MIN. being the centroid of the negative large control action and MAX. the centroid of the positive large control action. For any set of values for position and velocity errors, an output is produced. The rules relating the inputs to the output are listed in the table shown in Figure 3.1. All inputs correspond to a membership region which in turn fires a rule or multiple rules. These membership functions and rules have been designed and adjusted based on simulations, testing and a knowledge of hydraulic actuator characteristics.

LARGE POSITION ERROR

Referring to the table shown in Figure 3.1, large position error, positive or neg-

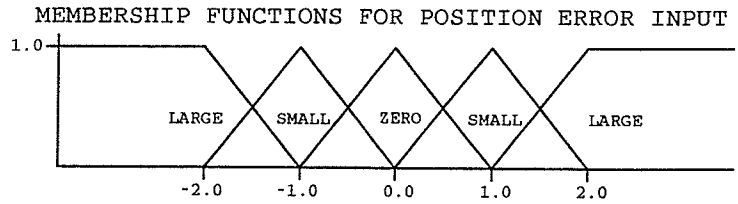

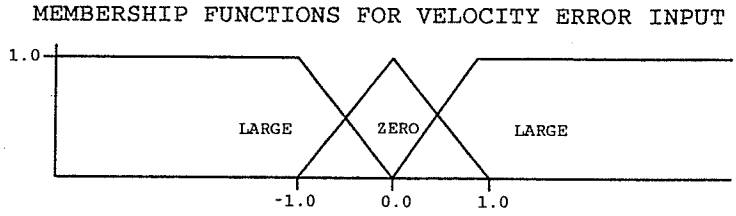

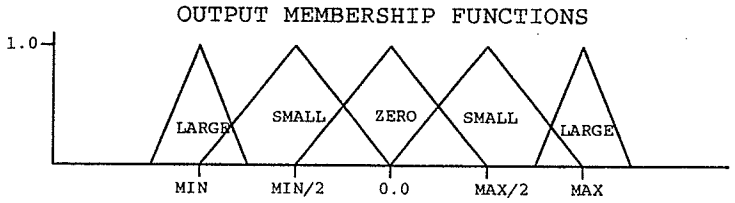

		Position Error				
		NL	NS	ZR	PS	PL
Velocity Error	NL	NL	NL	NS	PS	PL
	ZR	NL	NS	ZR	PS	PL
	PL	NL	NS	PS	PL	PL

PL positive large.
PS positive small.
ZR zero.
NS negative small.
NL negative large.

Figure 3.1: Membership functions and rule table for hydraulic actuators

		Position Error				
		NL	NS	ZR	PS	PL
Velocity Error	NL	NL	NL	NS	ZR	PL
	ZR	NL	NS	ZR	PS	PL
	PL	NL	ZR	PS	PL	PL

PL positive large.
PS positive small.
ZR zero.
NS negative small.
NL negative large.

Figure 3.2: Conventional rule table

ative, results in a maximum control output. This is required in order to have a response with a short rise time. The velocity error is not considered to be effective in this region.

SMALL POSITION ERROR

The rules associated with small position errors indicate a positive (negative) spool displacement for a positive (negative) position error no matter what the velocity error is. Note that for a zero velocity error or a velocity error that decreases the position error, a zero spool displacement stops the link; preventing it from reaching the required position. This leaves us with only a small control output. A large control action is only applied when the velocity error does not appear to reduce the position error, e.g., a case where a change in direction of travel is desired.

ZERO POSITION ERROR

This includes only one column of the table in Figure 3.1. Simulation studies showed that the rules belonging to this column contribute to the damping of the system. When the position error is zero, while there is a velocity error unequal to zero, a control action is applied with the same sign as the velocity error. The magnitude of this control is however small to prevent sustained oscillations at the set point.

A conventional control table with a diagonal orientation of rules, used in many applications including reference [8], is seen in Figure 3.2. This is not a truly diagonal table due to the small number of rules available and the need for a maximum control output when the position error is large. This is required to maintain a fast response no matter what the velocity is. The difference between the rules shown in Figure 3.1 and the conventional rule table can be found in only two rules. In Figure 3.2, when the position error is positive (negative) small, and the velocity error is negative (positive) large, then the control output is zero. The reason for this difference is that the

conventional rule table compensates for inertial effect at high velocities. This inertia, if not compensated for, will result in an overshoot of the desired position.

A 3-D surface of the control actions when using the hydraulic rule table in Figure 3.1 is seen in Figure 3.3(a). The control values are plotted for the input ranging from -2 to 2 for the position error and -1 to 1 for the velocity error. The solid lines are constant position and velocity error inputs and the dashed lines show the control height. The 3-D surface using the conventional rule table is shown in Figure 3.3(b). The difference between these two graphs is seen in the areas where the hydraulic and conventional rule tables are different, see Figure 3.1 and 3.2. On these 3-D surfaces a common input is present at point α. This point represents a small negative position error and a velocity error in the direction of the desired position. In the conventional rule table the value of control output is zero. In the hydraulic rule table the control output has a negative value which will continue to decrease the position error.

3.2 Tuning Controller Gains

The position and velocity errors are calculated as follows:

$$Position\ Error = (Desired\ Angle - Actual\ Angle) * P_e$$

$$Velocity\ Error = (Desired\ Velocity - Actual\ Velocity) * V_e$$

Where P_e and V_e are the position and velocity gains that put the resulting error values within the controller universe of discourse. The setting of these gains on the fuzzy controller can be a tedious and time consuming procedure. Each link may require a different setting because of different dynamic parameters. It would therefore be advantageous to tune these gains automatically, using an optimizing algorithm. The integral of position error, $e = Desired\ Angle - Actual\ Angle$, in a step input response is used here as a function to be minimized. Step response is easy to apply

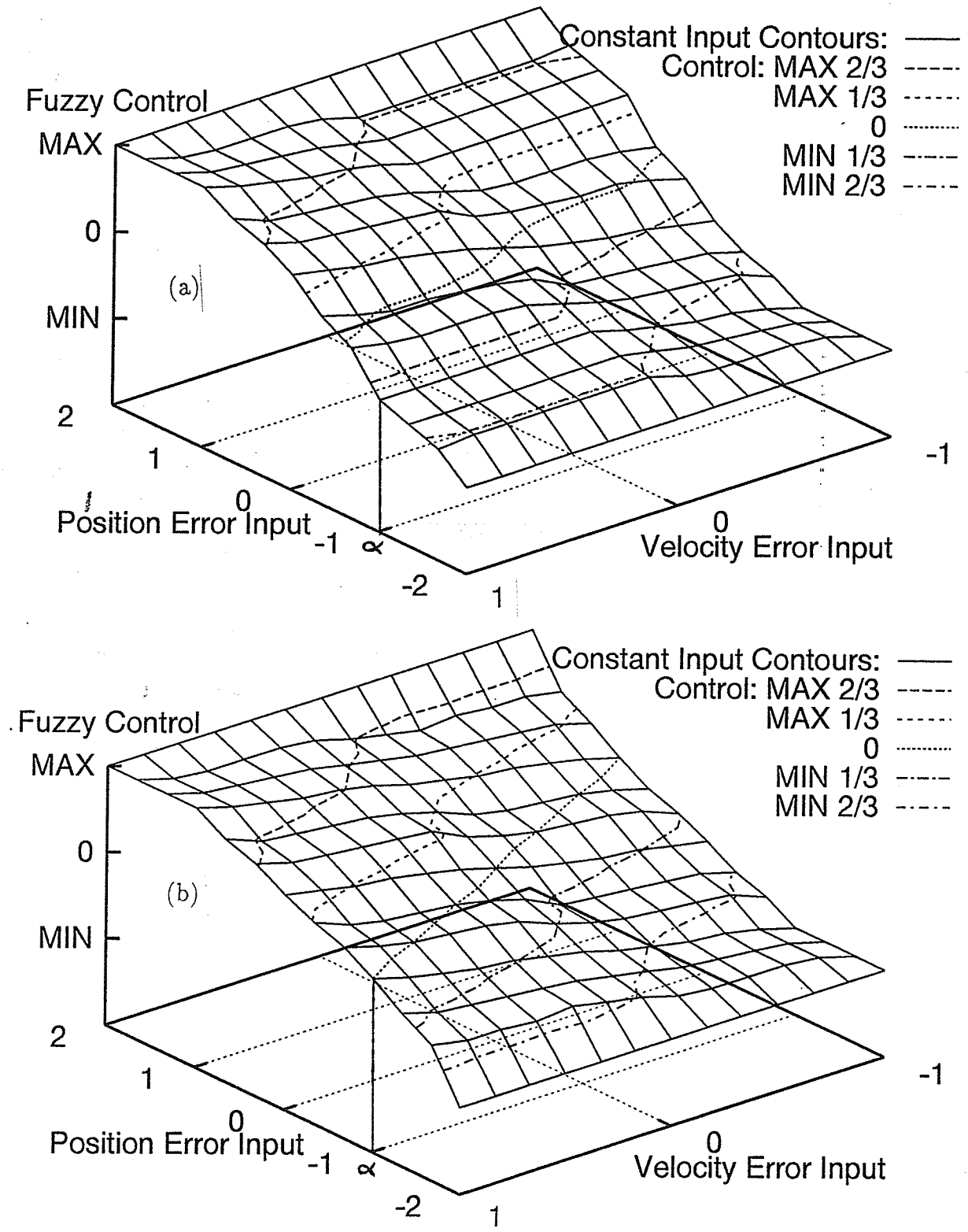

Figure 3.3: Control surfaces: (a) hydraulic rule table; (b) conventional rule table

and the minimization of error for the entire step response ensures both low rise time and overshoot. Any oscillations at the set point, because of the use of improper values for gains, is considered as error in the function evaluation.

The optimization problem is two dimensional, and the routine used in this thesis is based on the simplex method. The simplex method is a true N-dimensional optimization technique which does not incorporate line minimization [27,28]. It eliminates the problem of bracketing the minimum, is fast and does not require any derivatives. The simplex method is based on using a triangle (pyramid in the case of three dimensional optimization) with a performance error at each vertex. The performances are then compared and the next evaluation is performed in the direction opposite to the vertex with the worst performance. In this work, the performance error was simply chosen to be the accumulated position error ($\int edt$) over a sufficient period of time in a step input response. The performace of the simplex method will be detailed in Section 4.2.1.

3.3 Simulation Studies

The schematic of the hydraulic robot used in the simulation is shown in Figure 3.4. The robot runs on a constant pressure pump system and is controlled by closed-center valves. The structure and the physical parameters of the robot used in the simulation, were chosen to resemble the hydraulic robot used by Hanafusa et al. [22,26] at Kyoto University. The accuracy of the simulation results were previously verified by Al-Zaher [23]. The simulation of a hydraulic robot, used to evaluate the fuzzy controller, has proven to be a valuable tool in assessing the fuzzy rules. Performance of the hydraulic robot can be first observed in the simulation and effects of variation of several parameters can be examined before an actual implementation is carried out.

Proportional, proportional plus derivative and fuzzy logic controllers were first

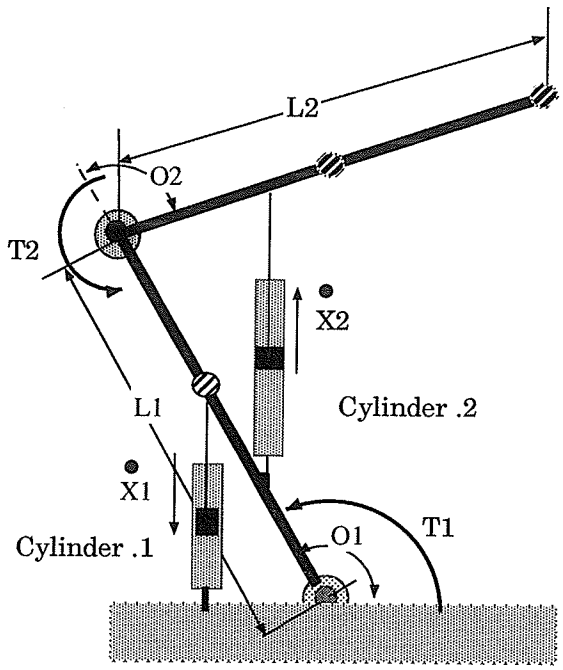

Figure 3.4: Hydraulic robot used in simulation [23]

tested in the simulation. These tests were done to understand what is possible with a PD controller and what would be expected from a fuzzy logic controller. A typical result is shown in Figure 3.5(a); link one of the robot was commanded to move from 60° to 120°. Referring to Figure 3.5(a), using only a proportional control, the response was not fast and exhibited some oscillations at the set point. Any further increase in the proportional gain resulted in a faster rise time but increased the undesirable oscillations. The addition of derivative control was attempted next. Fast rise time with a dampened response was very hard to tune in the PD controller. The response with a well tuned PD controller is shown in Figure 3.5(a). This figure also shows the result of applying a fuzzy controller with tuned gains. Even with a large overshoot the fuzzy controller response is dampened quicker than the PD controller (Note: this overshoot could be reduced). Figure 3.5(b) shows the control input for the three step responses. The proportional controller did not stay at the maximum control output

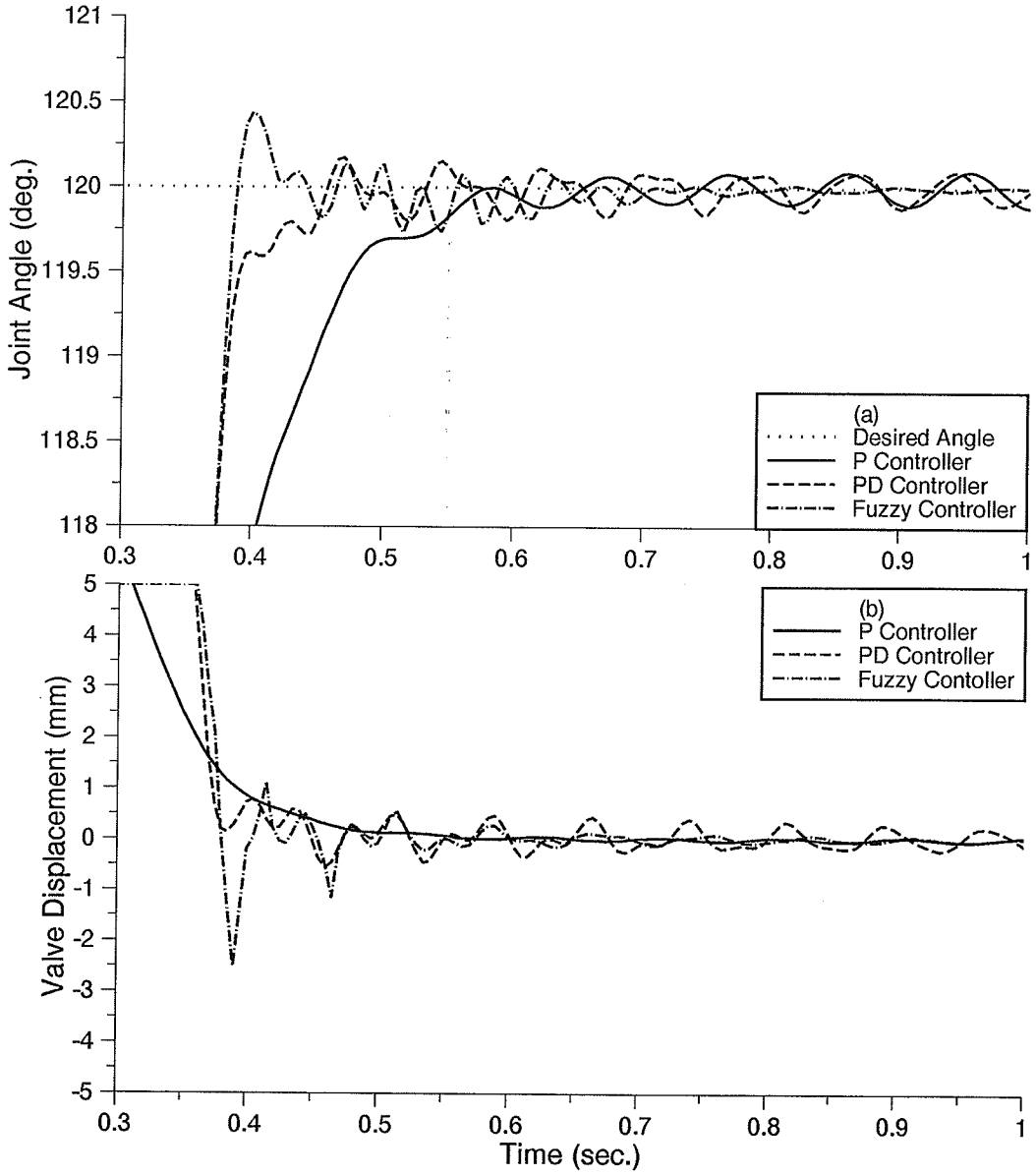

Figure 3.5: Link 1 step input response and control signal (simulation)

long enough to achieve a fast rise time. The PD controller produced larger control actions but became oscillatory at the set point. The output from the fuzzy controller assured a fast rise time and maintained a stable control.

These results highlight the basic characteristic of a fuzzy controller which implies that the stability and responsiveness can be tuned at the same time [8]. The fuzzy controller designed here maintained a fast, yet dampened response. This is due to the fact that the effect of the velocity error on the fuzzy control action is considered in union with the position error. This nonlinear characteristic of the controller is of great advantage and was not possible with a conventional PD controller with fixed gains.

In this example, the fuzzy control gains were tuned by the simplex optimization algorithm. Figure 3.6(a) shows the optimization which resulted in the global minimum. Here the performance error is graphed versus the number of iterations. The step input response at the start of the optimization is compared with the one after the optimization and is seen in Figure 3.7(a). The control values are shown in Figure 3.7(b). The maximum control output was maintained much longer in the optimum to ensure a fast rise time.

The simulation allowed the terrain of the accumulated error ($Performance\ Error = \int e dt$) with respect to the position and velocity error gains to be graphed. Figure 3.6(b) shows two cross-sections of the performance error surface for two different values of velocity error gains (V_e). The plot for $V_e = 0.9$ was the global minimum, found for the entire surface. The performance error at this point was 14.09 and the optimum position error gain was found to be $P_e = 2.0$. The trend of the performance error for $V_e = 1.8$ and for different values of P_e is also shown in Figure 3.6(b). It is a cross-section through a local minimum. The summation of error at this point was 14.13 for $P_e = 0.8$. This set of gains produced a response similar to the one in Figure 3.5 but with slight oscillations at the set point.

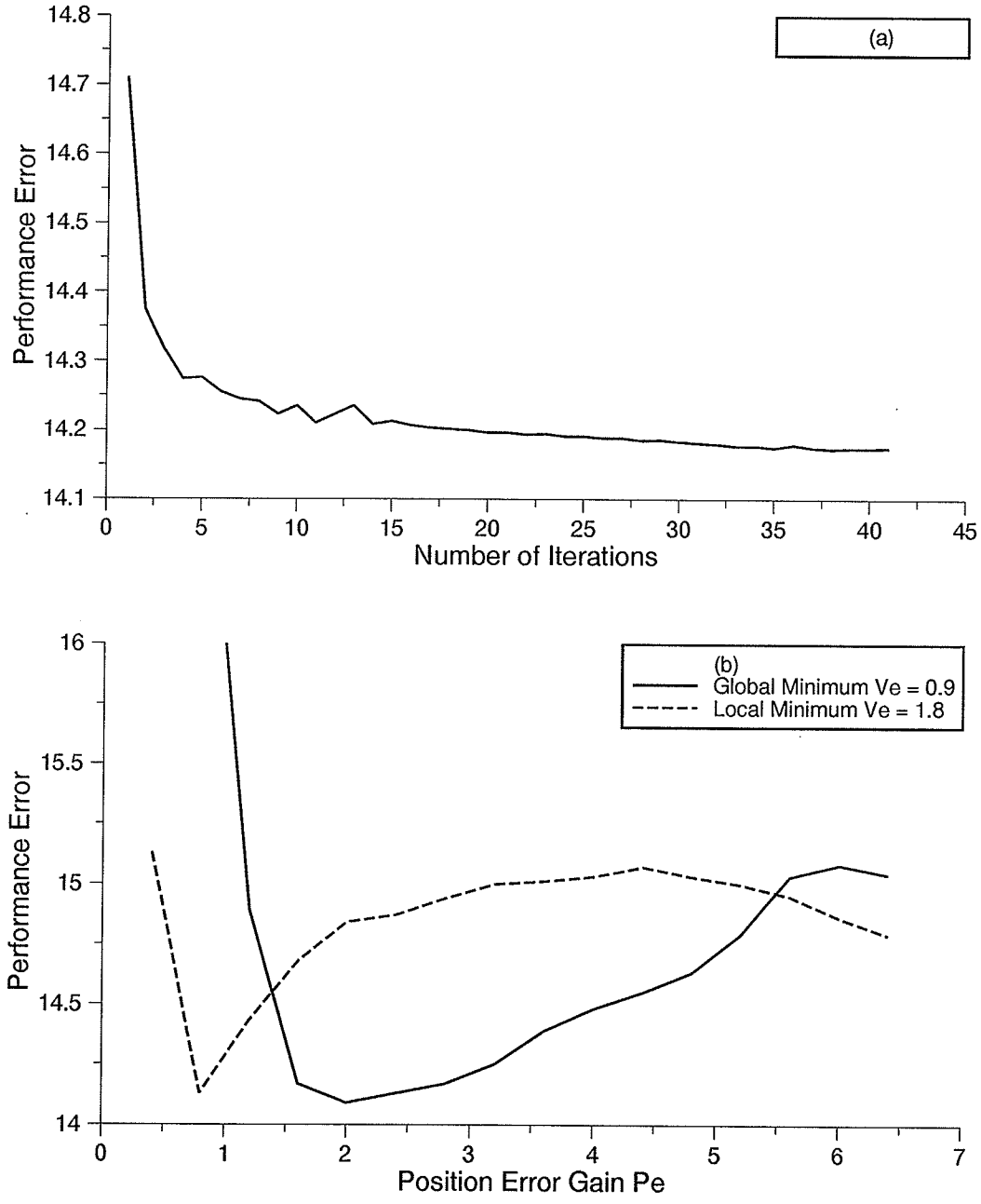

Figure 3.6: (a) Performance trajectory; (b) performance error vs. position error gains (simulation)

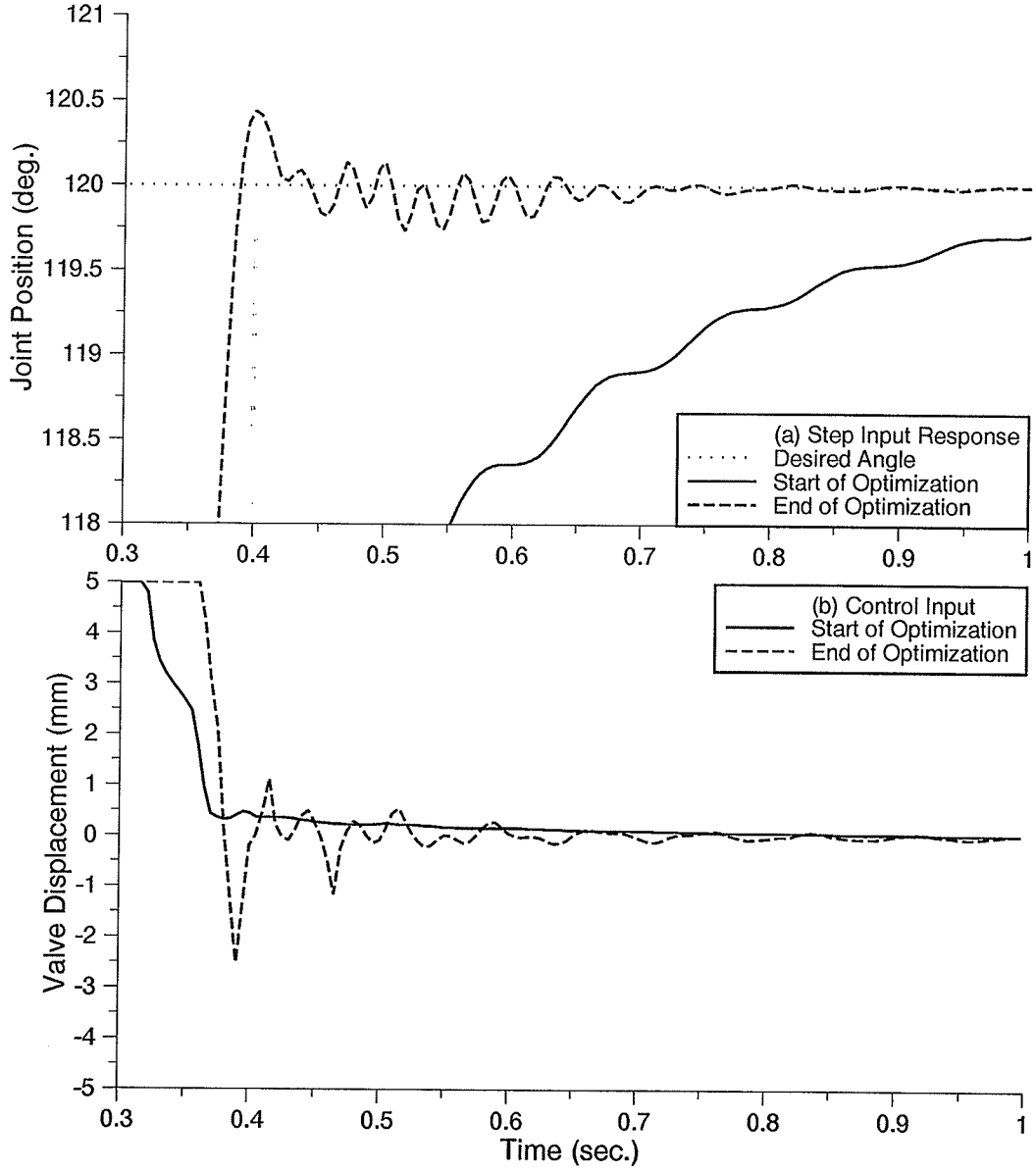

Figure 3.7: Responses at the start and the end of optimization (simulation)

The same step input, in an alternate region of the work space, was then applied to the simulation and a 3-dimensional mapping of the performance error vs. gains is shown in Figure 3.8. A global minimum can be observed visually at approximately $P_e = 1.2$ and $V_e = 0.6$ with performance error 13.89. A local minimum can also be observed at approximately $P_e = 1.2$ and $V_e = 2.0$ with performance error 14.12, this is roughly the same area as the original step input. This shows that a consistent minimum can be found for any step input.

In spite of the existence of local minima, the simplex method converged to the optimum position and velocity error gains, given different starting points. One problem with the simplex routine was that when using starting points with high values for gains (much higher than the optimum gains) the algorithm tended to be unstable, due to unstable response; therefore no minimum direction was obvious. As a result, optimizations were always done using small starting gains.

A similar optimization was performed using the conventional rule table shown in Figure 3.2. The optimum step response is seen in Figure 3.9(a). The rise time was slightly longer than the hydraulic and just slightly overshoots the desired. Here to maintain a dampened response, while still reaching the desired, the controller required input gains 50% higher than the hydraulic table optimum gains. The gains are $P_e = 3.0$ and $V_e = 1.35$. The reason for this increase is the rule that states: for velocity error of NL and position error of PS, then control output is ZR. This higher gain increases instability and decreases the range of non-maximum control for position error input. The optimum hydraulic control table gains, as applied with the conventional rule table, is shown in Figure 3.9(a). The lower gains resulted in a longer rise time and an actual position which stopped before reaching the desired then continued slowly. Control input trajectories are shown in Figure 3.9(b). These results show that the compensation for velocity is too much.

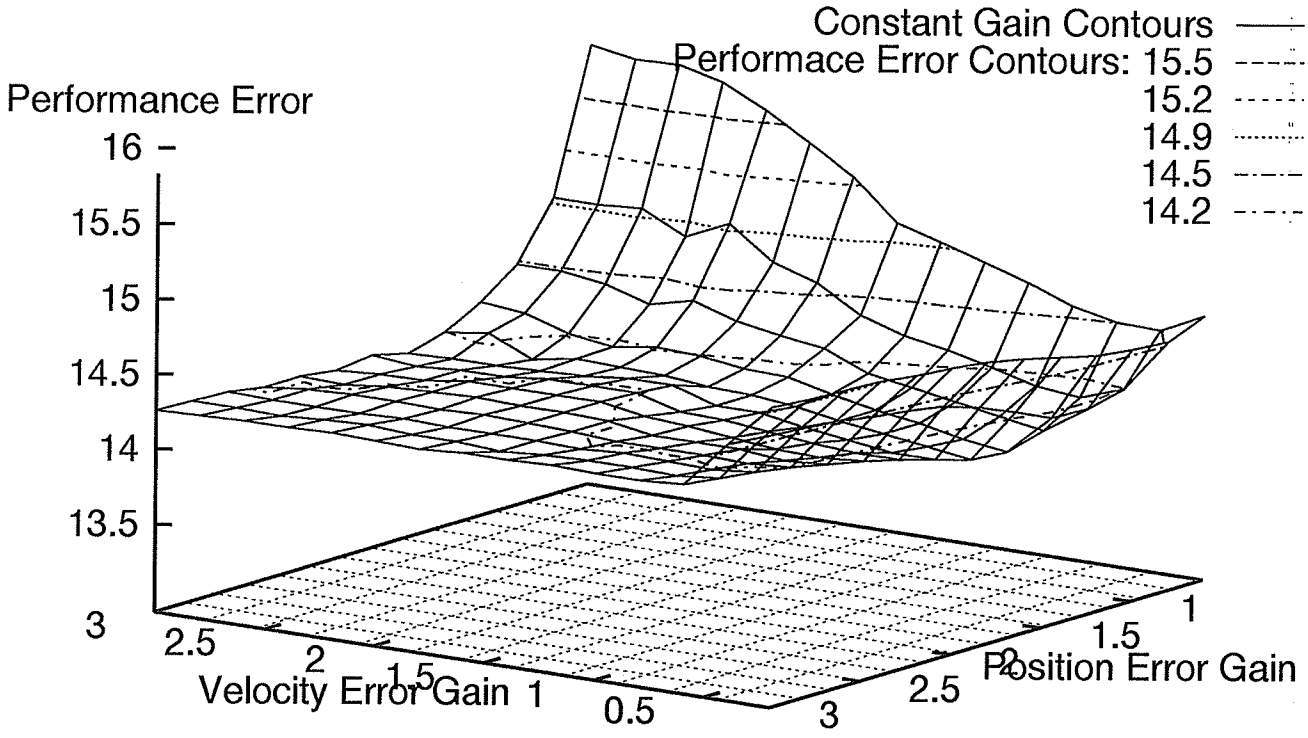

Figure 3.8: Performance error surface

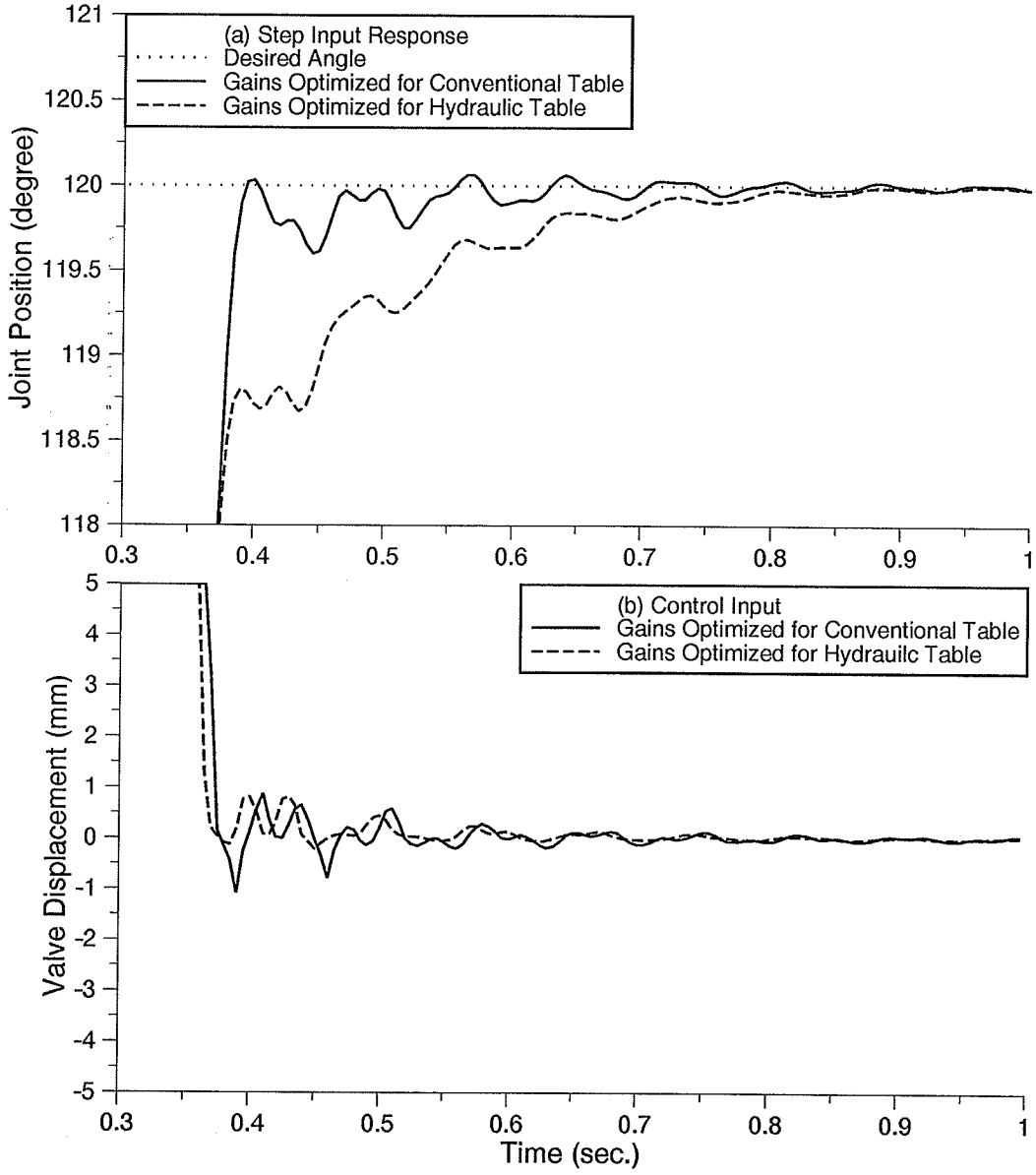

Figure 3.9: Response with a conventional rule table

Chapter 4

Experimental Studies

4.1 Overview of the Experimental Test Station

An industrial hydraulic robot (a Unimate MK-II) was retrofitted as a research robot to establish a platform for testing the control algorithms. The manner in which the computer was integrated into the system is shown in Figure 4.1. In a closed-loop system, connections to send a control signal and receive feedback are required. We have servovalves to control, and encoders to read the joint positions. The encoders generate digital signals. An interface was built to read the encoder signals, translate them into parallel binary and present them to the digital I/O card as shown in Figure 4.1. In this figure, the data link which starts at the absolute encoder interface indicates digital input from the encoders to the digital I/O of the computer. The servovalves regulate fluid-flow to hydraulic cylinders in proportion to the input currents. The Digital-to-Analog (D/A) card allow the computer to generate a valve current proportional to D/A voltage ($\pm 5 volt$ to produce $\pm 600 ma$ current).

When the PD-type fuzzy controller described in Section 3.1 was applied in the experiment, the acquisition of accurate actual velocity values for each link posed a

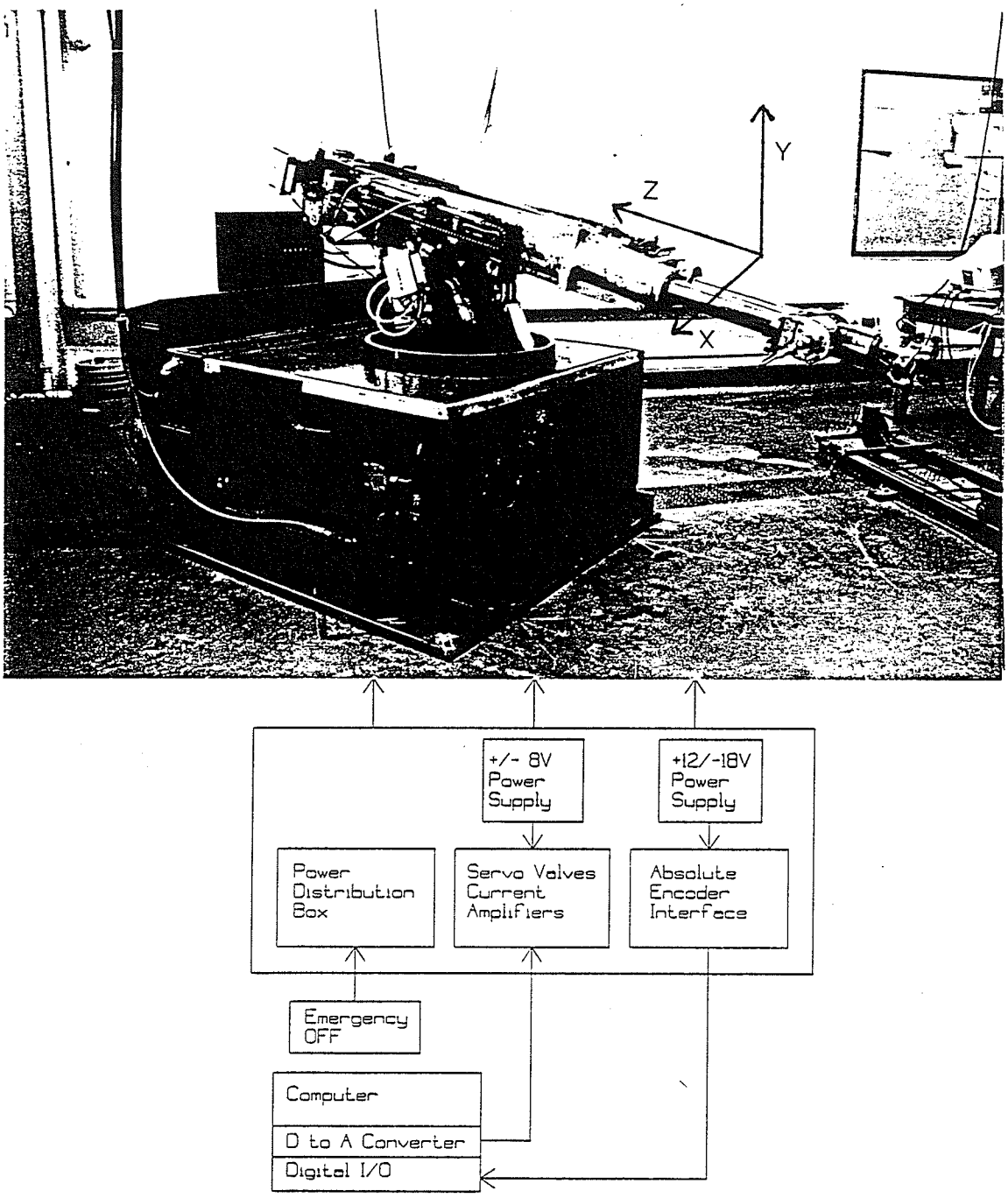

Figure 4.1: Experimental test station

problem. The simplest method to obtain these values was from the position encoders. A regression of joint encoder values was then performed to obtain the actual velocity. Regression of three previous joint encoder values was used initially in experiments.

Time was obtained from the internal clock of the computer. A routine asked for the present time at the start of each control loop. The time was accurate to 1/1000 of a second. Inconsistent control frequencies were a problem in the initial experiments due to data storage to a file approximately every tenth control loop. This problem was solved by keeping all the data in vectors and performing data file storage at the end of the experiment. With this arrangement the control frequency was maintained at a relatively constant level during experimentation.

Modifications to the conventional fuzzy membership functions, shown in Figure 2.2, were required for successful application of the fuzzy controller in simulation. These changes included widening of the zero output membership function by 100% and a reduction in the MAX output membership function by 50%. The reason for increasing the zero output membership function was the speed of value response due to the lack of damping or valve friction in the simulation. The decrease in the MAX output membership function was necessary to reduce its dominance over the other output membership functions.

Modifications to the fuzzy membership functions were also required for successful application of the fuzzy controller in experiment. Because of the friction and deadband present in the valves, the zero voltage output was then returned to its original width in Figure 2.2 but the MAX output remained at the decreased width; changes are seen in Figure 3.1. The zero voltage reduction resulted in larger control values when the position error was close to zero. These larger values were required due to the steady-state error observed in experiment. The steady-state error was the result of a 6% deadband in the spool displacement of the hydraulic servovalve, as specified by the manufacturer.

4.2 Single-Link Experiments

Preliminary experiments revealed that, an increase in P_e (position error gain) reduced the rise time but to the detriment of the overshoot and oscillations at the set point. This is also true in a conventional proportional controller. Decreasing P_e slowed down the response and resulted in a larger steady-state error. Similarly V_e (velocity error gain) operated much like a derivative gain in a conventional PD Controller in its damping ability. It also had a characteristic of over compensation (will be shown later), which resulted in sustained oscillations at the set point. Therefore an optimum set of gains was required.

4.2.1 In/Out Motion

Step Input Response and Gain Tuning

Figure 4.2(a) shows the In/Out step response of link 3 (link with In/Out motion in Figure 4.1). The response corresponded to gains $P_e = 2.0$ and $V_e = 1.0$. These gains were initially used in the optimization routine. The optimum gains were found by repeatedly performing the step response. The program evaluated the performance error, altered the gains and repeated the motion until the best performing gains were determined. The optimized values, found for this case, were $P_e = 3.87$ and $V_e = 1.21$ which resulted in the response shown in Figure 4.2(b). It is seen that the optimized response has a slight overshoot but the rise time was fast; it was stable and did not have oscillations at the set point. The steady-state error observed in the response was due to the 6% deadband in the spool displacement. This steady-state error resulted in a constant fuzzy control output [see Figure 4.2(b)] (Note: saturation of control occurs at 5 Volts). However, because of the deadband in the valve, the error was not eliminated. The plot of the performance error values as a function of the number of

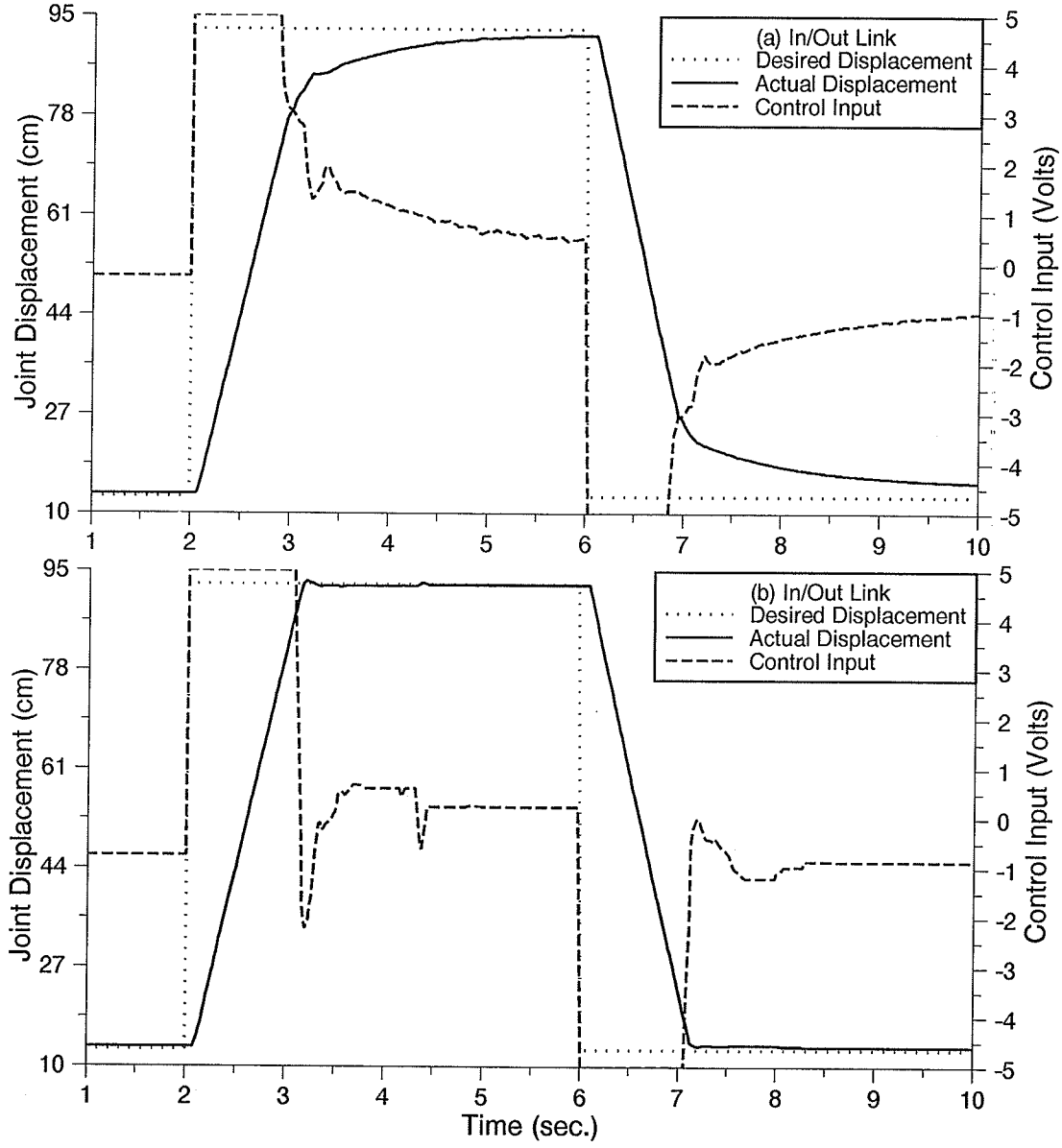

Figure 4.2: In/Out step response to a fuzzy controller: (a) start of optimization; (b) end of optimization (Note: saturation of control occurs at 5 Volts)

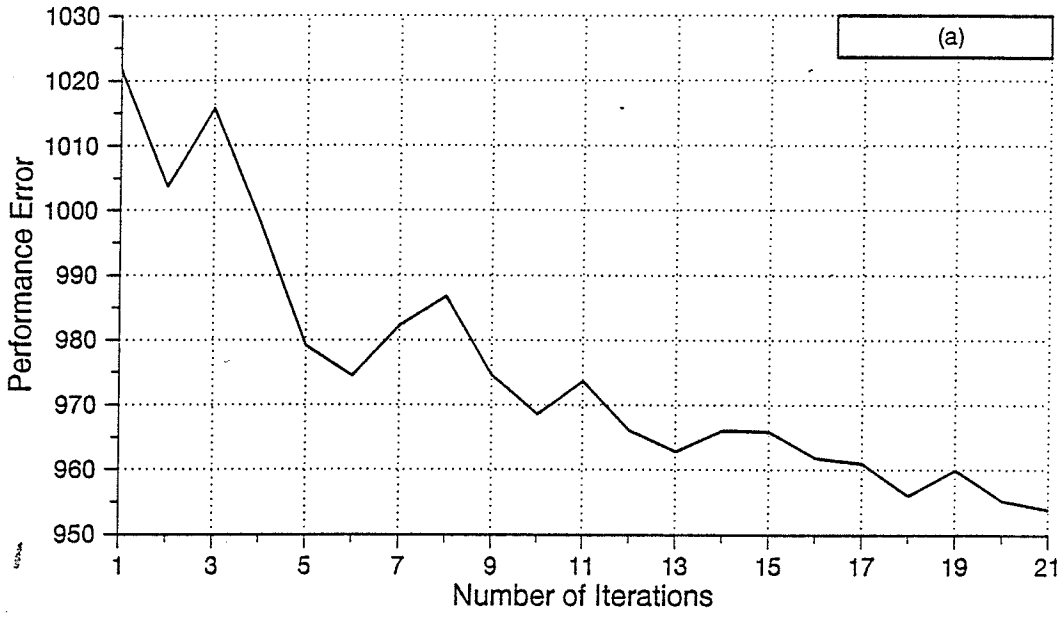

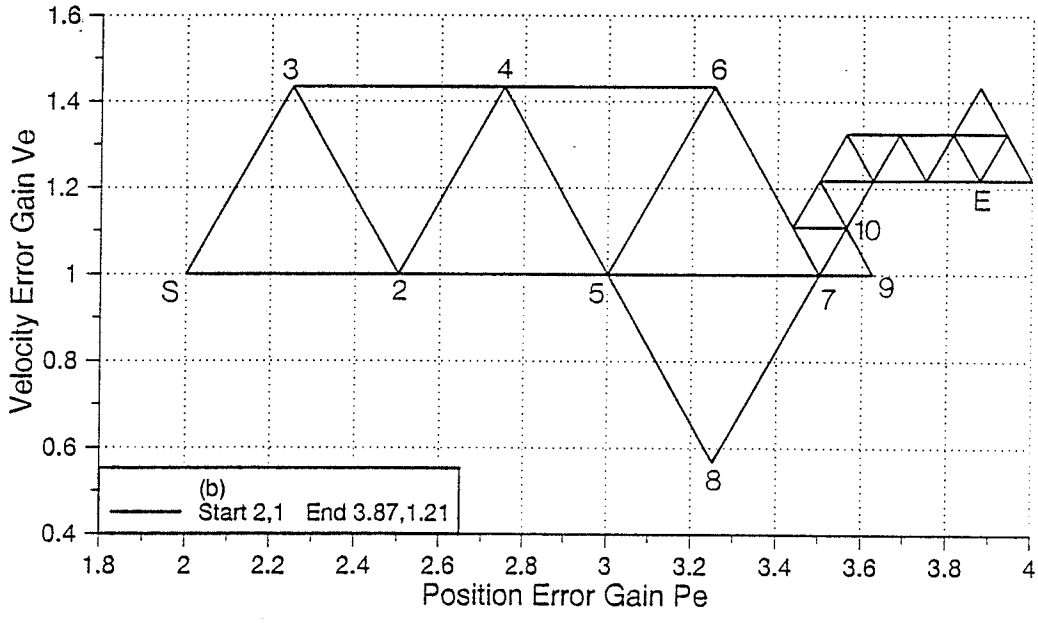

Figure 4.3: (a) Performance error changes; (b) mapping of sample optimization

trials is shown in Figure 4.3(a), and the actual operations of the method from the initial gains to the optimum is seen in Figure 4.3(b).

It should be noted that in some experimental results, an example is seen in Figure 4.2 (b) for the In/Out motion, the steady-state error due to the existence of valve deadbands was not obvious. This was a random occurrence and was not the result of the fuzzy controller. A steady-state error could have been observed for the same experiment if it was repeated. The maximum steady-state error was, however, limited to a value proportional to deadband.

Ramp Input Response

A ramp (constant velocity) input was then applied to link 3. The optimized set of gains found for the step input, were used in this experiment. The result is shown in Figure 4.4. The trajectory profile, which covered almost the entire extension of the link ($104cm$), included a gradual increase in the required velocity at the start and a gradual decrease to zero velocity at the end. This was done to observe how velocity error gain would react during the velocity transition and to ensure that a diverse and large number of rules were utilized.

The steady-state error presented in Figure 4.4 was unavoidable with the fuzzy controller designed here. There had to be a steady-state error in the hydraulic robot if it was to follow a ramp input. A zero velocity error and a zero position error would result in a closed valve and the link would stop. For the valve to open and the hydraulic robot to have a continuous motion there had to be a position error. The desired constant velocity was however achieved.

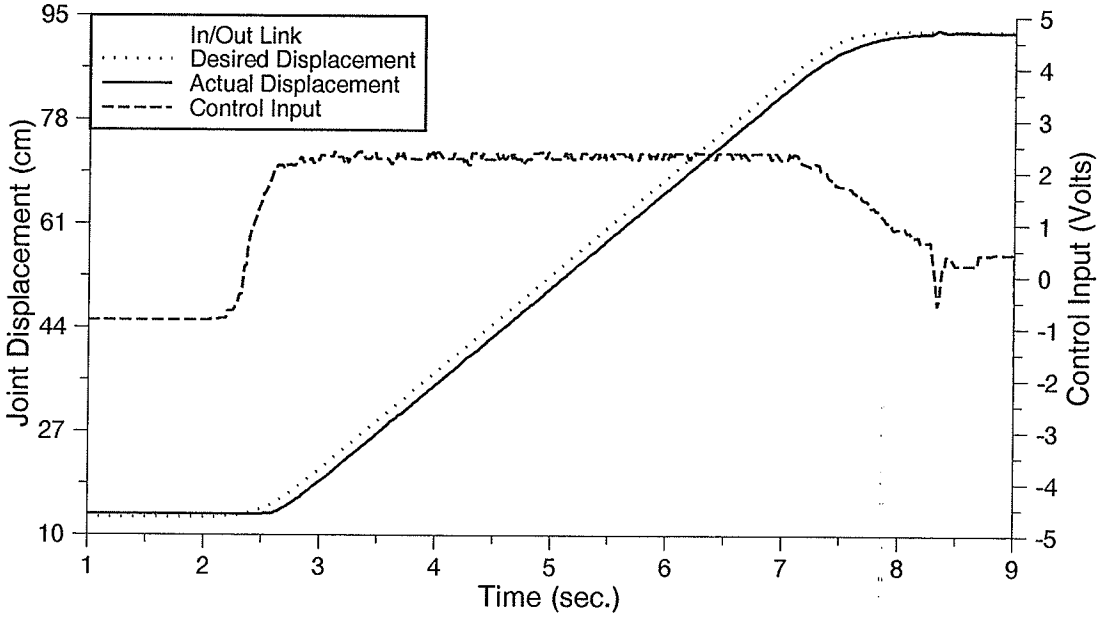

Figure 4.4: In/Out constant velocity (ramp) response

4.2.2 Up/Down Motion

Figure 4.5(a) shows the Up/Down motion of link 2 with the optimized fuzzy control gains. The optimized gains were found in the same manner as in the previous experiment, using step response evaluations. A conventional proportional controller was also applied to the same step input. The result is shown in Figure 4.5(b). The optimum fuzzy gains were $P_e = 11.4$ and $V_e = 2.4$, the proportional gain was $K_p = 15$. For a similar rise time, the proportional controller produced a large overshoot.

The firing sequence for the plot of position in Figure 4.5, is seen in Figure 4.6. At the start of the step response the position error was maximum and velocity error was zero (Note: for a step input response the desired velocity was zero). From this starting point the velocity error increased to a maximum and then returned to zero. If this graph is overlayed on the control table the order of firing is observed; for any given point on the input path multiple rules were fired. The controller was tuned sufficiently in that it was observed to proceed directly toward the center of the table

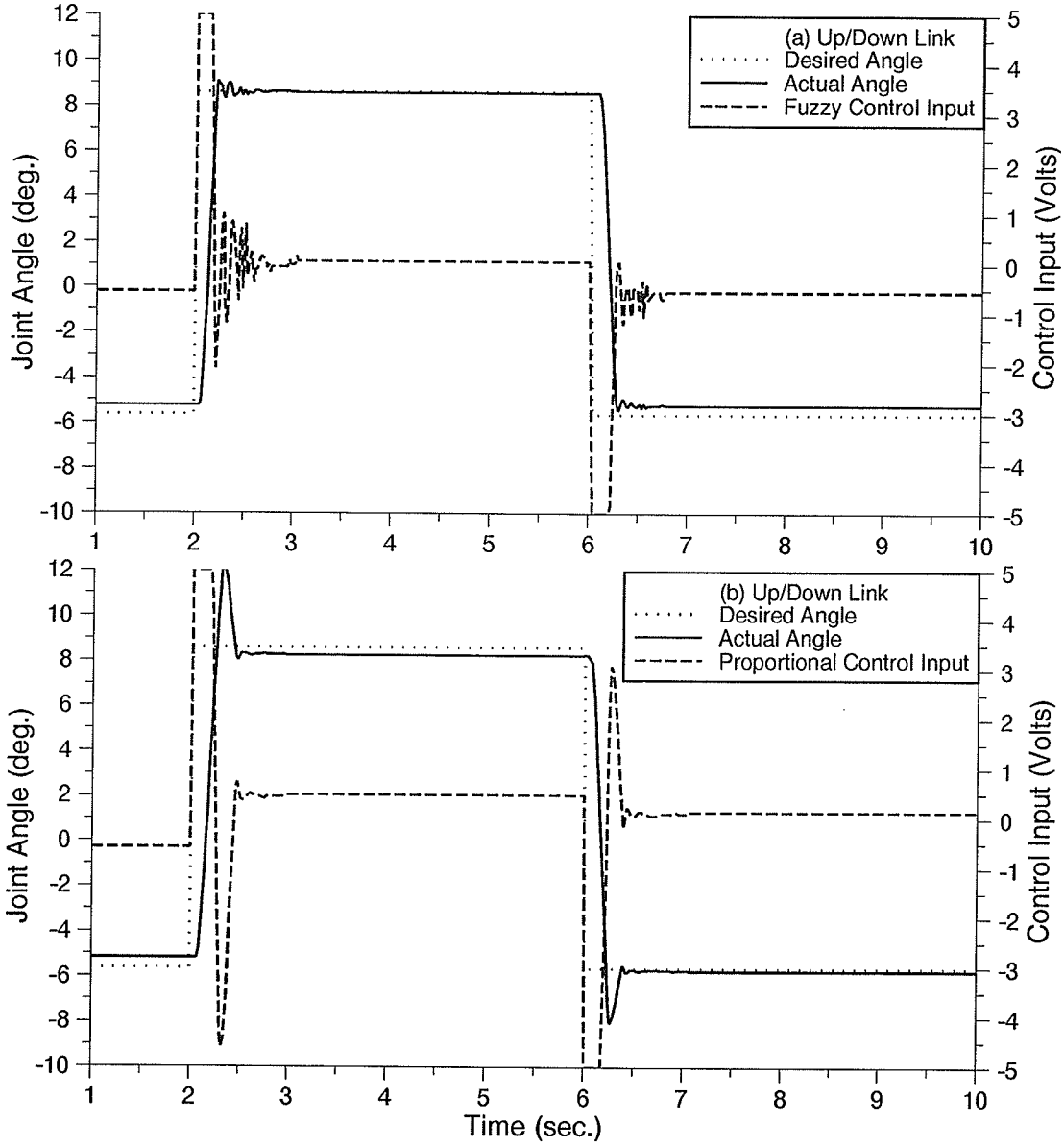

Figure 4.5: Up/Down step response: (a) with fuzzy logic control; (b) with proportional control

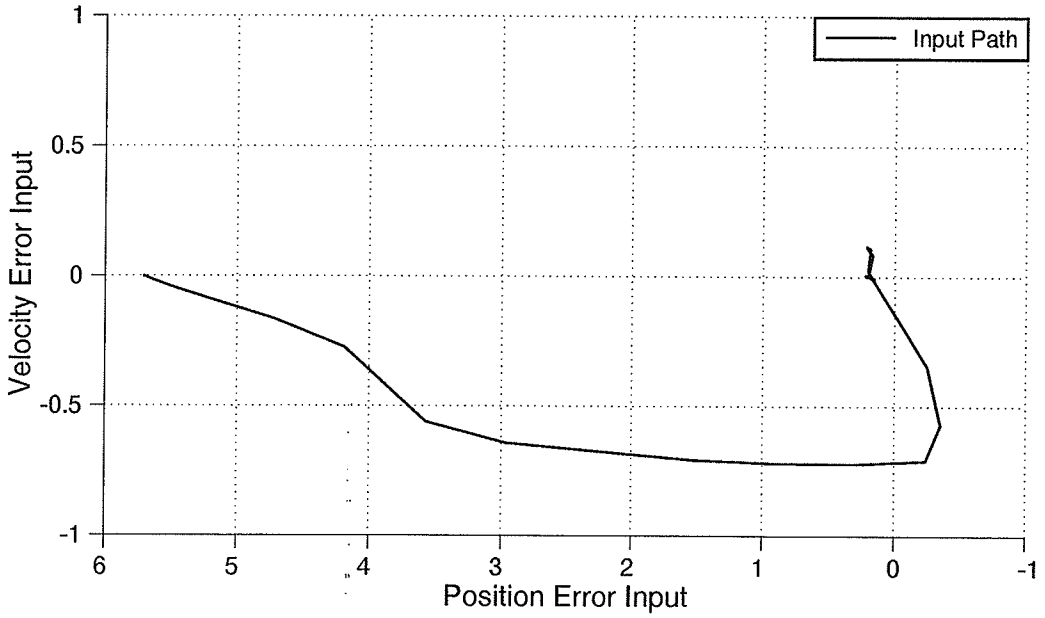

Figure 4.6: Phase diagram pertaining to Figure 4.5(a)

with small oscillations before settling. The steady-state position error observed in Figure 4.6 was due to the valve deadband (see also Figure 4.5).

The result of the ramp input for the loaded and unloaded link is shown in Figure 4.7(a). The same optimal gains as in the step input were used in this experiment. The robot was loaded with $45kg$ (a 25% increase in weight) of weight at the end effector, and the motion was in the upward direction. The total range of the motion was 37°. Referring to Figure 4.7(a), the steady-state error decreased for the unloaded case once the link passed its horizontal position. This resulted in a decreased control input for the unloaded arm; it remained constant for the loaded case. Increasing V_e did not affect the steady-state error as was expected. The velocity profiles are also shown in Figure 4.7(b) where the actual velocities are plotted against the desired velocity. It is seen that the loading did not affect the velocity response.

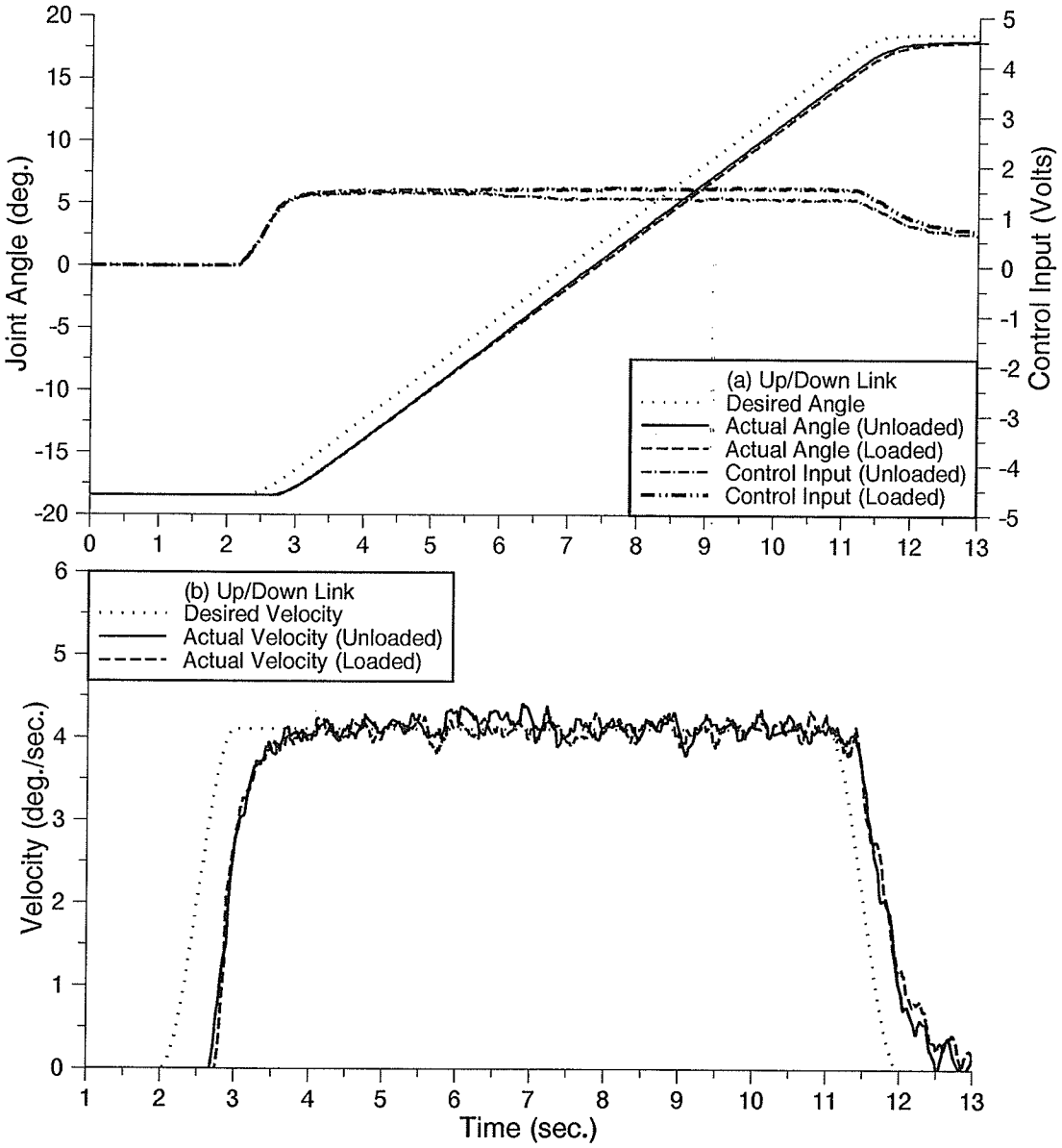

Figure 4.7: Up/Down ramp input response: (a) joint angle trajectory; (b) joint velocity profile.

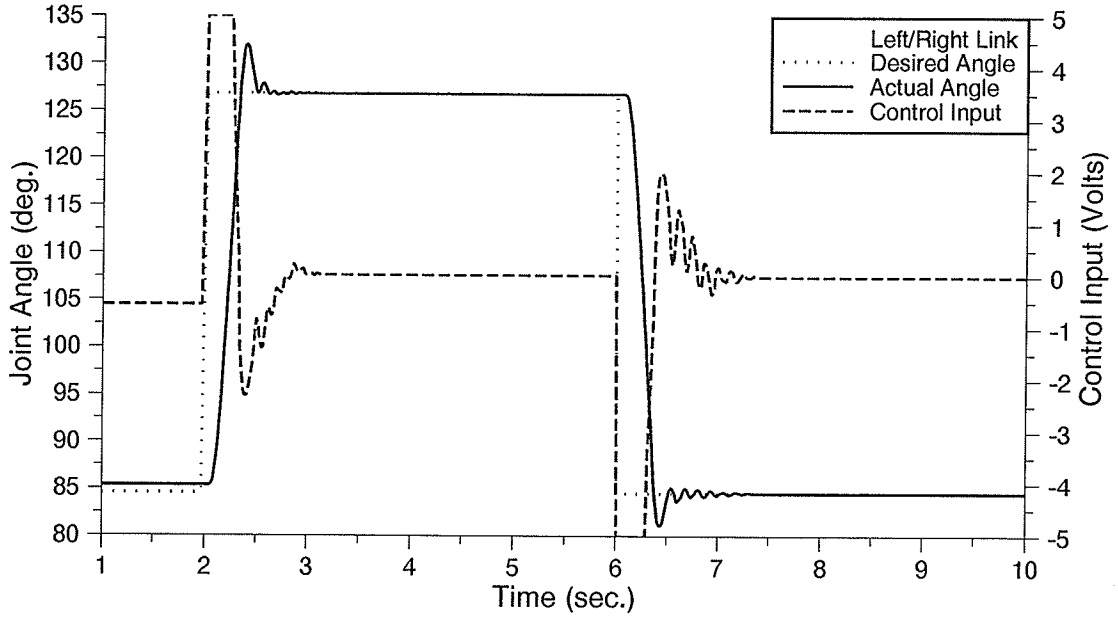

Figure 4.8: Left/Right step response

4.2.3 Left/Right Motion

The step response of link 1 during a Left/Right motion and with tuned gains (using the optimization routine) is shown in Figure 4.8. The optimum fuzzy gains were $P_e = 3.62$ and $V_e = 1$. The overshoot present in the step response was the result of an optimum rise time and the high inertia of this link. A fast rise time resulted in a performance error which was lower than any performance error produced with a decreased overshoot. The oscillations of the link, at the set point, were however dampened quickly. A balance has been reached between error due to overshoot and rise time in the final optimum gains. One may add a penalty function to increase the weight of the errors due to the overshoot. The optimization would then stop when a certain overshoot is observed.

We also performed a comparison between the velocity profiles of a loaded and unloaded ramp input response for link 1 (loading consisted of an extended In/Out link). The resulting responses were almost identical.

4.2.4 Additional Step Input Response Tests

Step size experiments were then performed to observe the effects of inertia, gravity and the usefulness of an optimum set of gains in different regions of the workspace. These experiments were applied to the Up/Down motion of link 2 only. A step response of 14.2°, in different regions of the workspace, was applied first. Figure 4.9(a) shows a test for a 14.2° step below the horizontal level to which the link falls short of the desired angle for both motions. When the step was moved above the horizontal, in Figure 4.9(b), an overshoot was visible for both 'up' and 'return' step responses. The absence of overshoot in the step response performed above the horizontal is believed to be the result of nonlinear hydraulic cylinder dynamics and gravity effects.

The responses to step inputs of 28.4° and 42.6° about the horizontal are seen in Figure 4.10. Overshoots for such larger step sizes were negligible. Smaller step input response tests were also performed for a starting point at approximately 5° below horizontal. The 7.2° step response in Figure 4.11(a) shows that the controller did reach the maximum $5volt$ output before it fell within the range of small position error. The size of the position error for the 3.6° step response in Figure 4.11(b) did not result in a maximum controller output. This was because the error was within the small position error at the start. The position error to which the link stopped was right on the edge of the valve deadband. The link did not attain the velocity required to bring it closer to zero position error. The 1.8° step input response is also seen in Figure 4.11(c).

4.2.5 Discussion

For all links, the optimal control gains were found in less than 25 iterations ($\approx 5.5min$). During the experiment, it was also observed that some starting points resulted in the algorithm ending at a velocity error gain local minimum. This was be-

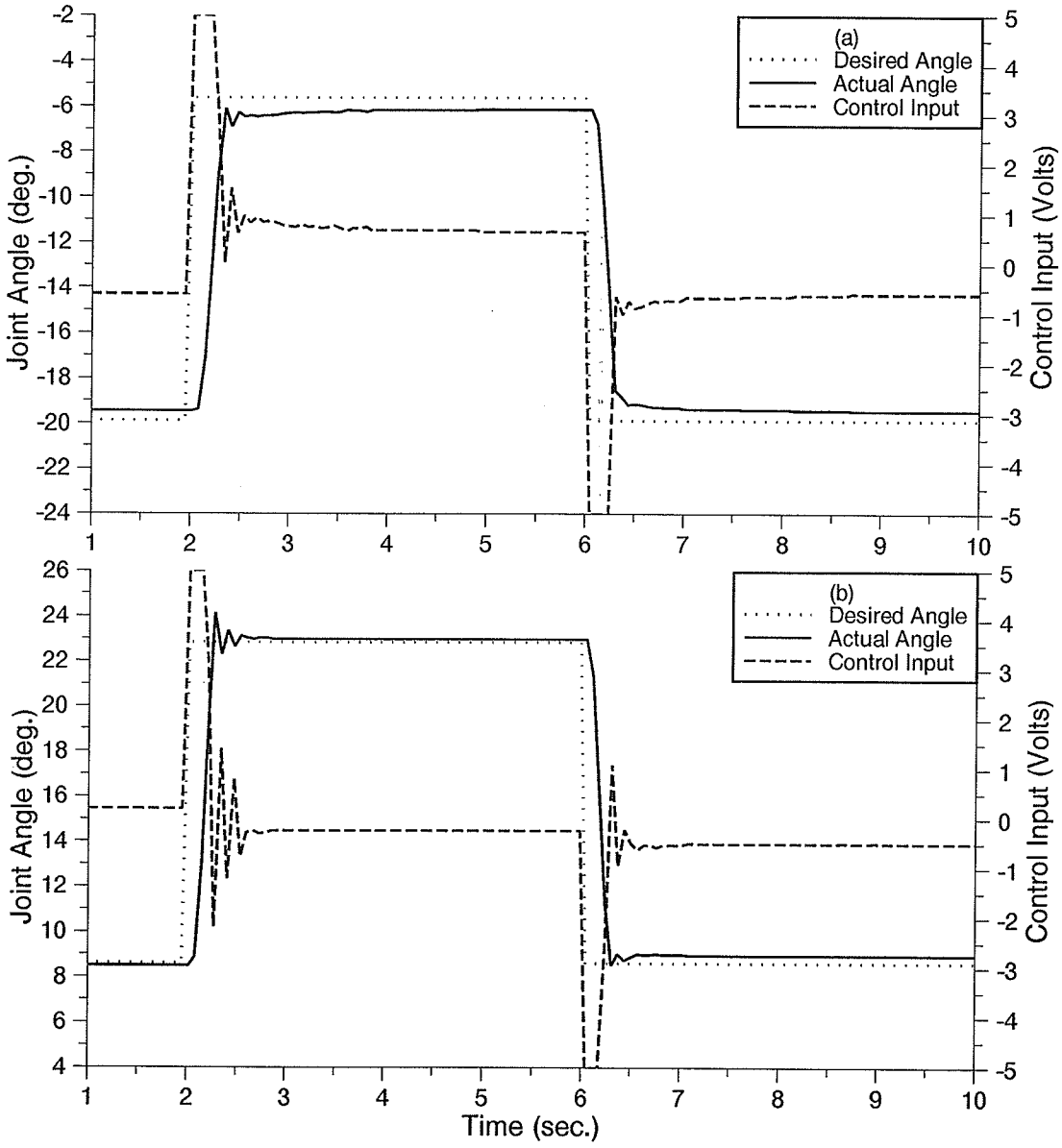

Figure 4.9: Up/Down step input responses (14.2°) with different starting points

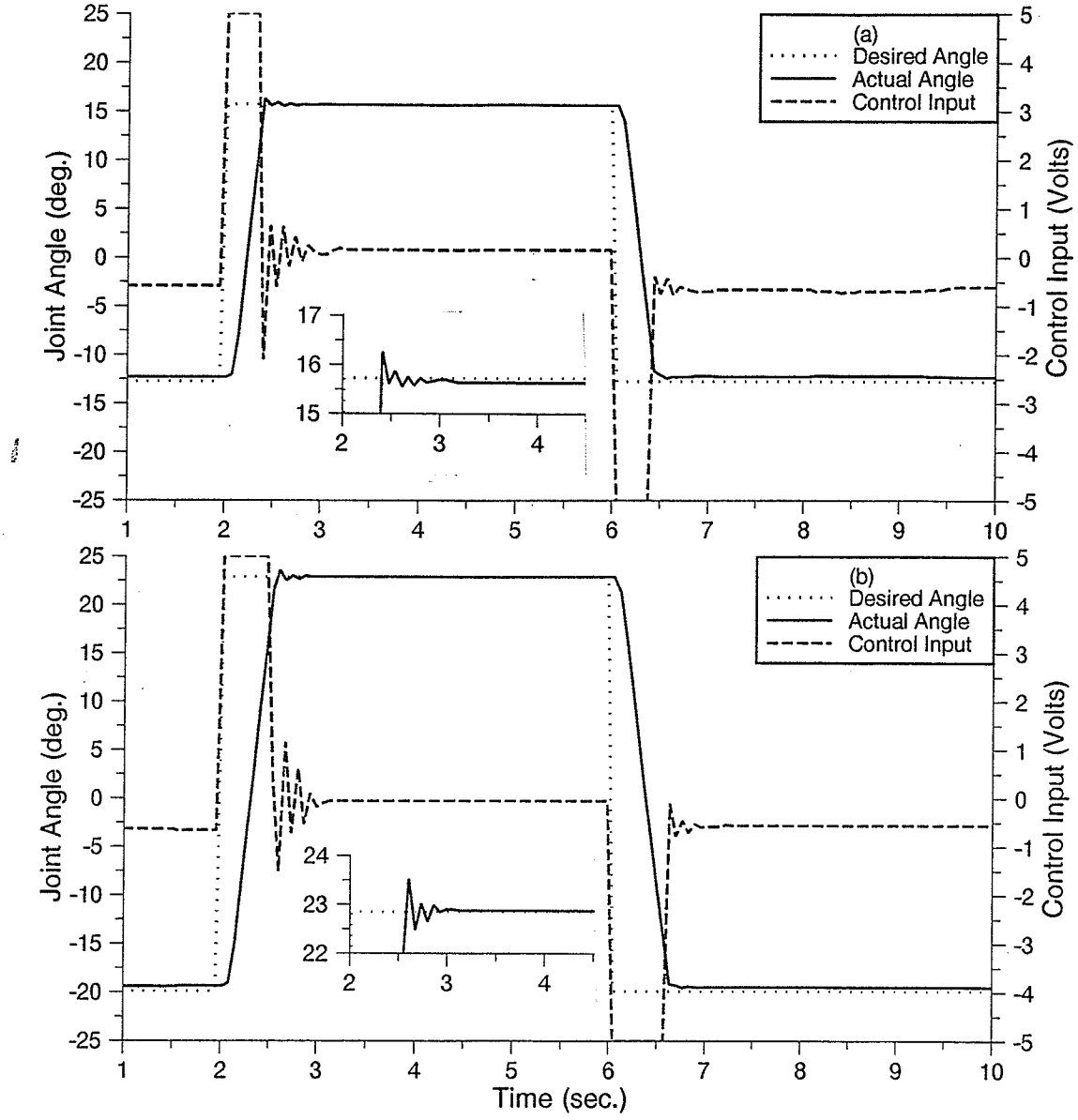

Figure 4.10: Up/Down step input responses with increased step sizes; (a) 28.4°; (b) 42.6°

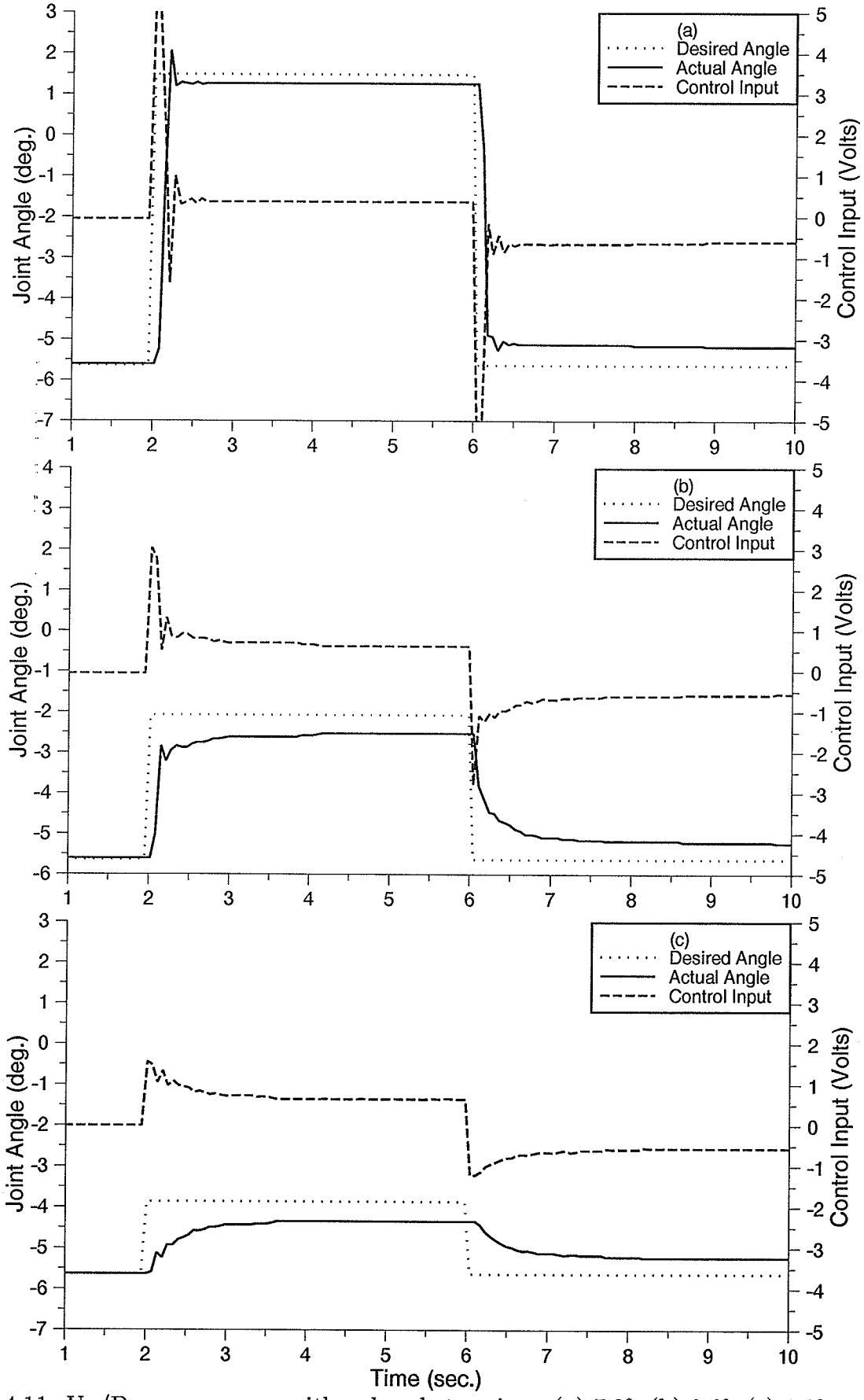

Figure 4.11: Up/Down responses with reduced step sizes: (a) 7.2°; (b) 3.6°; (c) 1.8°

lieved to be due to a random steady-state error size which was added to performance error during the optimization. Other reasons were encoder noise and robot nonlinearities which resulted in non-reproducible velocities in the step input. For such cases the results from the optimization trials (with different starting points) were compared and the gains corresponding to the lowest performance error were chosen as optimal gains.

The application of various step inputs demonstrated that the optimum gains found by the optimization routine could be utilized for a variety of step sizes and regions of the workspace without a new set of optimum gains required.

It was found that adjusting the P_e gain to eliminate steady-state error in a step response could not be achieved. A decrease in the steady-state error was possible, but it was not eliminated completely. An elimination could not be achieved with the other tuning parameters either. Therefore, a steady-state error elimination method is required. In the above experiments, and all experiments to follow, the control frequency was $\approx 60Hz$.

For velocity plots the ten-point regression of joint encoder values was performed. Noise in the encoders was eliminated this way and the regression was believed to be close to the actual velocity. During actual implementation of a step input, a 3 point regression of position was used to find actual velocity in the control calculation. When trajectory tracking was applied, a 30 point regression was used to produce a better result since the controller became less sensitive to noise and velocity variations which were present.

Normally when one does a regression of points with respect to time, the result is related to the average of time at which each measurement took place. This means that somewhere in the middle of the 30 points, the regressed value is accurate. In the application of regression to this fuzzy controller it was impossible to predict the

15 or so points which occurred in the future. Therefore, regression of the previous 30 encoder joint values, was accurate for 15 control intervals before. Using this method for the current control calculation created a problem in that the controller was acting upon information which was slightly delayed (at 60Hz sampling frequency the delay was $15/60 = 0.25$ seconds). The calculation of actual velocity did not represent the present state of the system, and zero velocity error could not be achieved. This delay could be addressed in future work.

There are a few possible solutions to the problem of shifted velocity profile. One is to somehow shift the desired velocity to match up with the actual velocity. The other solution would be to increase the control frequency so that the 30 point regression is calculated within a shorter time period. This would greatly reduce, but not eliminate, the shift. It is not advisable to decrease the number of regression points because of the measurement noise.

4.2.6 Effect of Fuzzy Logic Parameters on Step Input Responses

The fuzzy logic parameters considered in this thesis are the width and peak values of the output membership functions of the fuzzy controller. The effect of changing these parameters is similar to changing the gains for a certain range of the controller inputs. When tuning these parameters, as applied to a ramp input, the effect was not noticeable. To truly understand how fuzzy logic parameter tuning affects the response, the controller inputs must cover a wide range. A step response appeared to be more useful, and was therefore used here to examine the fuzzy logic parameters. The experiments were performed on the Up/Down motion of link 2.

Small Voltage (PS and NS) Output Peak Values

Increasing the small voltage output centroid, i.e., peak values of PS or NS output membership functions [see Figure 2.4(b)] produced larger control values for small position errors. This increase in peak values was not expected to affect the output of the controller at close to zero position error values. This change altered the rules with PS and NS output membership functions. Referring to the rule table in Figure 3.1, 6 out of 15 rules with output PS and NS were affected.

When the peak value of the output control belonging to small voltage output membership function was decreased by 25%, the control reaction for small position errors became smaller. This change slowed down the response close to the desired angle, this is seen in Figure 4.12(a). The link stopped short of the desired angle because the control action resulting from the small error membership function was reduced. Similarly, increasing in the peak value by 25% and 50% resulted in the response shown in Figures 4.12(b) and (c), respectively. The increase in peak values increased the control actions at small errors. The link came closer to the desired angle and even produced an overshoot for the 50% increase.

Zero Voltage (ZR) Output Width Value

The change in zero voltage output width was expected to alter the local scaling factor of the controller for position and velocity errors close to zero. This alteration changed only the control actions close to the center of the rule table in Figure 3.1, for output voltage ZR. Increasing the width of the zero output membership function, as shown in Figure 2.4(c), increased the weight of this output when it was used in the 'COA' calculation.

Figure 4.13(a) shows the step input response of the Up/Down link with 25% increase in the width of the zero control output. The response looks similar to the

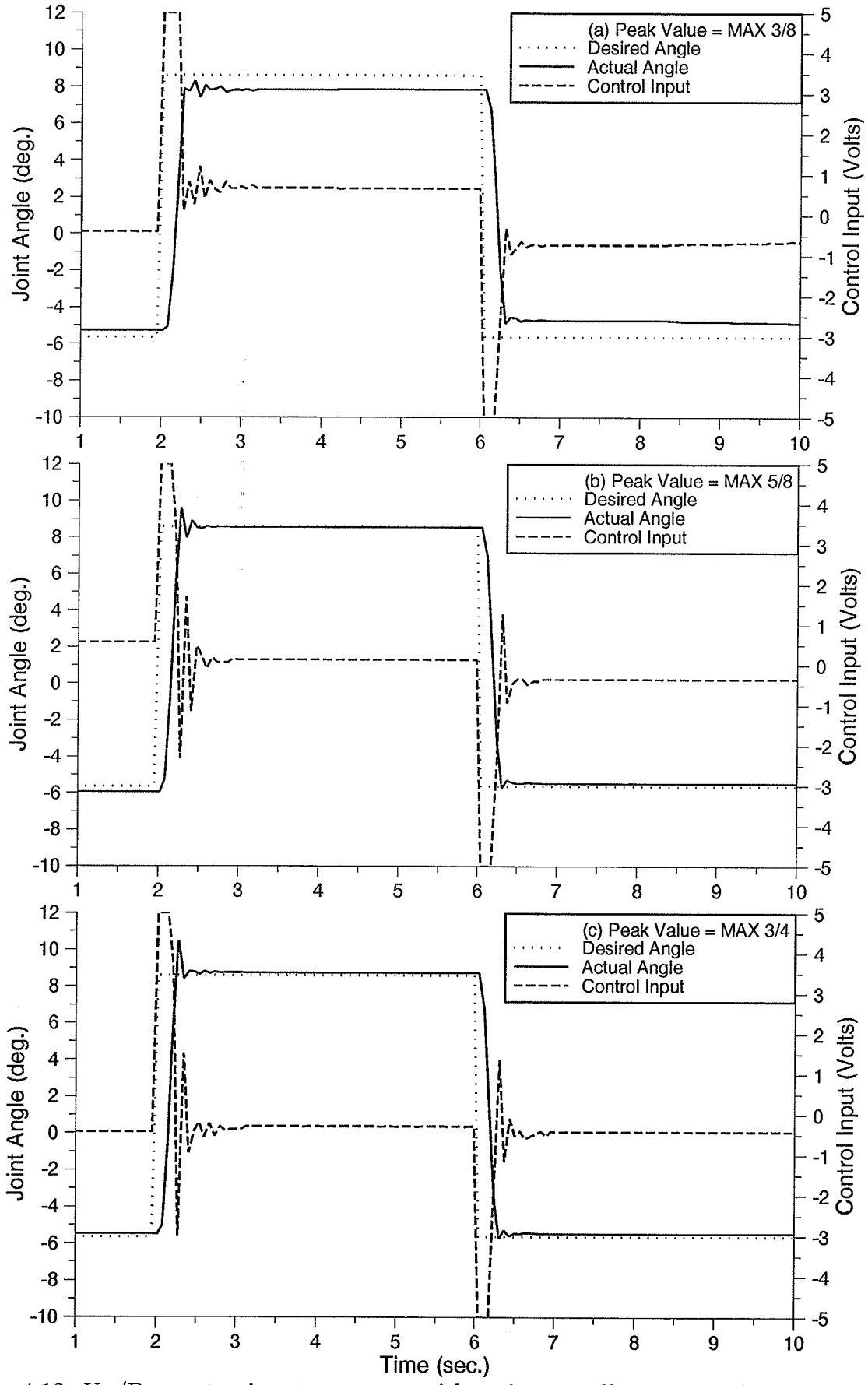

Figure 4.12: Up/Down step input responses with various small output peak values

case when the small voltage peak value was decreased [Figure 4.12(a)]. Control values close to zero error were lower in magnitude as compared to Figure 4.5(a), and the link did not reach the desired position. Width was then decreased by 50% and 75%; the responses are seen in Figures 4.13(b) and (c), respectively. For this decrease, the control output close to the zero position error was larger because zero voltage output was less dominate in the 'COA' calculation.

The reduction in the zero output width had relatively the same effect as increased peak value of the small output, for reasons of dominance. The difference between these two changes was in the oscillations about the desired position with a decreased zero output width. Here control values have been increased at the center of the control table not the surrounding area. These higher control actions greatly reduce the steady-state error to the detriment of stability. Therefore, a decrease in the zero voltage output width may induce sustained oscillations about the set points.

4.2.7 Response to Conventional Rules

The conventional rule table sets the control output to zero for a small positive (negative) position error with large positive (negative) velocity error. Referring to Figure 4.14, the application of the conventional rules did in fact send a zero voltage before the desired angle was reached. This is clearly seen in the return motion of the Up/Down link of Figure 4.14. The zero voltage as well as the deadband made it impossible for the link to reach the desired position. The gains here were not the optimum for the conventional rule table but simply the optimum found for the hydraulic rule table shown in Figure 4.5(a). Experiments with the optimum set of conventional rule gains can only be found in the simulation results of Section 3.3, Figure 3.9. Referring to Figure 3.9 it was found that the conventional rule table required 50% higher gains to achieve a step response similar to the hydraulic rule

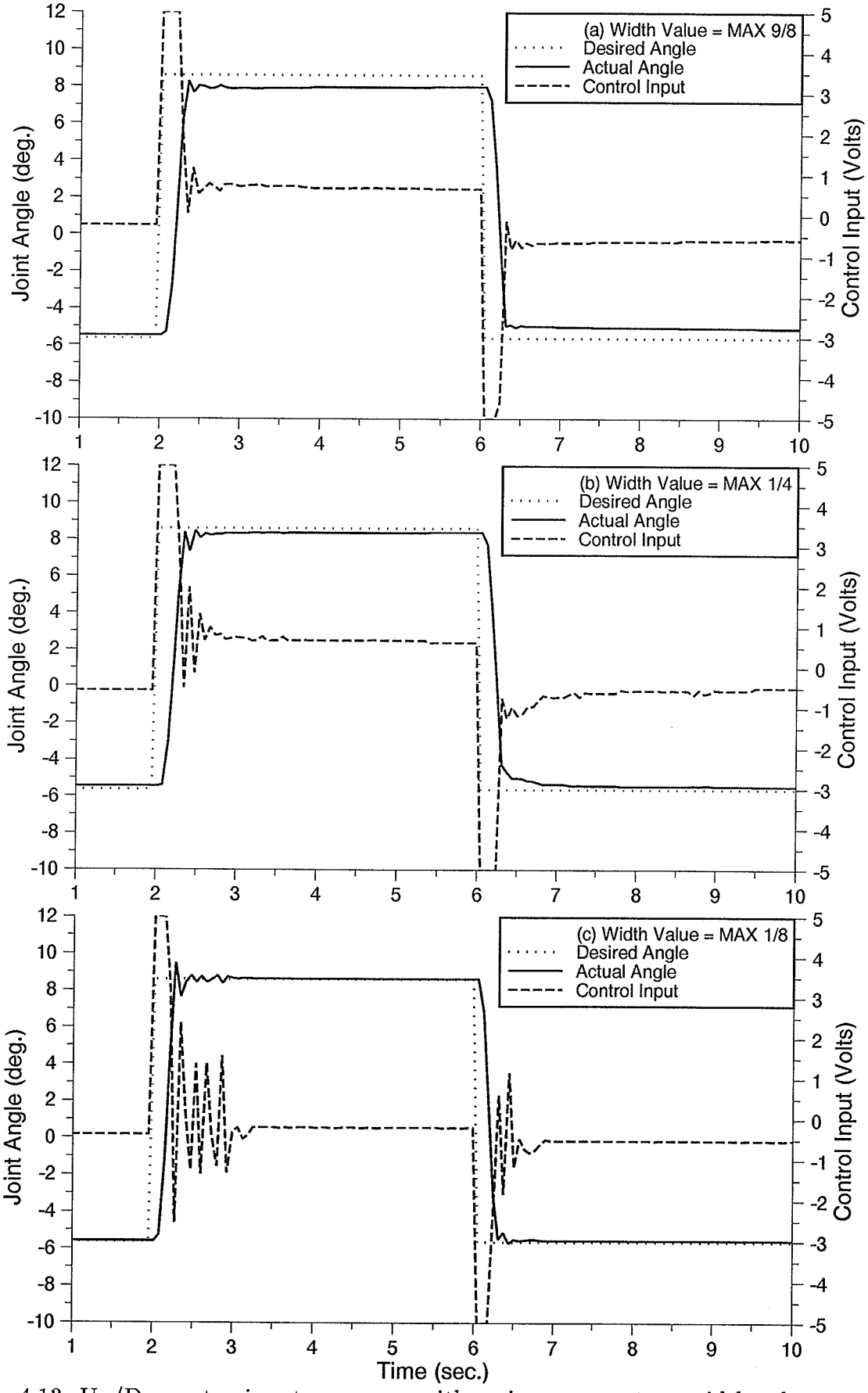

Figure 4.13: Up/Down step input responses with various zero output width values

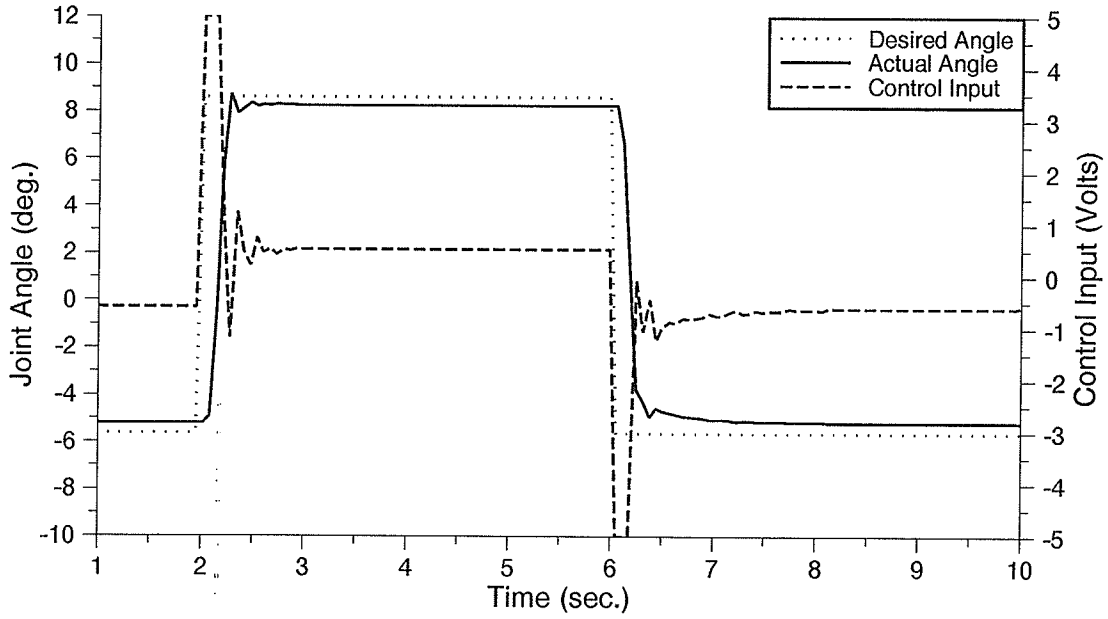

Figure 4.14: Up/Down step input responses with conventional rules and optimum gains used for hydraulic rules

table. Higher gains, however, may adversely affect the stability. The conventional rule table compensated for velocity to a degree which was not necessary in hydraulic robot control.

4.2.8 Effect of Controller Gains on Trajectory Tracking

It is known that the area of the rule table close to the zero velocity and position errors required tuning for stability (zero output width values) and the areas surrounding it required tuning for responsiveness (small output peak values). Tuning controller gains P_e and V_e, on the other hand, altered the universe of discourse of an input, therefore the entire controller behaved differently.

For trajectory tracking response, as opposed to step input response, position and velocity errors remained within a small to zero range. Therefore, the inputs to the controller remained small, and rule firing remained close to the center of the rule

table. For this case the controller inputs are relatively constant and any change in fuzzy logic parameters was relatively the same as increasing P_e and V_e. Therefore fuzzy logic parameters were not examined here.

Effect of P_e Gain

A trajectory input response with best performing gains is seen in Figure 4.15(a). The trajectory corresponds to a 3-link trajectory tracking to be discussed in Section 6.2.4. The effect of increasing and deceasing P_e on the response is seen in Figures 4.15(b) and 4.15(c). Increasing the P_e gain by 100%, reduced the steady-state error but did not eliminate it. Also, the controller became sensitive to the position error and oscillations in control were observed. For a 75% decrease in P_e gain, the size of the steady-state error was increased and the controller had trouble following the desired trajectory.

Effect of V_e Gain

Increasing the V_e gain 20 times decreased the velocity error in the system. This can be seen in Figure 4.16(a). A high value for V_e gain, however, puts the P_e and V_e gains in conflict with each other. The Controller alternately increased the speed of the link, due to the V_e gain, and when zero position error was reached, a much smaller control signal was sent.

The result of setting V_e to zero is seen in Figure 4.16(b). The results show that the P_e gain alone performed well enough to result in an actual velocity profile which was close to the desired angle; however a delay in motion was noticeable at $t \approx 21sec$, when the link starts from rest.

The velocity profiles for the trajectory in Figures 4.15(a) and 4.16 are shown in Figure 4.17(a). There was a shift, or delay, in the actual velocity as compared to the

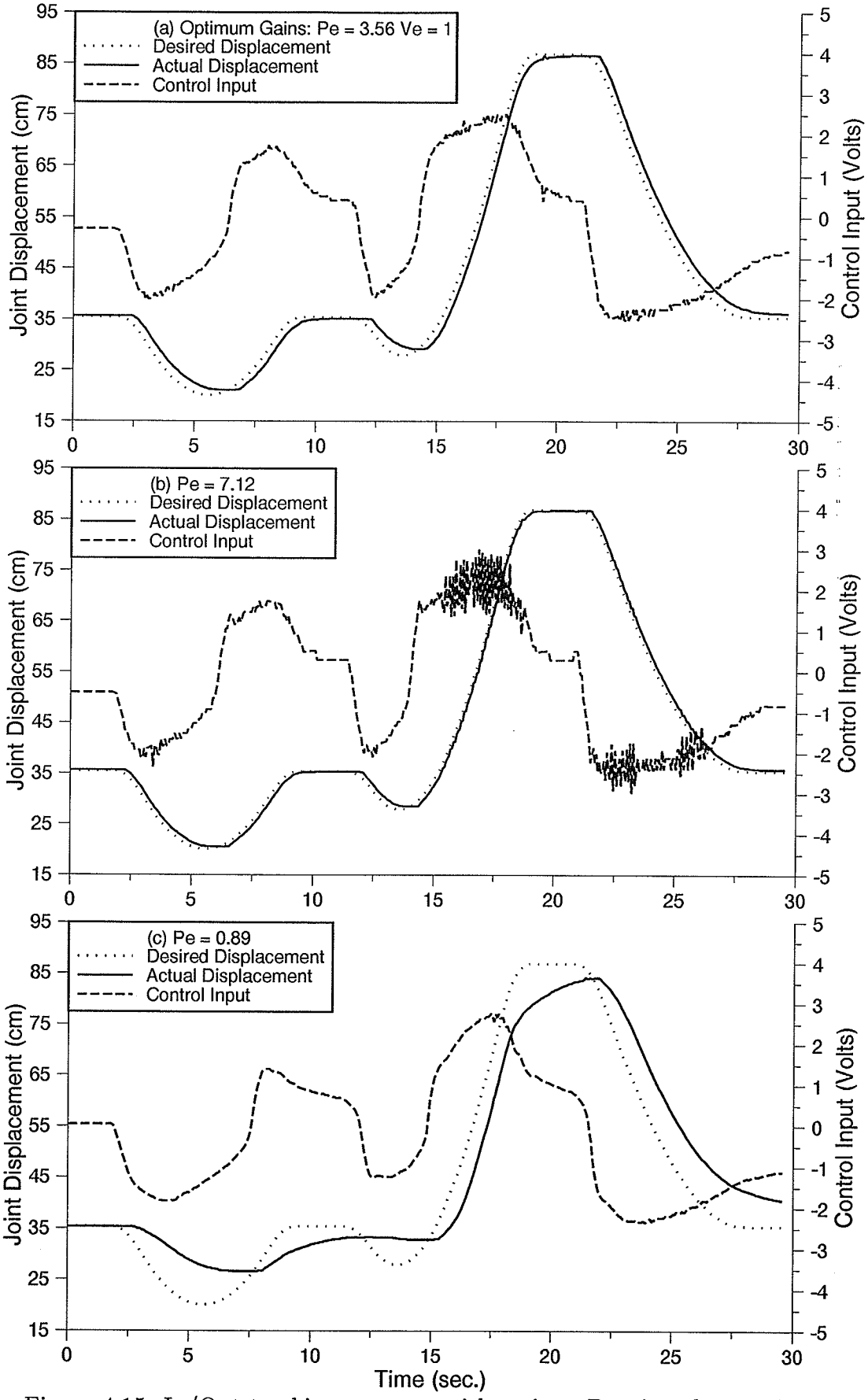

Figure 4.15: In/Out tracking response with various P_e gain values

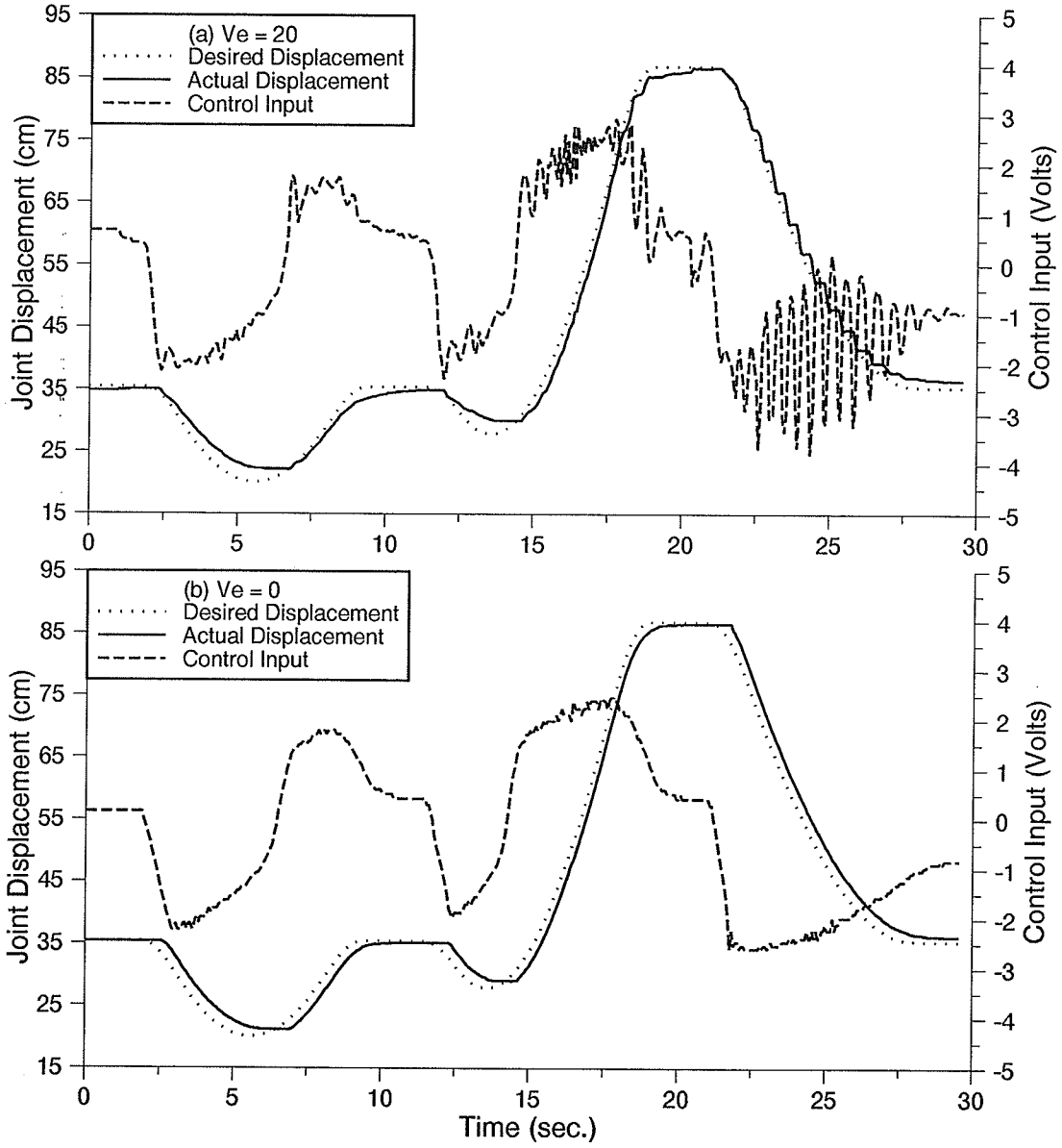

Figure 4.16: In/Out tracking response with various V_e gain values

desired velocity just as the actual position was shifted from the desired position. The zoomed in view of the first 10 seconds [see Figure 4.17(b)] indicated that increasing the V_e gain brings the actual velocity closer to the desired velocity at the velocity transition; but as position and velocity errors were eliminated, the valve displacement was decreased and the link slowed down. The optimum V_e gain smoothed the response and did not over compensate for velocity error.

4.2.9 Speed Control

Figure 4.18(a) shows the PD-type fuzzy controller applied to the trajectory used in Figures 4.15 to 4.17 at 1/5 the speed. The magnitude of the control values were smaller in Figure 4.18(a) than in Figure 4.15(a). The slower speed was still stable and there was a decrease in the steady-state position error. A slower desired velocity in a ramp input resulted in a smaller valve displacement. This small valve displacement was directly proportional to a small steady-state error. The velocity profile for this trajectory is seen in Figure 4.18(b). The desired velocity seems to be followed closely. The coulomb friction of the link evidently delayed the motion at the start.

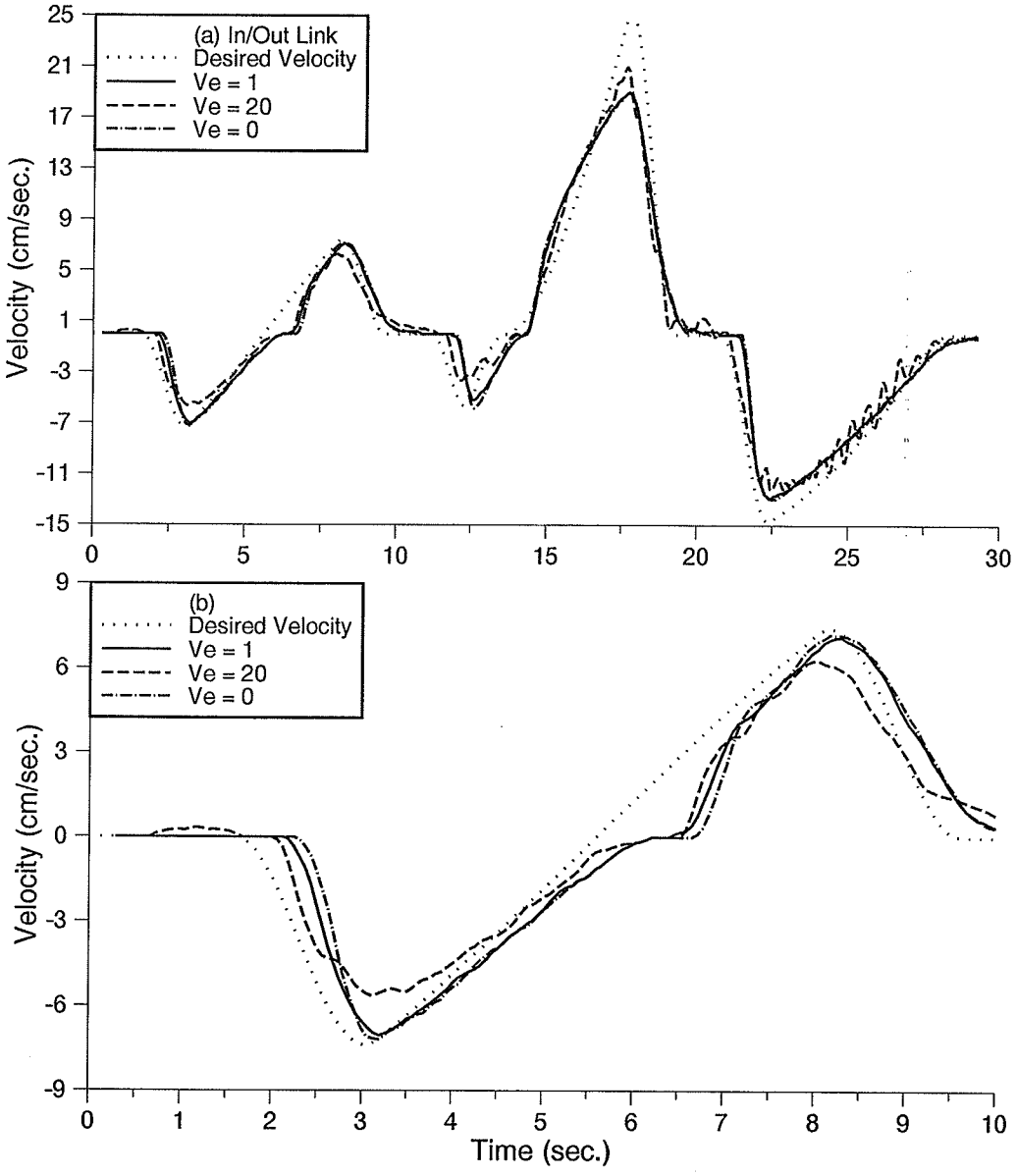

Figure 4.17: Velocity profiles pertaining to Figures 4.15(a) & 4.16: (a) full trajectory; (b) enlarged view

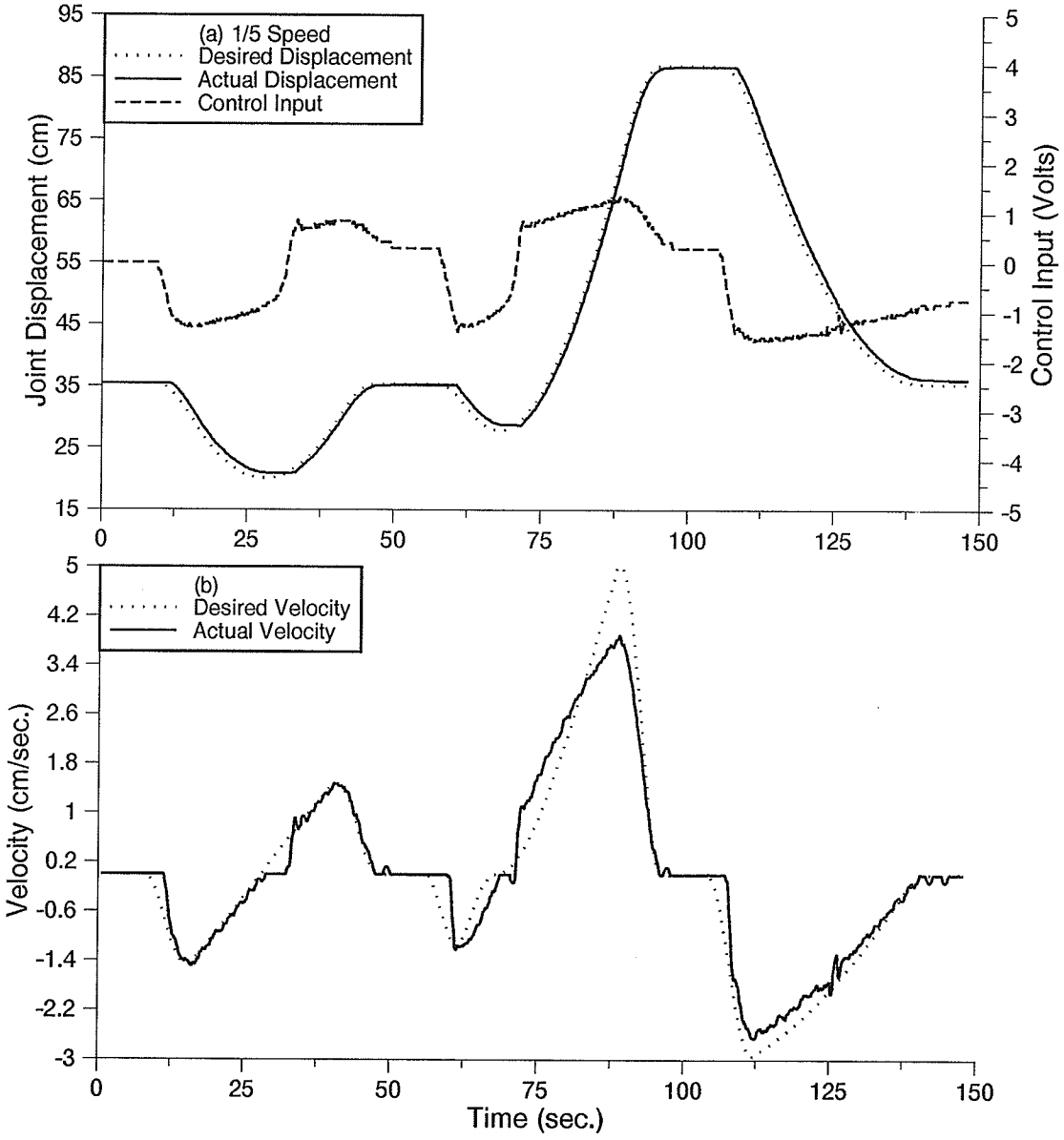

Figure 4.18: In/Out trajectory response at reduced speed: (a) position and control; (b) velocity profile

Chapter 5

Steady-State Error Elimination

5.1 Sources of Steady-State Error

Figure 5.1 shows the results of applying the PD-type fuzzy controller to link 2 (link with Up/Down motion) of the hydraulic robot shown in Figure 4.1. Both step and ramp input responses are shown. The response to the step input [see Figure 5.1(a)], for well tuned gains, was fast with acceptable overshoot and no oscillation at the set point. The steady-state error is due to the deadband in the servovalve which produced a non-zero control action. By changing the gains one can reduce the steady-state error but this may adversely affect the stability; for example, increasing the position error gain caused oscillations in control action [see Figure 4.15(b)]. It is also seen that the position error was different in size from one step to another. Dry friction, in the form of stick-slip, in the hydraulic servovalve as well as asymmetry in the deadband are believed to contribute to this phenomenon.

Figure 5.1(b) shows the response to a ramp input. The same control gains as in the step input were used in this experiment. The trajectory profile, which covered almost the entire extension of the link, included a gradual change in the required

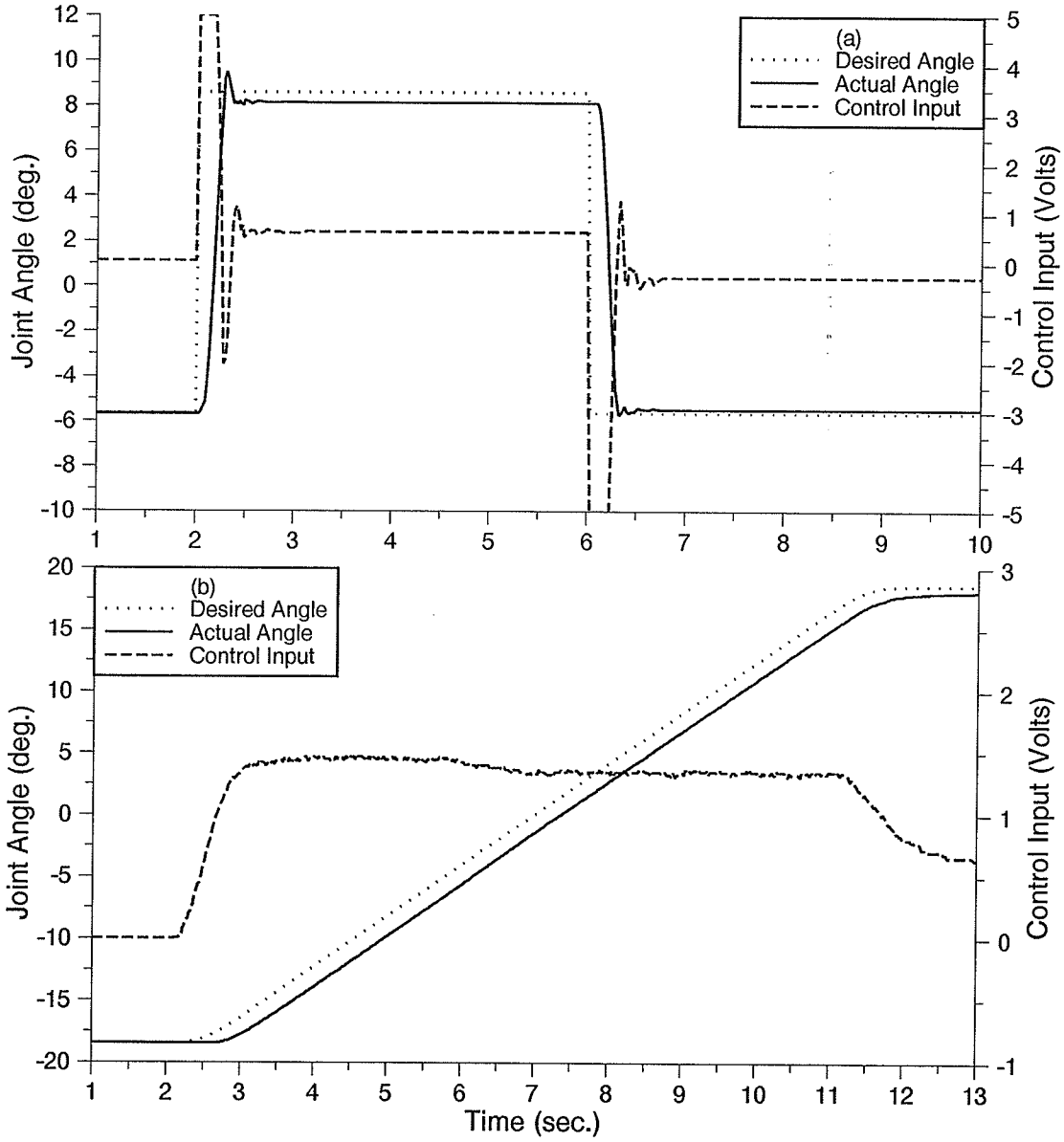

Figure 5.1: Up/Down response with PD-type fuzzy control: (a) step input; (b) ramp input

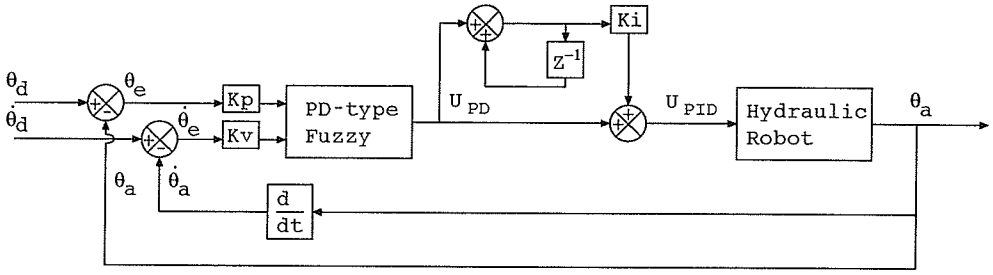

Figure 5.2: PID-type fuzzy control block diagram

velocity at the start and at the end. A constant position error is seen when following a ramp input. This is expected since, in order to follow a ramp input, the valve must remain open; thus, some error must be present in the ramp. A zero position and velocity error would result in a zero valve displacement and the motion would stop.

5.2 Steady-State Error Elimination

5.2.1 Step Input Trials

The focus in this chapter is placed on developing algorithms that can work *in parallel* with the PD-type fuzzy controller. With this goal, the PID-type controller shown in Figure 5.2 was first constructed. Referring to Figure 5.2, the output from the PD-type fuzzy controller was accumulated to produce a PI-type fuzzy control action which was scaled and added to the PD-type fuzzy controller. The result of applying the method to a step input similar to that of Figure 5.1(a), is shown in Figure 5.3(a). The result shows [see Figure 5.3(a)] an overshoot and a fairly long period of recovery. The steady-state error was however eliminated. Increasing the scale factor K_i resulted in a larger overshoot, although, the desired angle was achieved faster. The total control action is the summation of both contribution lines in Figure 5.3(b). The role of the PI control action at the beginning of the motion seems to be meaningless since, the

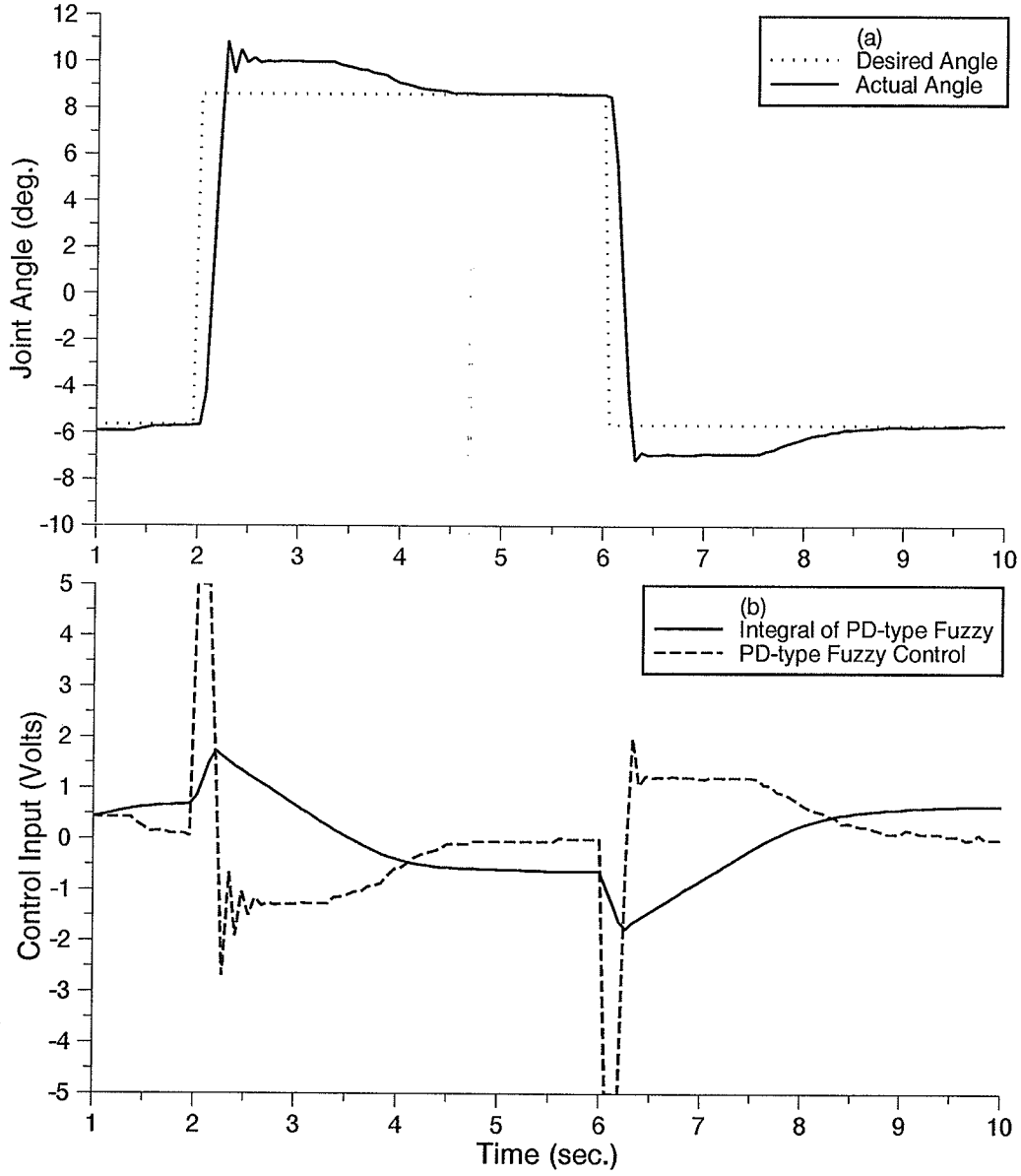

Figure 5.3: (a) Up/Down step input response with PID-type fuzzy control; (b) control inputs

maximum control action was already provided by the fuzzy PD control part. The slow recovery from the overshoot as partly due to winding down the unnecessary control action accumulated at the beginning of the motion. This recovery period can be reduced by introducing the anti-windup strategy described by Astrom and Hugglund [29]. The method, however, is effective only during the controller output saturation. It also requires the introduction of an additional gain called 'tracking time constant' which was reported to be sensitive to systems with derivative actions [29]. Based on these observations, two strategies are introduced which produce satisfactory results.

Reset error integral control action. Referring to Figure 5.4, the steady-state error is eliminated by adding a control based on the summation of error. The integral controller was activated depending on the status of the response; it resets itself otherwise. The rules that decide when to activate the integral controller are listed below:

Rule 1. If the velocity error is within fuzzy zero then start or continue integrating the error. The integral control contribution varies with degree of membership in zero velocity error μ;

$$U_{(I)} = \sum_{t=0}^{t} (\mu K_i)(\theta_d - \theta_a)$$

μ scales the integral action and governs the rate of increase of the integral of error.

Rule 2. When the velocity error is not within a 'fuzzy zero' region, reset and disable the integrator.

A zero velocity error is the indication of a system which has come to a steady-state and the controller (in this case the PD-type fuzzy controller) has done all it could to reduce the error in the system. In such a case, the integral control becomes active; degree of which depends on the degree of membership (μ) of the velocity error in the region of fuzzy zero.

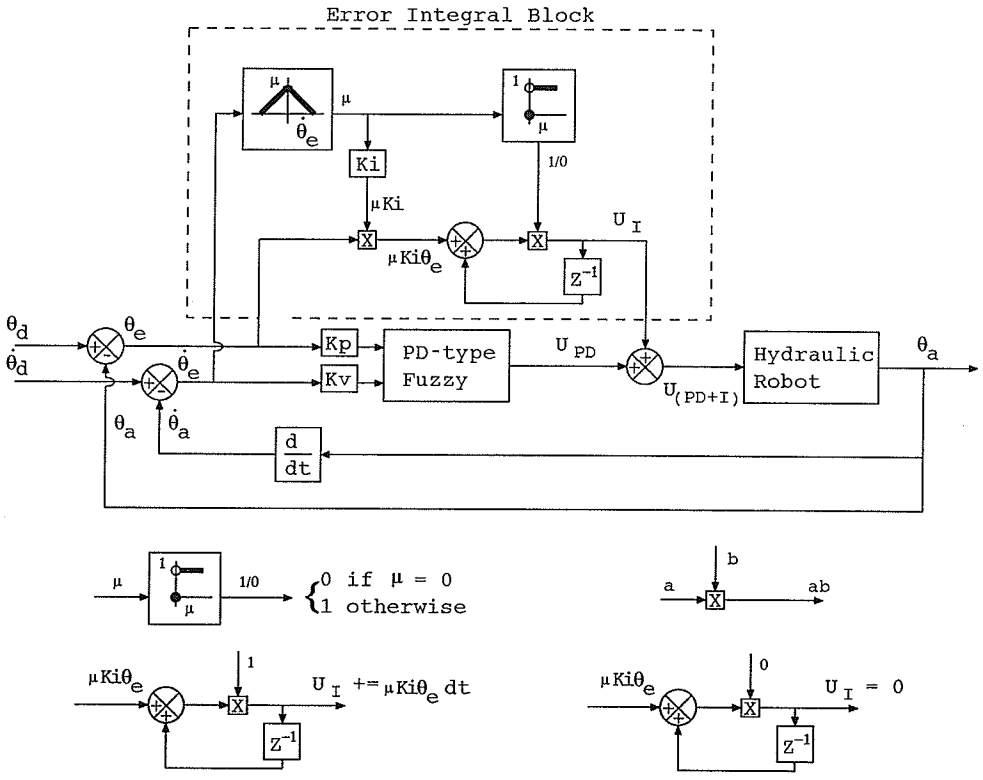

Figure 5.4: PD-type fuzzy plus reset error integral control block diagram

The result of application of the scheme to a step input is seen in Figure 5.5(a). The response was better than the one with PID-type fuzzy controller (Figure 5.3a). At the beginning of motion, the desired velocity matched (in a step input it is set to zero) the actual velocity of zero which resulted in a zero velocity error. The integral was therefore activated at the beginning of the step input but was soon deactivated (see Figure 5.5b). The integral control action became active once again when the output was close to the desired set point. The slow accumulation of error resulted in an added control which eliminated most of the steady-state error. The PD-type fuzzy control contribution eventually went to zero, and the control action from the integral block was just enough to keep the valve at its deadband limit.

Reset offset integral control action. The reset error integral controller has a characteristic that any desired action is not instantaneous. A certain time is required until the controller reaches the appropriate level. The reset offset integral control action is designed based on the fact that at the fuzzy zero velocity error region, the PD-type fuzzy control output is essentially a measure of the steady-state error (see the rule table in Figure 3.1). This measure can therefore be utilized as an added control, namely offset integral. Figure 5.6 shows the block diagram. The offset integral is updated by increasing/decreasing its value by an amount equal to the current fuzzy PD control action and remains active as long as the velocity error is within the range of fuzzy zero. This fuzzy zero region is similar to the zero velocity error in Figure 3.1 but 1/10 of the size. When the velocity and position errors reduce to zero, the PD-type fuzzy control output goes to zero and the offset integral value remains constant. When the velocity error exceeds the fuzzy zero neighborhood, the offset integral is set to zero and remains inactive.

The application of this strategy to a step input produced a result shown in Figure 5.7(a) which was slightly better than the one belonging to the reset error integral method [see Figure 5.5(a)]. The offset integral contribution to the control is seen in

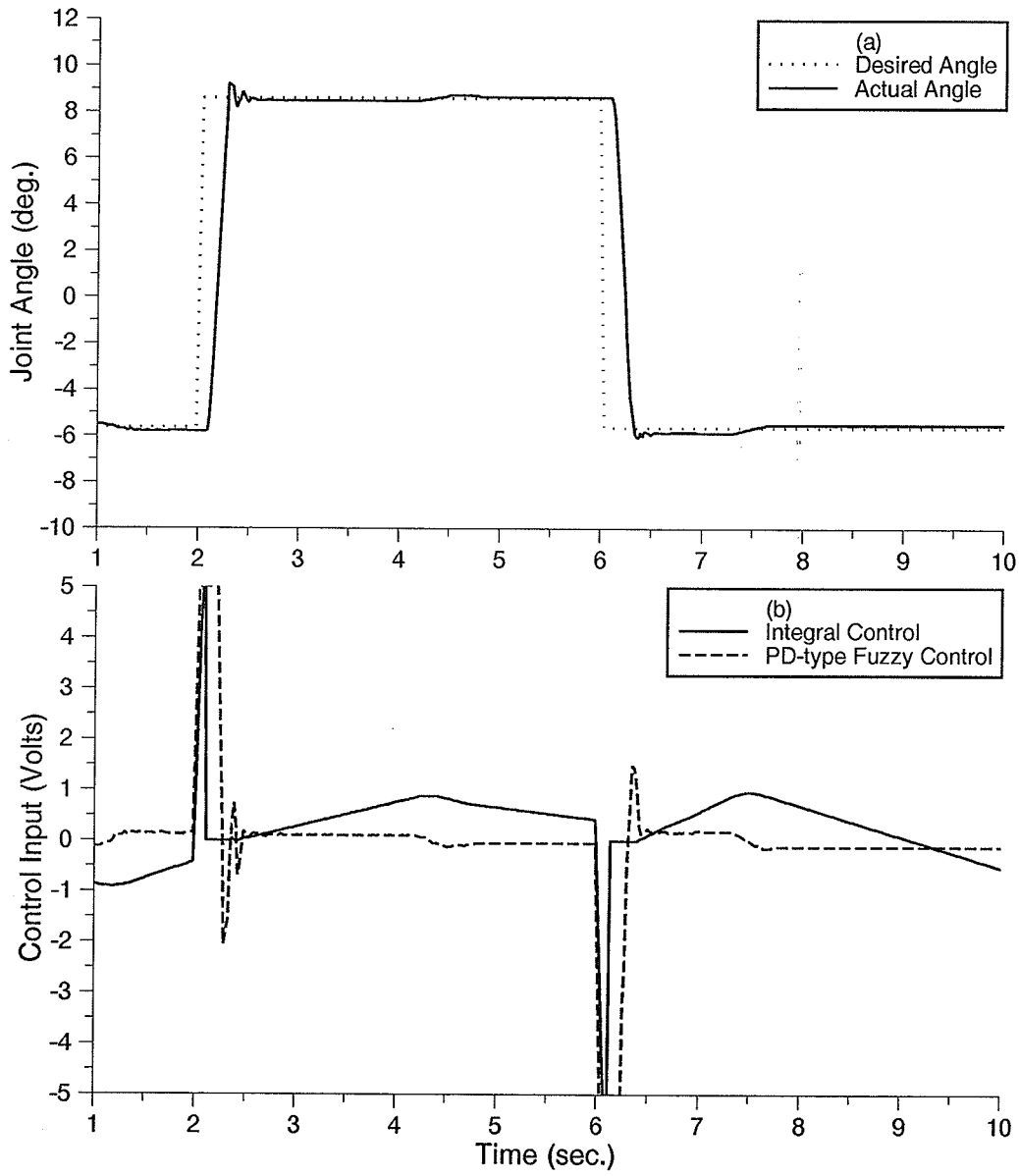

Figure 5.5: Up/Down step input response with reset error integral control; (b) control inputs

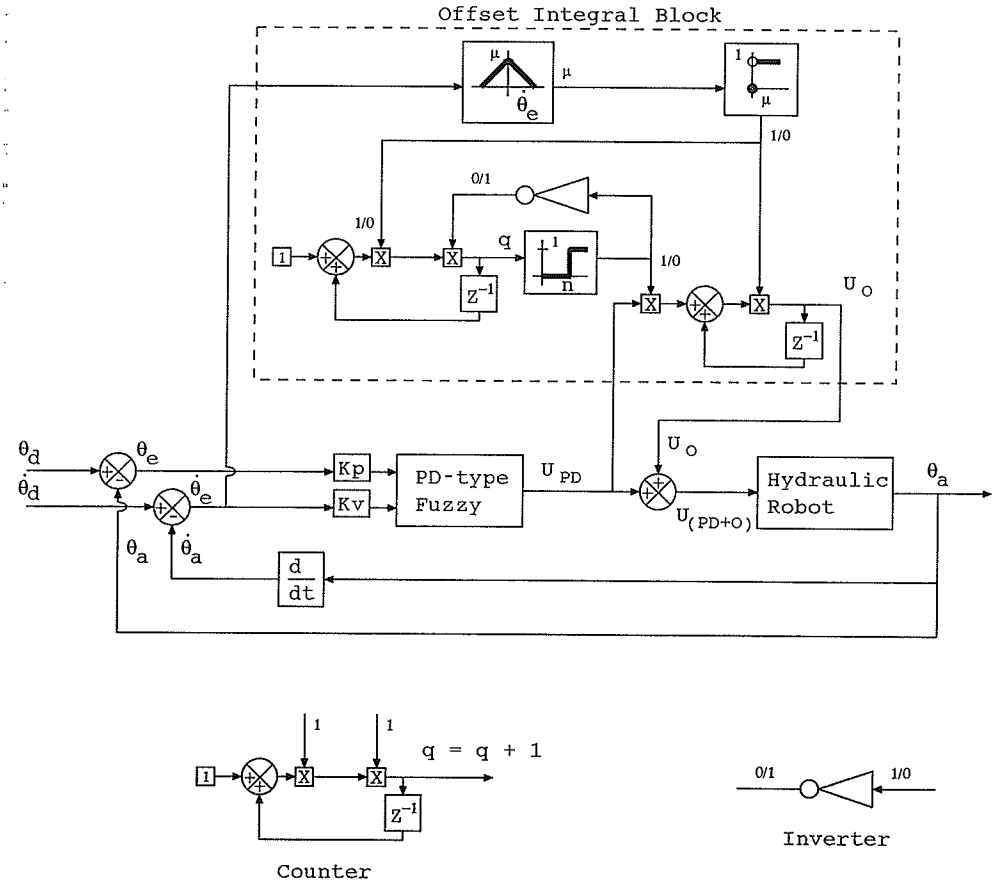

Figure 5.6: PD-type fuzzy plus reset offset integral control block diagram

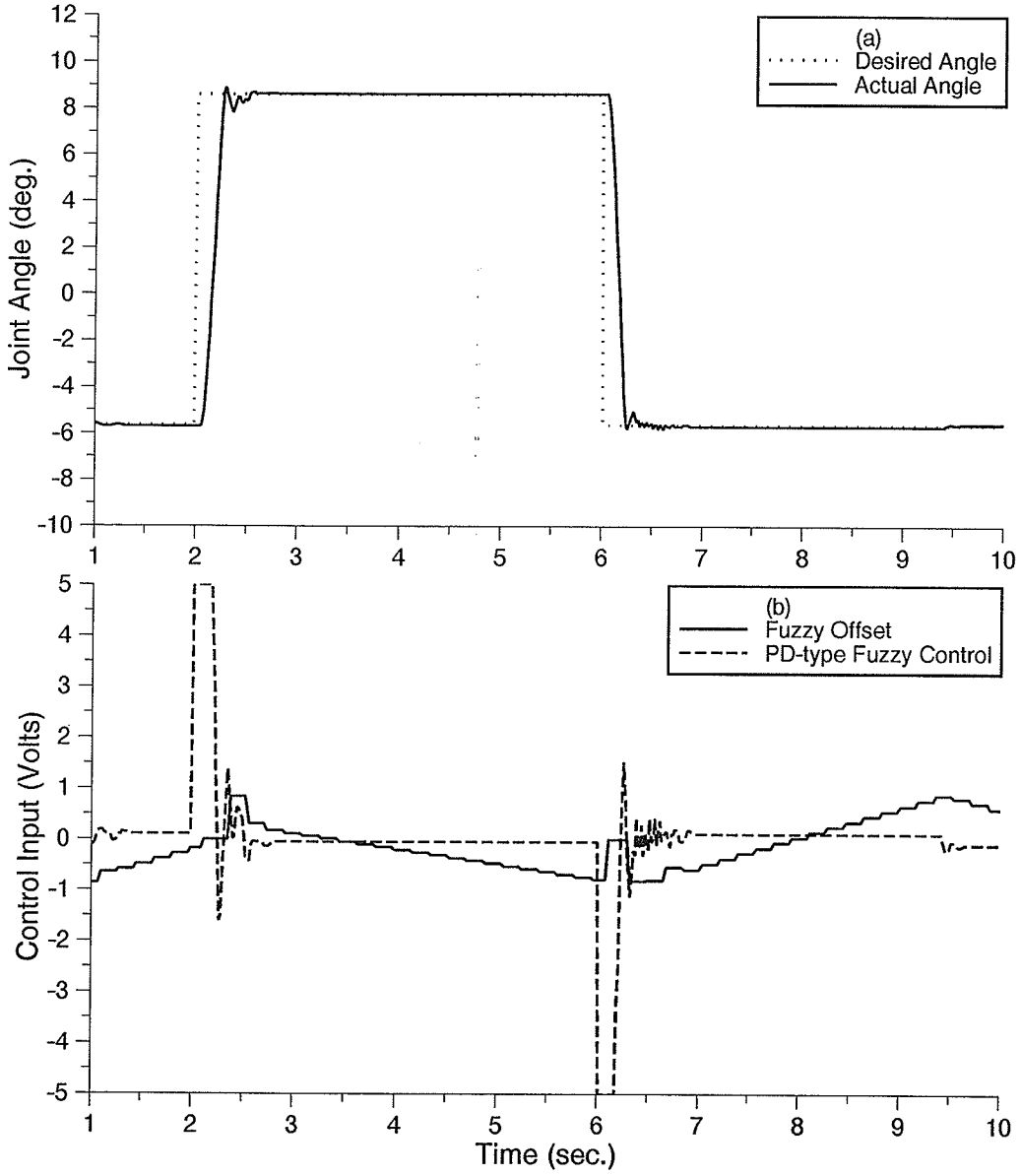

Figure 5.7: (a) Up/Down step input response with reset offset integral control; (b) control inputs

Figure 5.7(b). As soon as the velocity error fell within fuzzy zero region, a value equal to the current fuzzy PD control action was assigned to the offset integral. As a result, the time between the method activation until a rough measure of the steady-state error control was achieved, became shorter with this method. The rate at which the offset integral was updated was approximately $5HZ$. A faster rate did not allow enough time to observe the full effect of the offset integral and the system became unstable. A slower rate resulted in a slow elimination of steady-state error.

5.2.2 Ramp Input and Trajectory Tracking Trials

The response to the ramp input, using the PD-type fuzzy plus reset error integral controller, is shown in Figure 5.8(a). The ramp input was followed almost exactly; the slight errors at the beginning and at the end of the ramp were quickly recovered. The integral contribution to the control was smooth and stable for the duration of the ramp. Similar performance was observed when the PD-type fuzzy plus reset offset integral controller was applied to the same ramp input [see Figure 5.8(b)]. The same gains used for the step input responses were applied for this case. The performance of both methods were found to be satisfactory.

The trajectory tracking experiment involved two links; link 2 with a rotating joint and link 3 with a prismatic joint. The simultaneous motion of these two links allowed the endpoint to follow a Cartesian vertical straight line. The speed used in the tracking experiments was $\approx 30cm/s$ in the vertical direction. The PD-type fuzzy plus reset integral controller was applied first. The resulting vertical Cartesian position is shown in Figure 5.9(a). The vertical path is followed very closely with small deviations from the desired trajectory. The maximum deviation from the required constant horizontal distance was $2.5cm$. The error peaks seen in the horizontal direction, were the result of high dry friction at the prismatic joint of link 2. With reference to

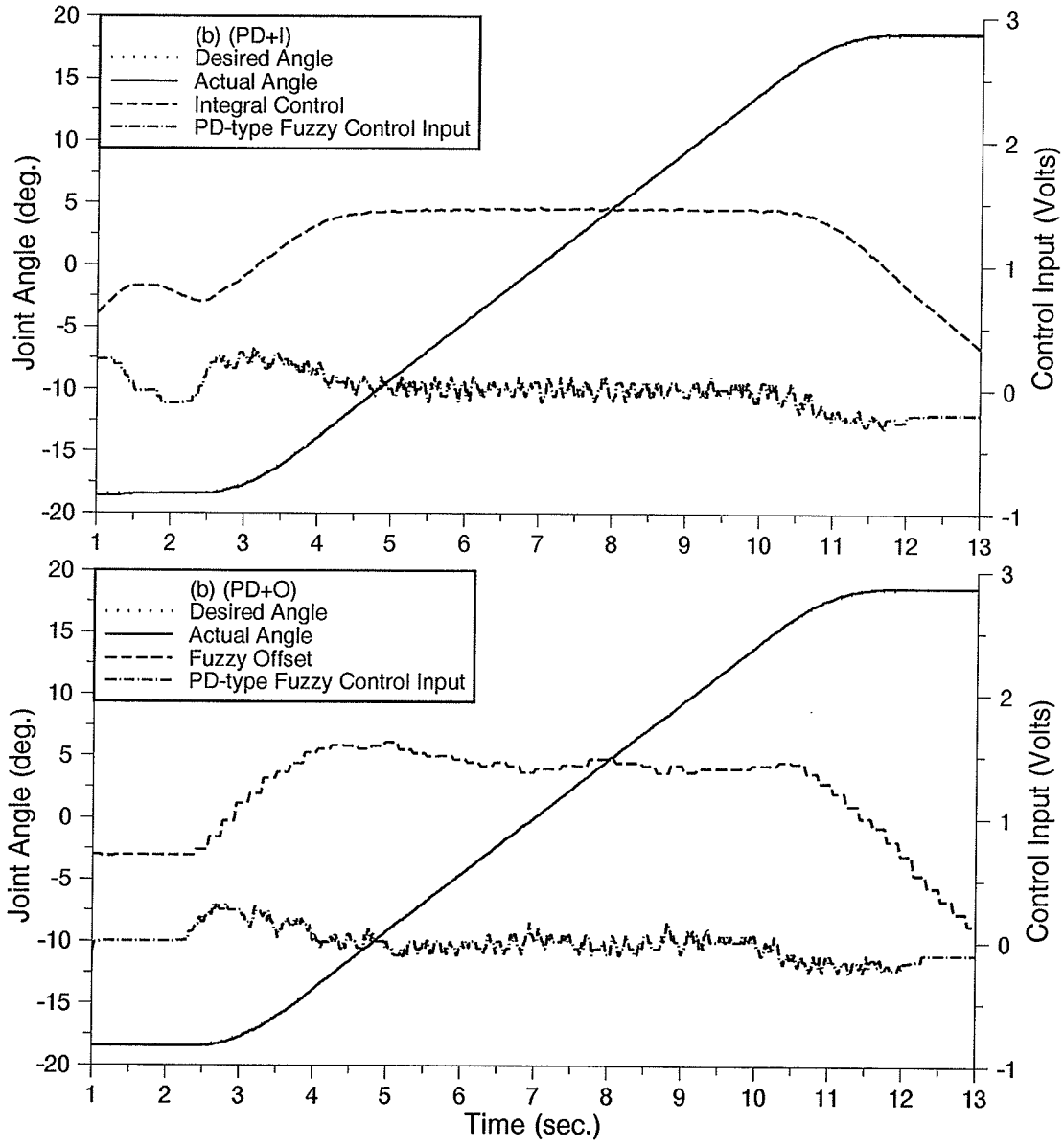

Figure 5.8: Ramp input response of Up/Down link: (a) with PD-type fuzzy plus reset error integral; (b) with PD-type fuzzy plus reset offset integral

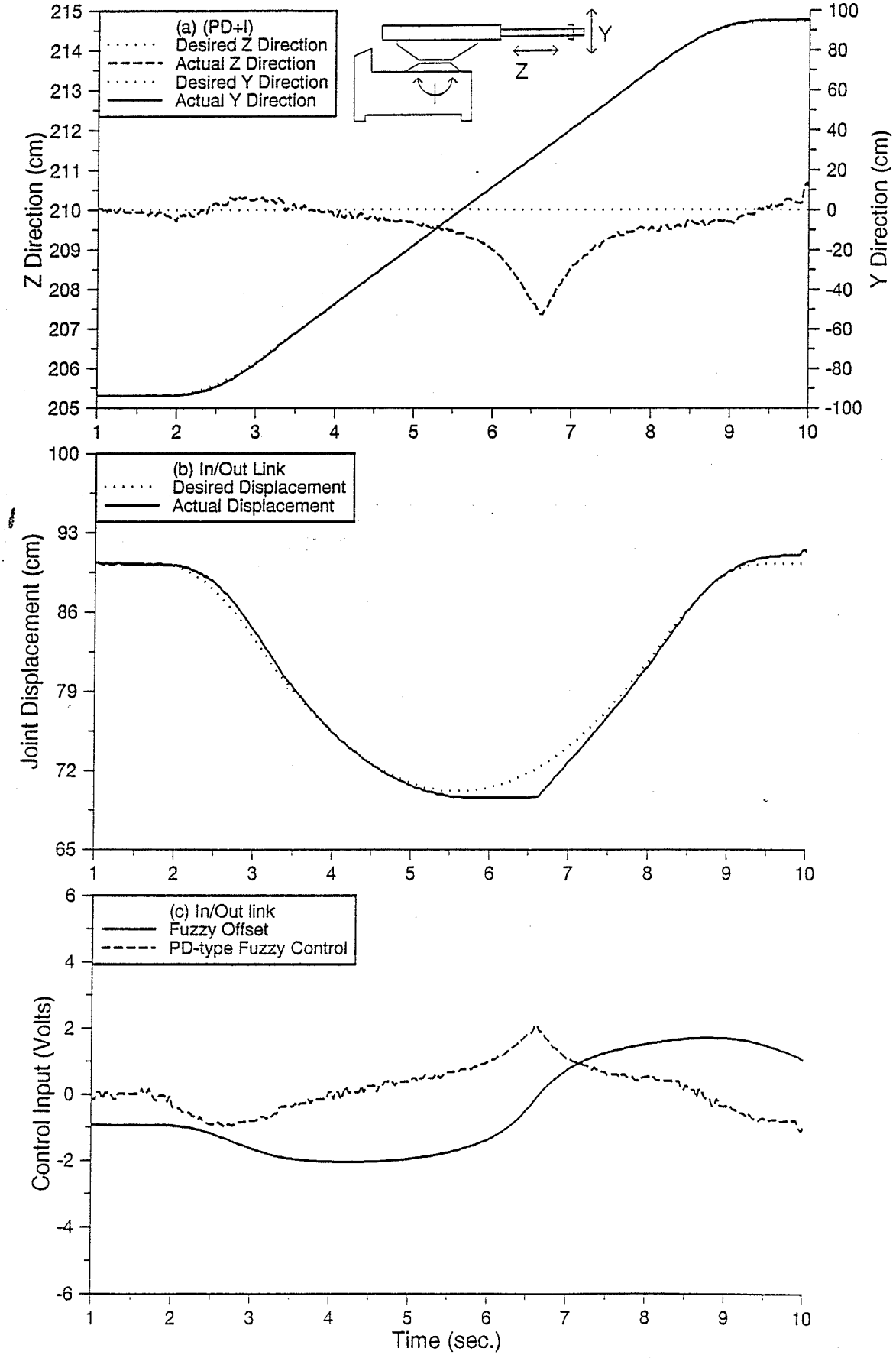

Figure 5.9: Trajectory response with reset error integral control

Figure 5.9(b), these error peaks coincide with the maximum deviation of link 2 from its desired displacement. The maximum errors occurred when link 2 started to move or changed its direction of movement. In addition to dry friction, the internal integral action of the reset integral block contributed to the peak observed at time $t \approx 6.6s$. Referring to Figure 5.9(c), the integral required time to wind-up to a positive value.

The effect of loading for the above trajectory was also studied, and the results were compared with the ones without load. Figure 5.10(a) compares the resulting horizontal displacements, and Figure 5.10(b) compares the resulting vertical velocities. The weight of the load was approximately $25kg$. As is seen, the performance of the controller did not deteriorate significantly. The only difference observed was the increased error peak in the horizontal displacement at the beginning of motion where link 2 was fully extended. The increased weight resulted in an increased dry friction at the prismatic joint.

The PD-type fuzzy plus reset offset integral controller was then applied to the same trajectory. The maximum error of the horizontal position was about $1.5cm$ which is seen in Figure 5.11(a). The In/Out response of link 2 [see Figure 5.11(b)] was mainly responsible for the horizontal deviation. The control inputs applied to this link are shown in Figure 5.11(c). Compared with the reset error integral action, shown in Figure 5.9(c), the offset integral changed at a faster rate than the integral. Loading did not affect the horizontal or vertical errors of the trajectory noticeably (see Figure 5.12).

The PD-type fuzzy plus reset offset integral was found to be slightly faster, in terms of computation time, and required less attention in the tuning of the updating rate gain. The magnitude of each increase in the reset offset integral method was governed by the PD-type fuzzy controller; therefore, it was able to adjust its measure of the steady-state error quicker than the reset error integral.

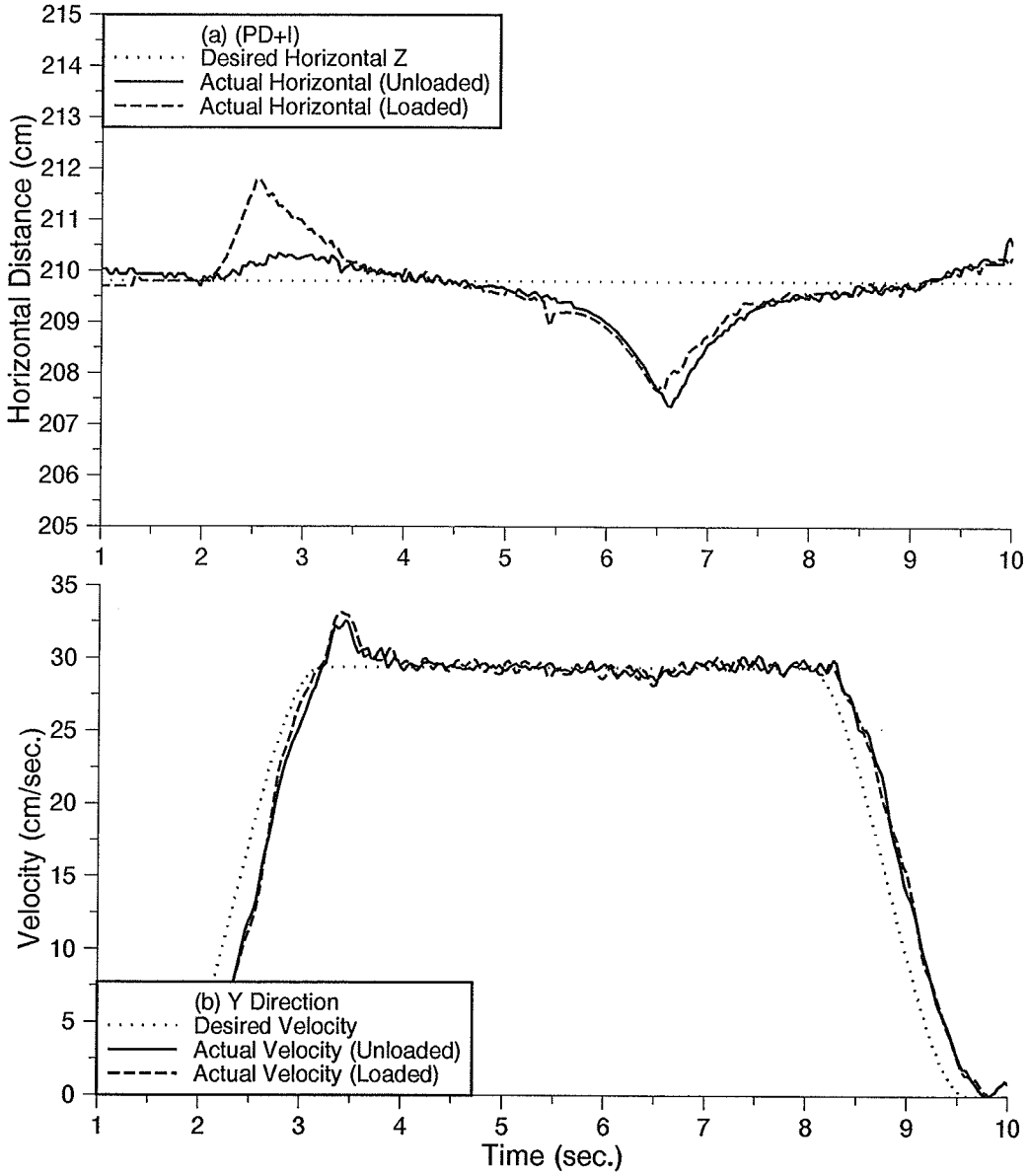

Figure 5.10: Trajectory response loaded/unloaded: (a) horizontal deviation; (b) vertical velocity profiles

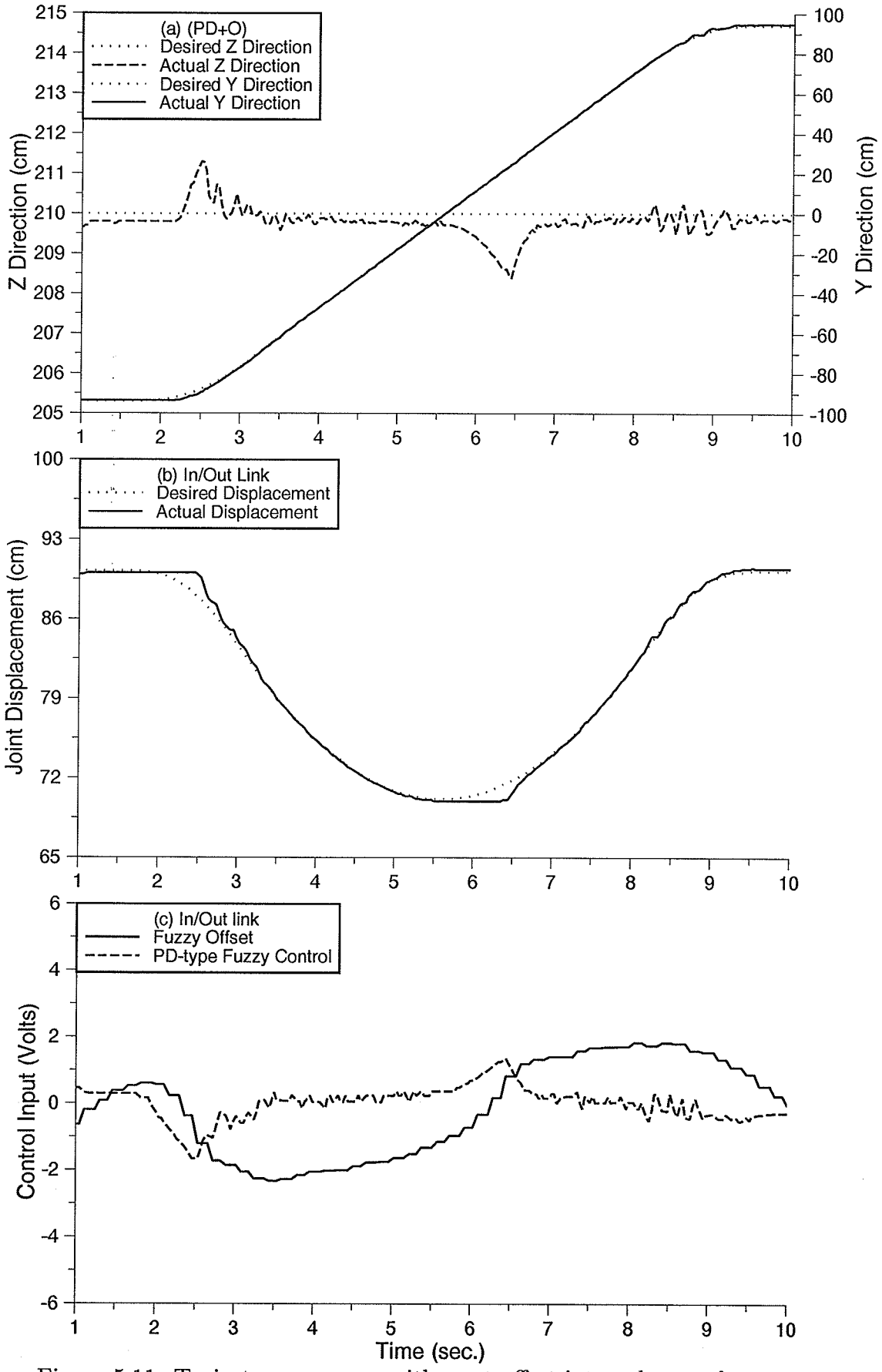

Figure 5.11: Trajectory response with reset offset integral control

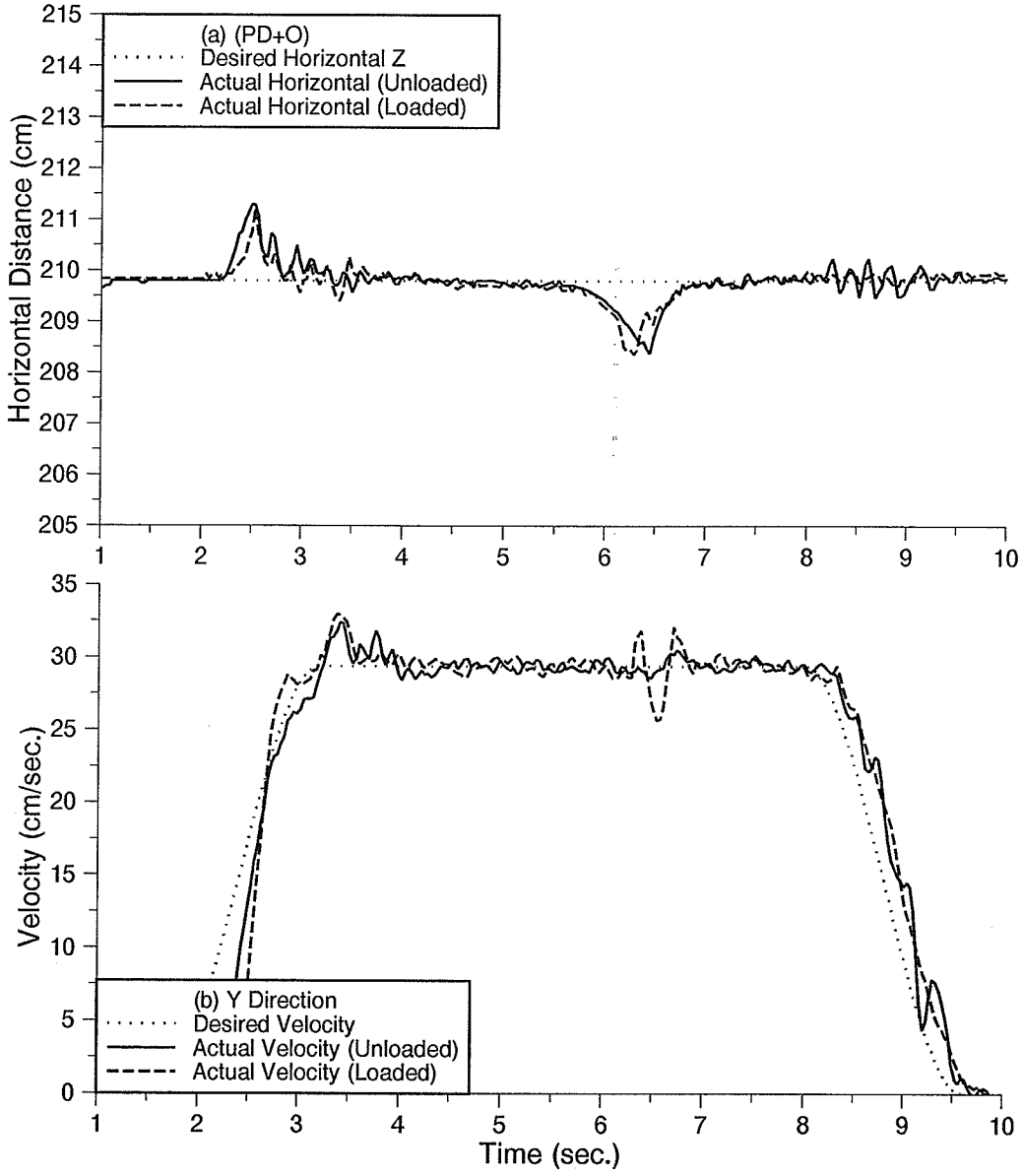

Figure 5.12: Trajectory response - loaded/unloaded: (a) horizontal deviation; (b) vertical velocity profiles

Chapter 6

Experimental Studies with Reset Offset Integral

This chapter examines how the changes in P_e and V_e gains affect the response of the PD-type fuzzy plus reset offset integral controller, and therefore give an idea of how to go about tuning for a particular response. The main focus of this chapter is the examination of reset offset integral for trajectory tracking. This section also examines the effect of updating rate on the reset offset integral. The fuzzy logic parameters and rule tuning were not attempted in this section. This is because the reset offset integral is only active for fuzzy 'zero' velocity error. This state is only achieved after all the PD-type fuzzy controller fuzzy logic parameters and rules have brought the system to some degree of stability.

6.1 Tuning the Control Gains

6.1.1 Effect of P_e gain

The simple PD-type fuzzy controller is inexact by nature. It uses a steady-state error in a ramp input to maintain a constant valve displacement. This, as was observed earlier, resulted in a shifted actual position profile. With the addition of the offset integral, the exact positioning became possible.

The tracking response of the PD-type fuzzy plus reset offset integral controller is seen in Figure 6.1(a) for the In/Out link. Once the offset integral was added, the steady-state error was eliminated successfully. The PD-type fuzzy controller was tuned to have a sharp increase in control output for small position errors to compensate for the effects of deadband and stiction on the system. This was not necessarily the optimum controller design when the offset integral method was added. However, a redesign of the tuning parameters was not necessary because the response was adequate.

The effect of a 75% increase in the P_e gain is observed in Figure 6.1(b). The oscillations were due to the PD-type fuzzy controller which over compensated for small position errors. The increased oscillations at high gain were also due to the offset integral update. An increase in the P_e gain increased the size of control actions and therefore had an unstable effect on an update of the reset offset integral.

The effect of 75% decrease in P_e is seen in Figure 6.1(c), there was no serious deterioration in the rate at which the steady-state error was eliminated. Figure 6.1 can be compared with Figure 4.15 in which the same gains were used but without reset offset integral. This demonstrated that the setting of the PD-type fuzzy controller gains did not require as careful attention as the PD-type fuzzy when operating alone. When using lower position error gains, However, the offset integral took longer to

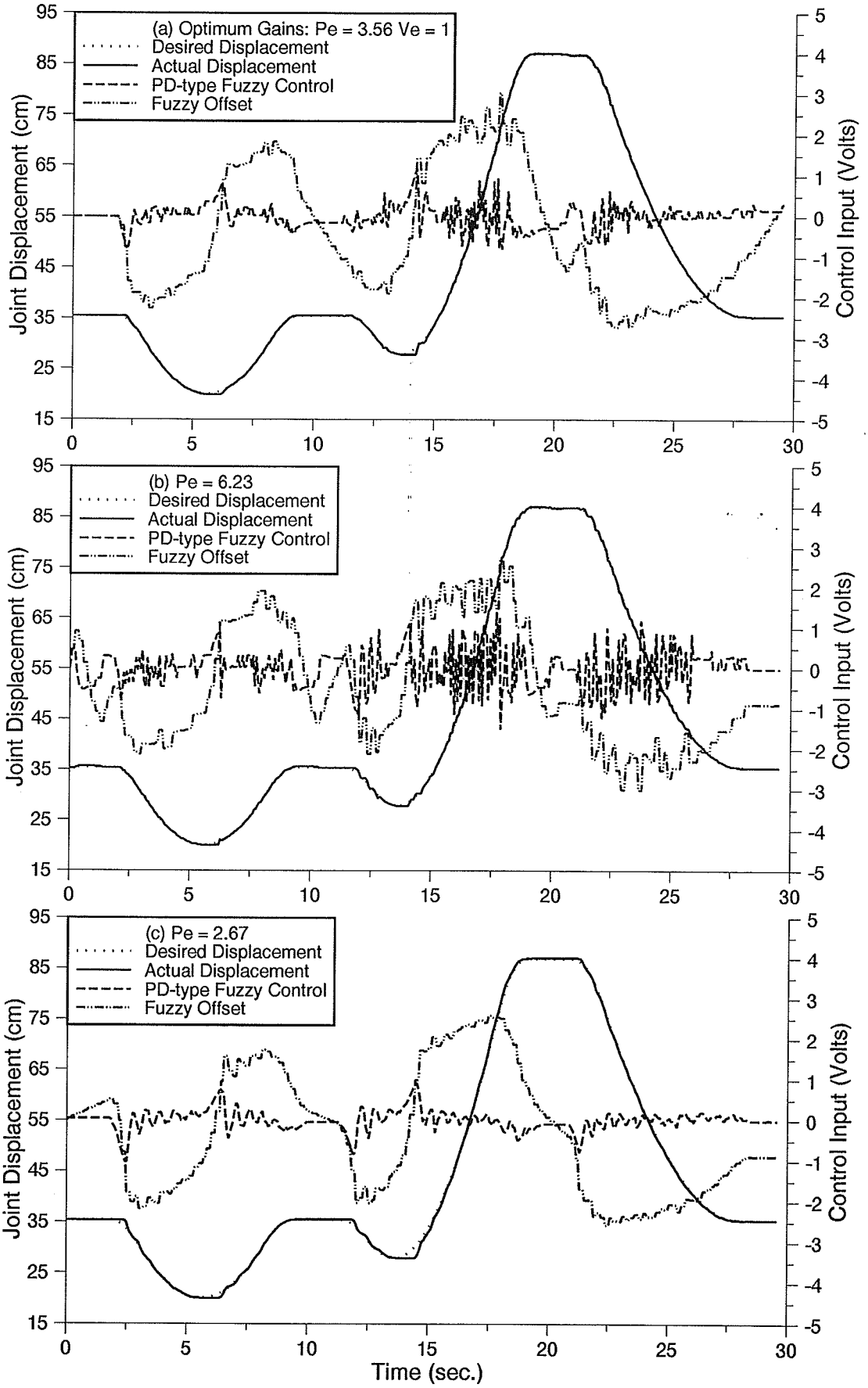

Figure 6.1: Effect of P_e gain with reset offset integral control

wind down when the velocity changed direction. This was due to a lower magnitude of PD-type fuzzy controller outputs.

6.1.2 Effect of V_e gain

Referring to Figure 6.2(a), an increase in V_e by 20 times is observed. An interesting characteristic is seen at $t \approx 18sec$. V_e gain was more dominant over the P_e gain. The actual position exceeded the desired position in an oscillatory manner. The V_e gain tried to speed up the link and the P_e gain then brought the position back to the desired position. When V_e gain was less dominant over the P_e gain this conflict was eliminated. This characteristic is similar to Figure 6.1(c) in which P_e was set at a lower value and V_e was the more dominant. The actual position exceeded the desired position for sections of this response, and no correction was done due to the decreased P_e gain. This was the direct result of the 30 point regression to find actual velocity mentioned in Section 4.2.8. The PD-fuzzy plus reset offset integral controller could not achieve both zero position and velocity errors for a changing desired position and velocity. A zero error for both was possible only when the desired velocity was constant.

V_e gain still had an important effect on control. An oscillation in position in Figure 6.2(b) at $t \approx 20sec$ was due to a V_e gain which had been set to zero, this is seen in Figure 6.3(a). There was no compensation for velocity as the In/Out link passed the desired position. The V_e gain compensated for the velocity of the link as it approached the desired position.

Figure 6.3(a) also compares the velocity trajectory for three different values of V_e. The actual velocities followed the desired velocity closely but oscillated about the desired velocity, just as actual position did. Referring to Figure 6.3(b), the three V_e performed in a similar manner to Figure 4.17(b). Comparing the responses to three

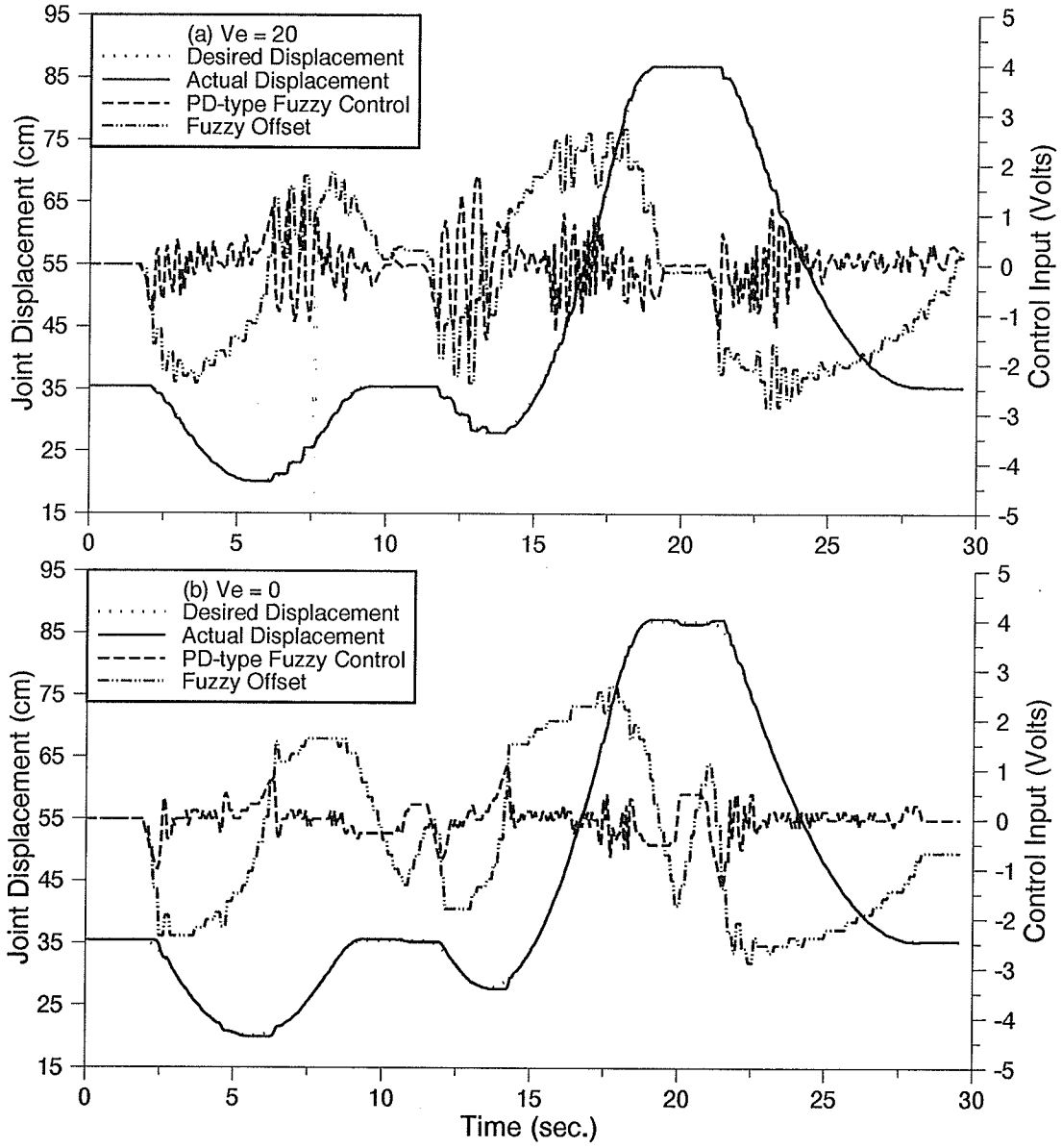

Figure 6.2: Effect of V_e gain with reset offset integral control

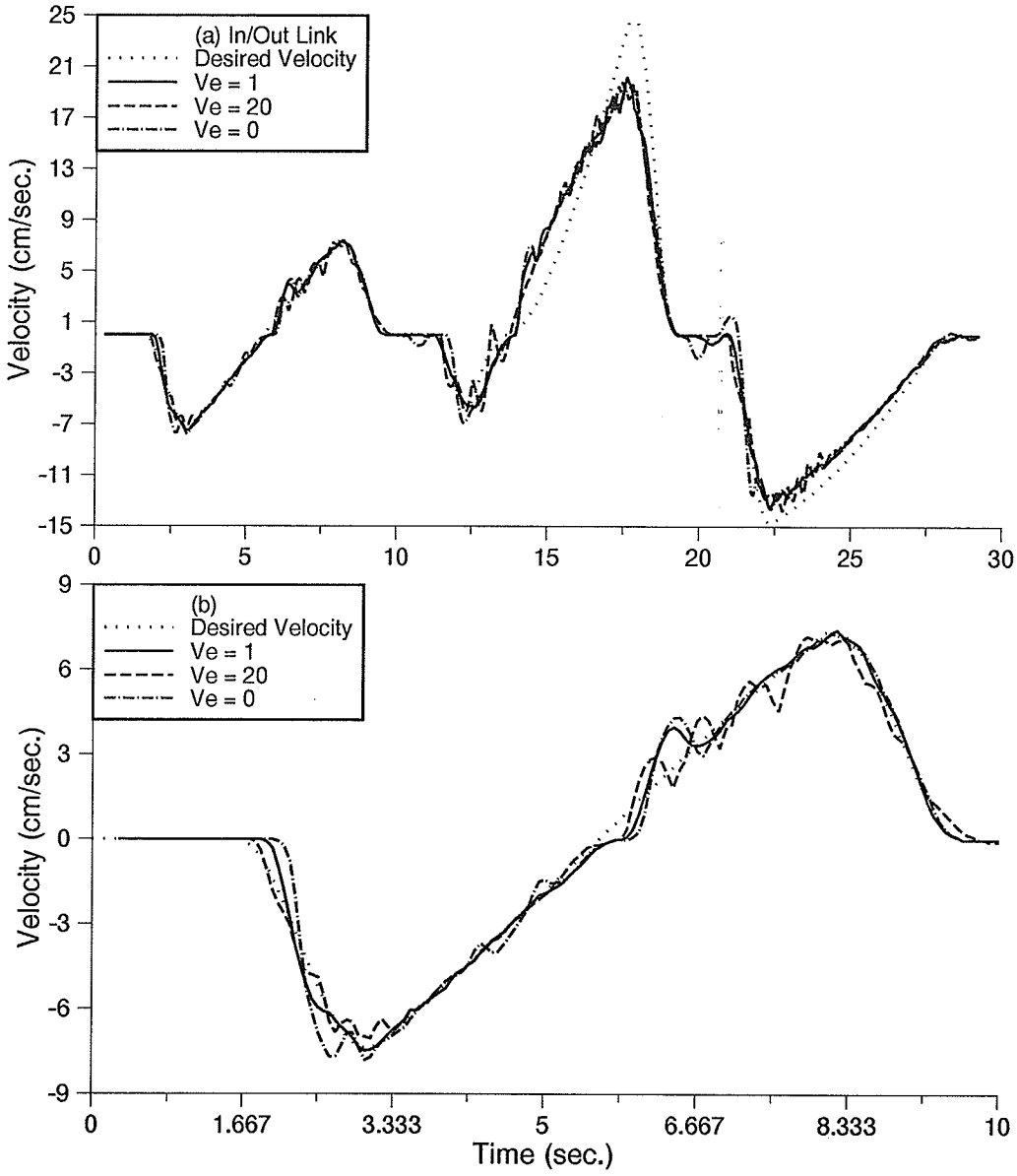

Figure 6.3: Velocity profiles: (a) full trajectory; (b) detailed view

V_e gains at $t \approx 3sec$, the higher the gain, the closer the actual velocity was brought to the desired velocity. A higher V_e gain also increased oscillations.

6.1.3 Effect of Offset Updating Rate

The updating rate was an important parameter in the reset offset integral controller. If the frequency was too small, the rate of steady-state error elimination was slow. The rate at which the offset wound down to zero, given a change in the desired direction, took longer if the updating frequency was increased. This trait of winding down was also shared by the other integral type controllers which were tested, but the correction was not as long with the offset integral and stability was maintained. For all experiments with offset in Chapter 5, and previously in this chapter, the rate of updating was 6Hz ($q = 10$).

The effect of a decrease in the updating frequency by 50%, (i.e., $q = 20$) is seen in Figure 6.4(a). At $t \approx 14sec$, this frequency did not seem to be fast enough. The delay due to winding down increased. When updating frequency was increased by 100% (to $q = 5$ intervals) the winding down occurred faster, but to the detriment of stability. This is seen in Figure 6.4(b). Referring to Figure 6.4(b) at $t \approx 20sec$, there was a large oscillation in the offset integral which was trying to eliminate the steady-state error when the link was brought to a stop. Here the rate of update is unstable and winds up and down too fast. Both the increase and decrease in update frequency produced a reasonable response. As with the setting of P_e and V_e, gain when the offset integral was active, the exact setting of updating rate was not a necessity. A further increase in updating frequency resulted in simply an integral of PD-type fuzzy control values with an integral gain of one. This gain was too high and resulted in oscillations and instability.

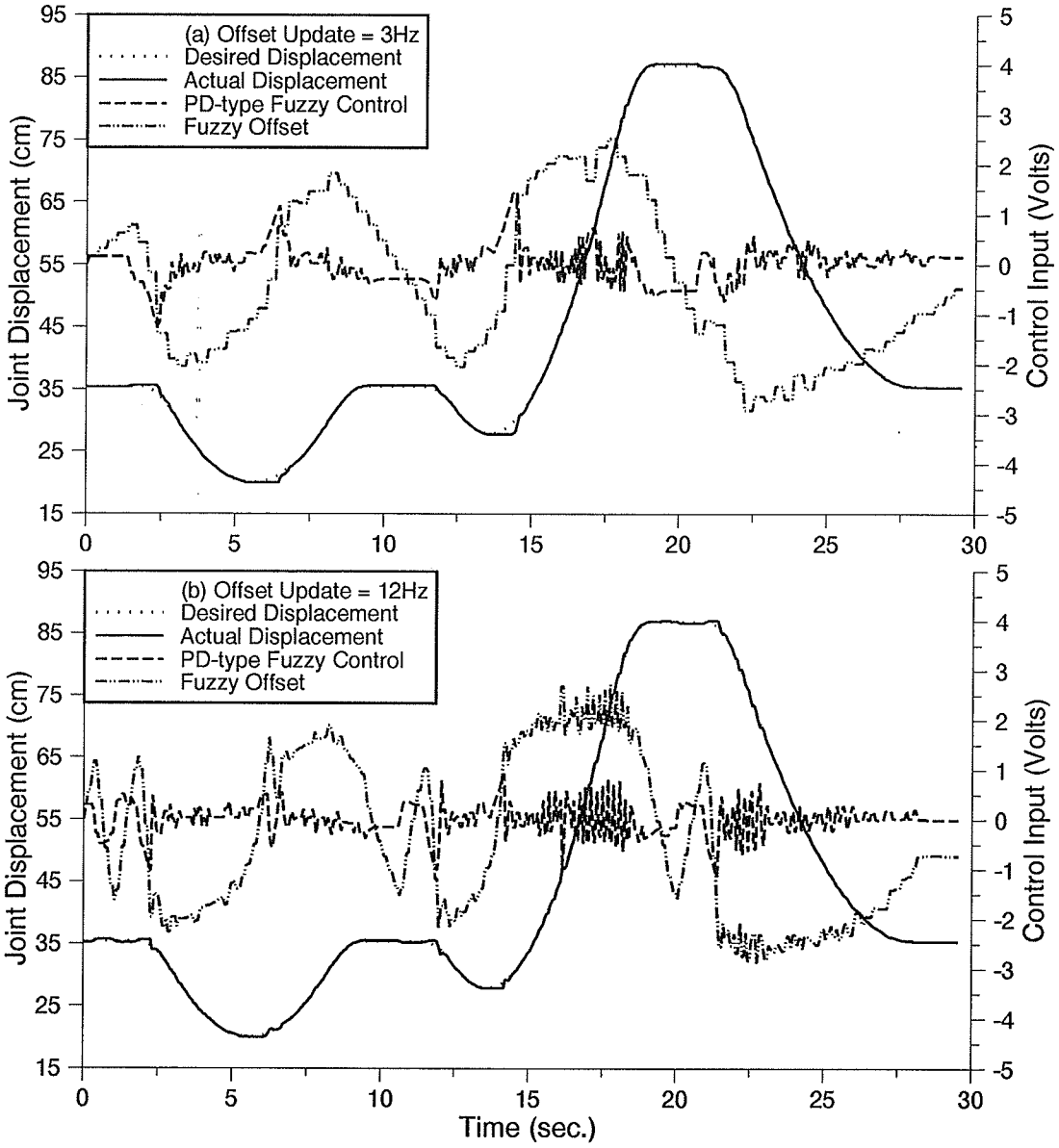

Figure 6.4: Effect of updating frequency: (a) low frequency; (b) high frequency

6.2 Additional Experiments

6.2.1 Step Input Responses

Different step sizes, as in Section 4.3.1, were applied to the PD-type fuzzy plus reset offset integral controller. These step inputs included 7.2°, 3.6° and 1.8°. With the addition of the offset integral, the steady-state error was reduced substantially for the 7.2° step, as is seen in Figure 6.5(a). The offset integral also performed well for the 3.6° step input shown in Figure 6.5(b). The control action from the PD-type fuzzy alone was not large enough to bring the link closer to the desired at $t \approx 2.25sec$. This was the point where the link would stop in the absence of the offset integral.

Due to the slow speed of the link, a velocity error which exceeded fuzzy zero did not occur to deactivate the offset integral at the start of the step response in the 1.8° step input shown in Figure 6.5(c). This resulted in an overshoot on the 'return' motion, which was quickly corrected. The overshoot was due to an update of the control action when the highest control output from the controller was still present. The results in Figure 6.5 display a robust nature.

6.2.2 Tracking Control

Speed control was also performed for the In/Out link trajectory. Figure 6.6 shows the response with increased speed. In Figure 6.6(a), at $t \approx 8sec$, the deactivation of the offset integral is observed, at this point the offset control input goes to zero and a steady-state error was present. Here the velocity error exceeded fuzzy zero due to the increased size of steady-state error and the resulting lag in actual velocity as compared to the desired velocity. The velocity error falls within fuzzy zero and the elimination of steady-state error activated at $t \approx 11sec$. This off/on characteristic is

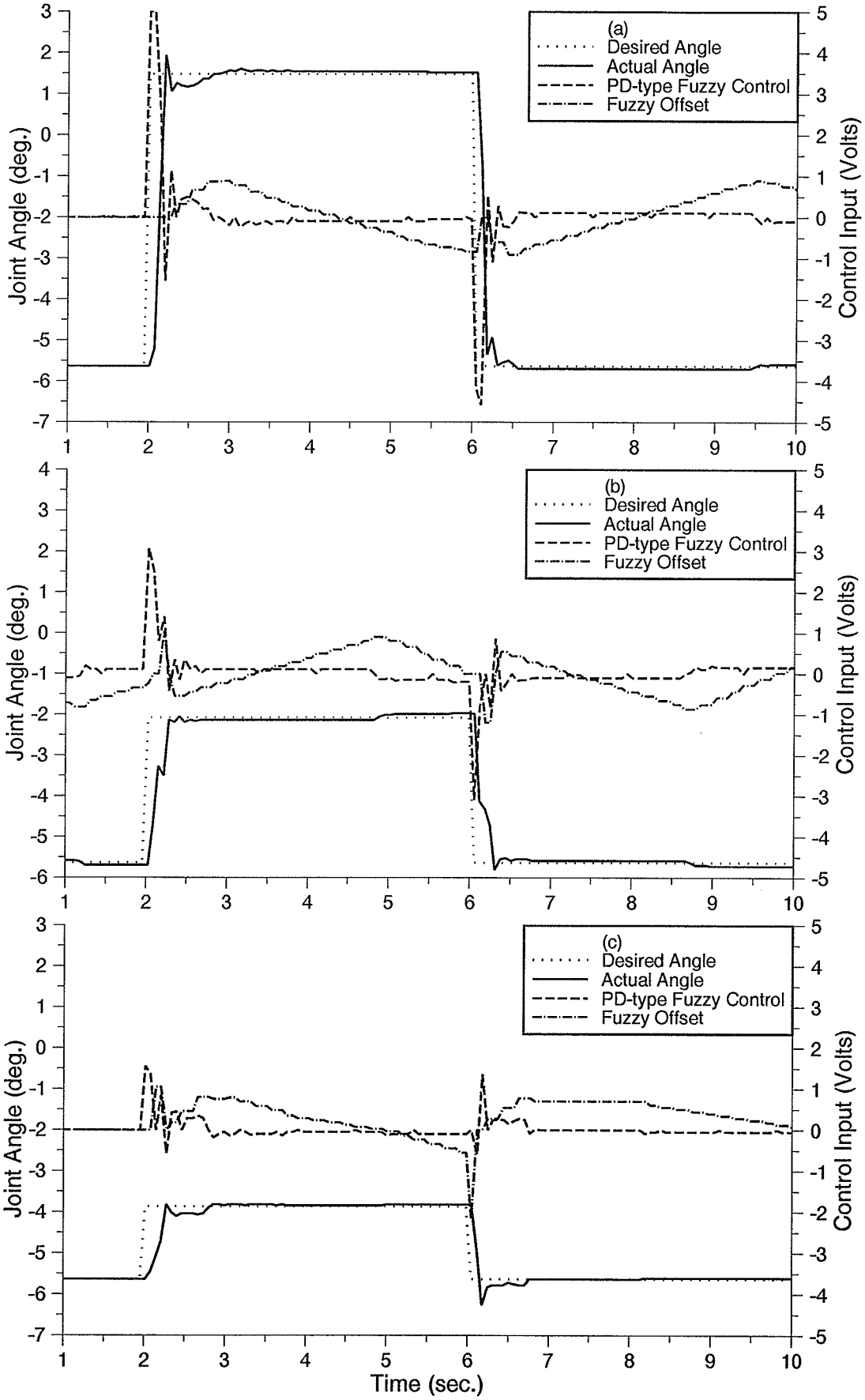

Figure 6.5: Response to different step input sizes

inherent to the reset part of the controller and occurred when the zero velocity error state could not be achieved due to increased steady-state error.

When the tracking speed was further increased, the delay in the method activation became longer. This is seen in Figure 6.6(b) where the speed was increased by a factor of four. When the offset was deactivated, as it was between $t \approx 3$ *to* $4sec$, there was a steady-state error present. Here the trajectory was identical to the result for the PD-type fuzzy acting alone (this result were not included in this thesis due to space). Fuzzy offset activation could be achieved by increasing P_e or V_e gains, which make the controller more responsive. An increase in the P_e gain of $\approx 50\%$ was then applied. The result is seen in Figure 6.6(c). The gains reduced the steady-state error of the response and as a result the method was activated for longer periods, but it did not eliminate the on/off characteristic entirely. This on/off characteristic could only be eliminated by increasing the fuzzy zero velocity error range.

The speed of the desired position input was then decreased to 1/5 of the original speed and the trajectory tracking experiment was repeated. As is seen in Figure 6.7(a), the steady-state error has been reduced. The control magnitudes were at much lower values and no oscillations in the position were observed. This displayed the stability of the offset integral at decreased velocities. The velocity profile is seen in Figure 6.7(b). Here the desired velocity was followed closely for the first part of the trajectory, but with obvious oscillations about the desired values. Even at slow speeds this oscillation was present.

6.2.3 Repeatability Test

Experiments were then performed to show repeatability of the controller. A 42.8° step response performed at the beginning of experiments, and once again after the machine had been in operation for one hour. There was no noticeable difference

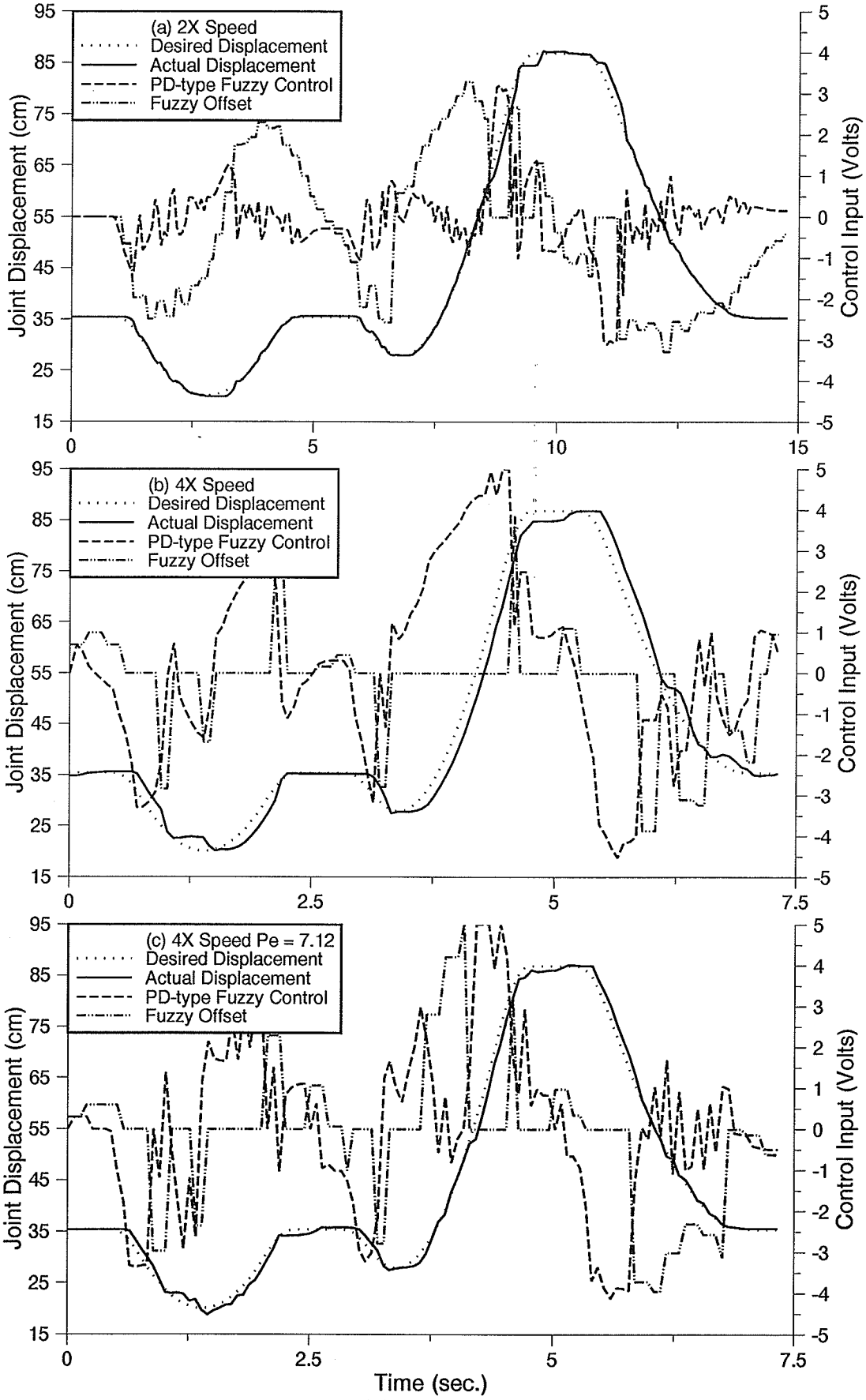

Figure 6.6: Effect of increased speeds: (a) 2X; (b) 4X; (c) 4X with increased gain

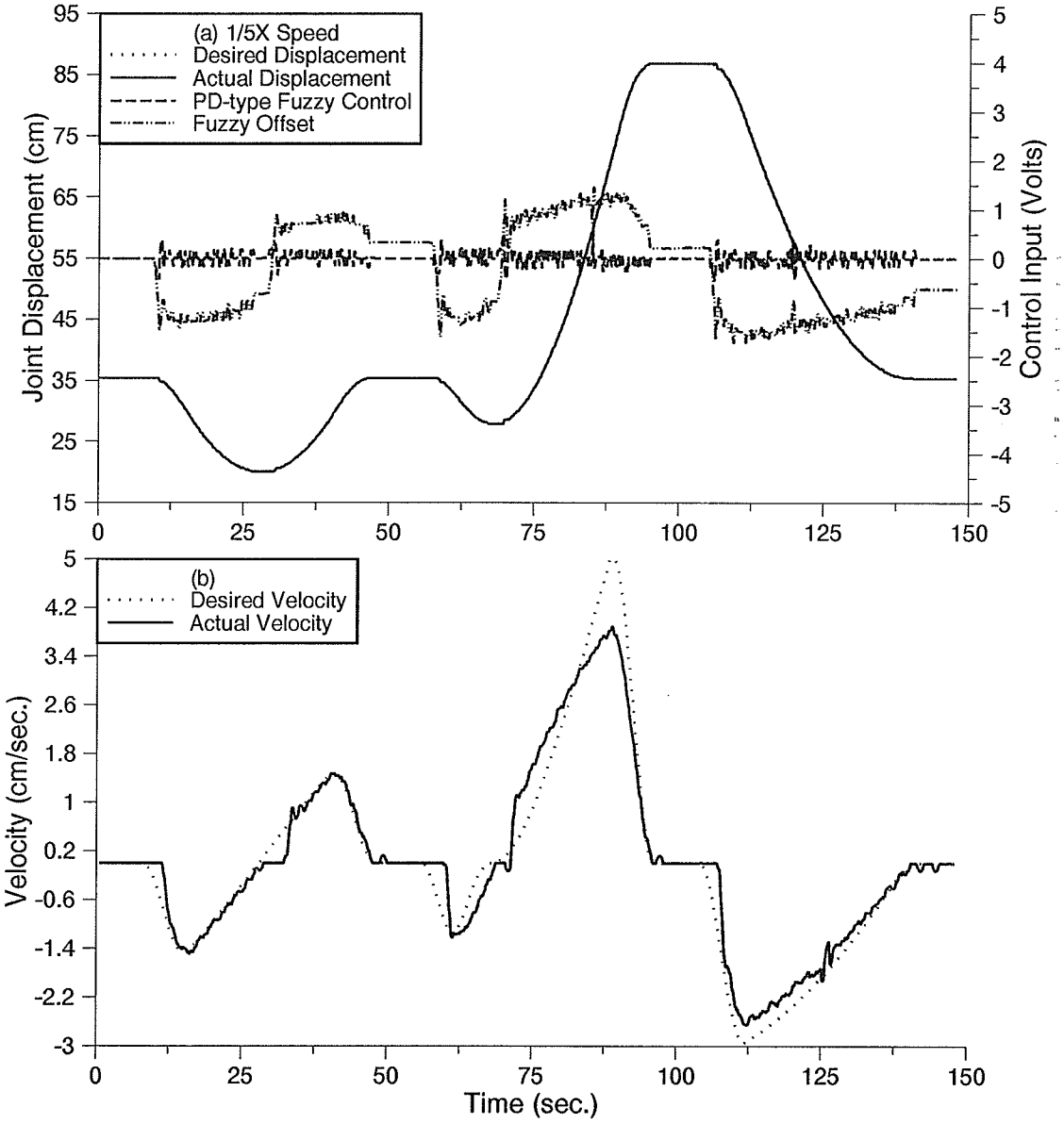

Figure 6.7: Effect of reduced speed: (a) position and control inputs; (b) velocity profiles

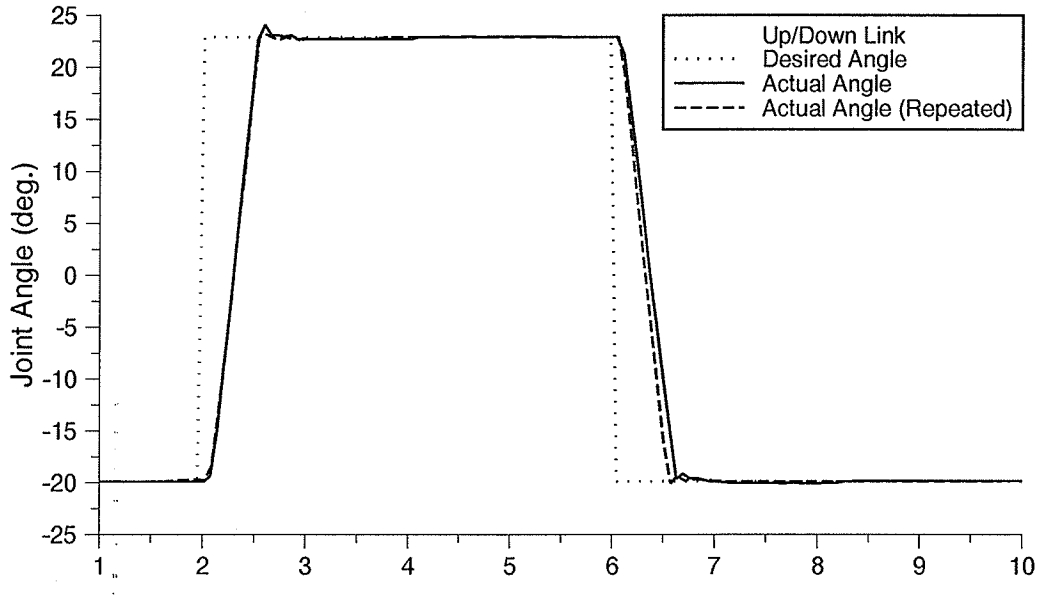

Figure 6.8: Repeatability test

between the two. Both are seen in Figure 6.8. The reason for the slight difference in the return motion was an inconsistent pump pressure, this was unavoidable with the industrial hydraulic robot.

6.2.4 Multi-link Position Control

Trajectory tracking experiments using three links were then performed on the industrial hydraulic robot using the reset offset integral. A triangular trajectory was applied with the end-effector moving in the $X - Y$ direction, while maintaining a constant Z direction distance [refer to Figure 4.1]. At a slow speed, the trajectory was performed in 30 seconds and the results are in Figure 6.9(a). The actual path did not deviate much from the desired position until the change in direction. This, as observed earlier, was due to the winding down of the offset integral method. The end-effector traveled 142cm in $\approx 10sec$ along the horizontal and vertical, and 201cm in $\approx 10sec$ on the diagonal.

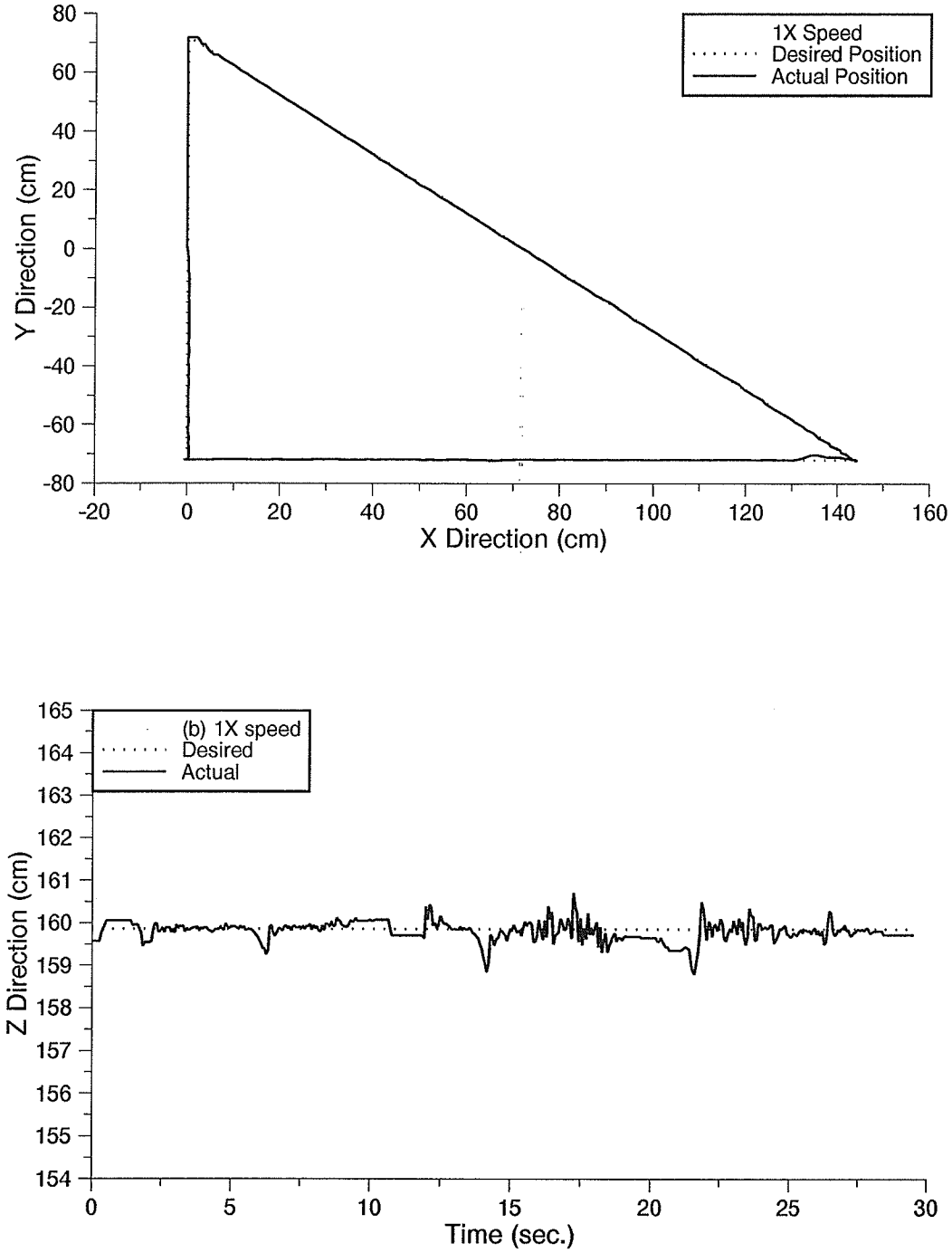

Figure 6.9: Endpoint multi-link trajectory tracking: (a) XY direction; (b) Z direction

The response of the In/Out link is observed in Figure 6.1(a) with the velocity profile in Figure 6.3(a). The trajectory for the other two links are seen in Figure 6.10(a) and 6.11(a) and the velocity profiles in Figure 6.10(b) and 6.11(b). During the ramp input sections of the Up/Down trajectory, between $t \approx 3$ *to* $8sec$, both velocity and position errors have been almost eliminated. Accuracy was possible because the actual velocity lag, or shifting, did not have an effect at this point. The velocity profile was smooth until $t \approx 22sec$ were the winding down of the method occurred. This caused a delay in the links motion and oscillation in the links velocity during the correction.

The Left/Right link has the same characteristics but oscillations about the desired velocity seem to be larger due to higher inertia. During $t \approx 0$ *to* $12sec$ the desired velocity was zero and the desired position was constant. This resulted in a winding up of the method to attempt to eliminate the small position error present at this point. When the windup exceeded the stiction and deadband, an overshoot occurred because the control system was not fast enough to compensate for this instantaneous motion.

The result of the position control for speed 1.6 times faster than the one shown in Figure 6.9(a) is illustrated in Figure 6.12(a). The deviation in the Z direction has increased in Figure 6.12(b). The speed of the trajectory was further increased four times. The results are shown in Figure 6.13. The trajectory was followed sufficiently but the end effector did oscillate about the desired position. The error in the Z direction increased to $\approx$ 5cm [Figure 6.13(b)]. On the diagonal the end-effector traveled 201cm in $\approx 2.5sec$. The reason for the decreased accuracy was the activation and deactivation of the offset integral, similar to the results in Figure 6.6(b). This could also be attributed to the control frequency which was not twice the bandwidth, the bandwidth of the system was too small for the desired input frequency, or the fuzzy zero velocity error range was too small for proper activation. At low speeds, the off-

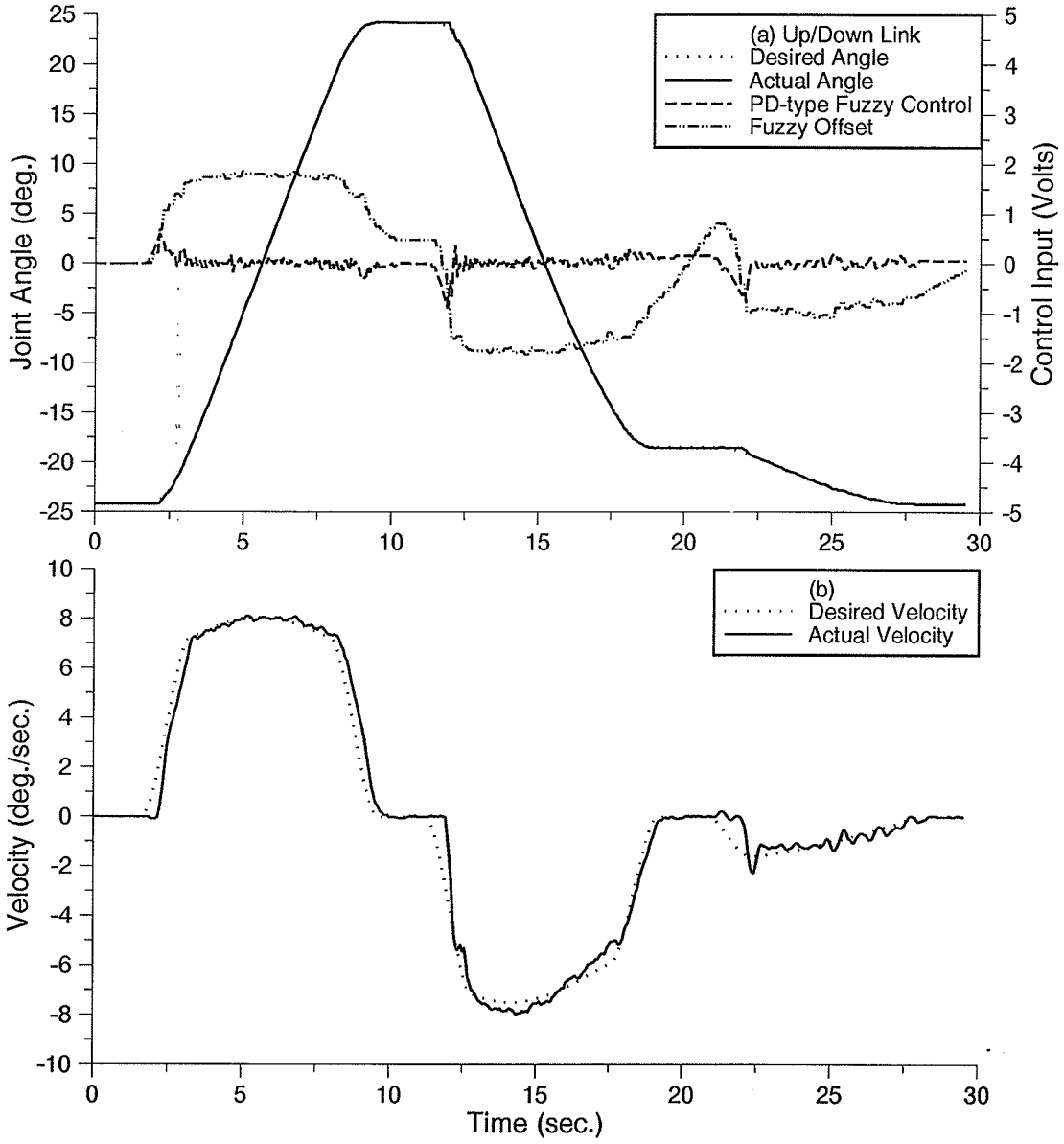

Figure 6.10: Up/Down response pertaining to Figure 6.9: (a) position and control inputs; (b) velocity profiles

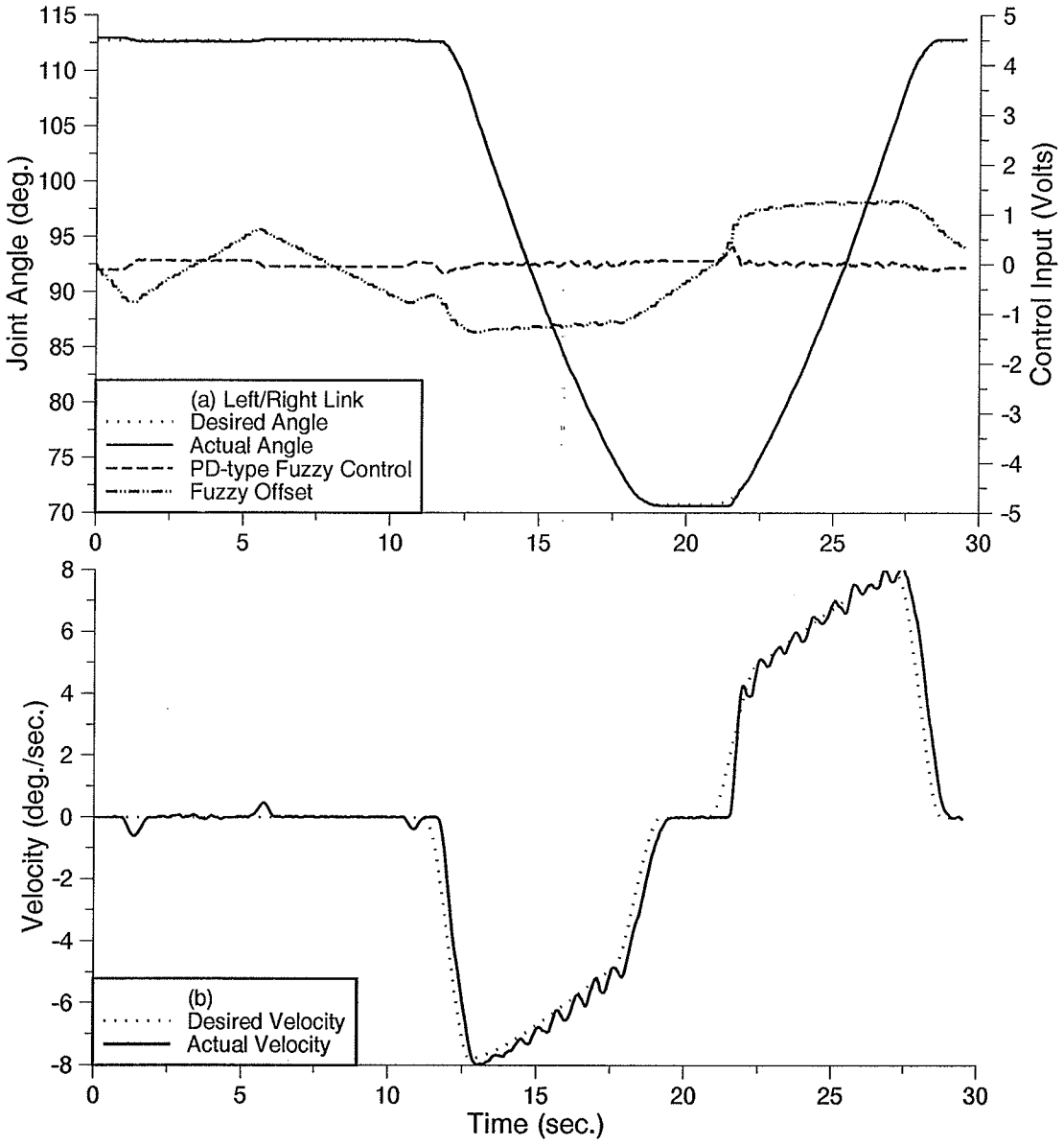

Figure 6.11: Left/Right response pertaining to Figure 6.9: (a) position and control inputs; (b) velocity profiles

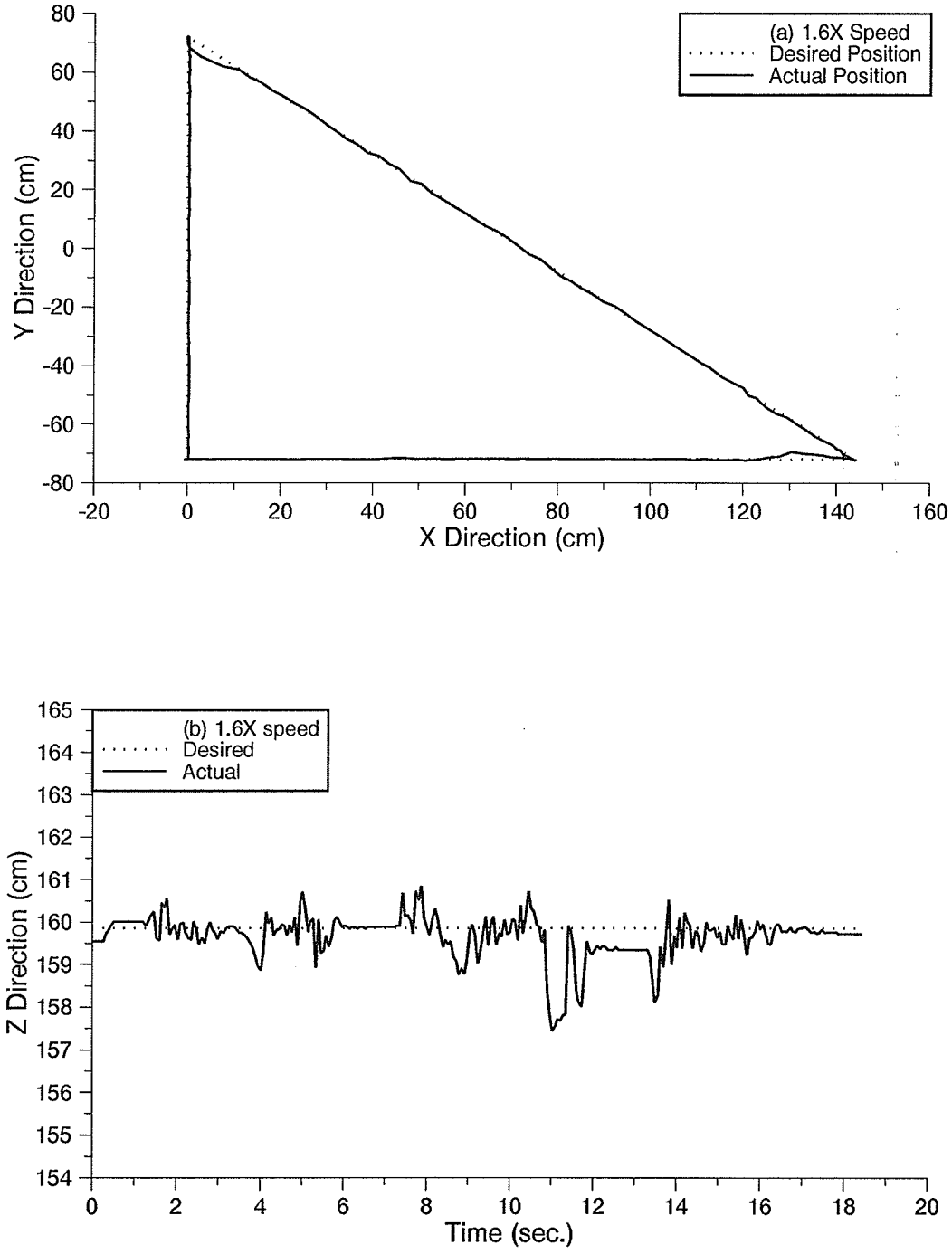

Figure 6.12: Effect of increased speed (1.6X): (a) XY direction; (b) Z direction

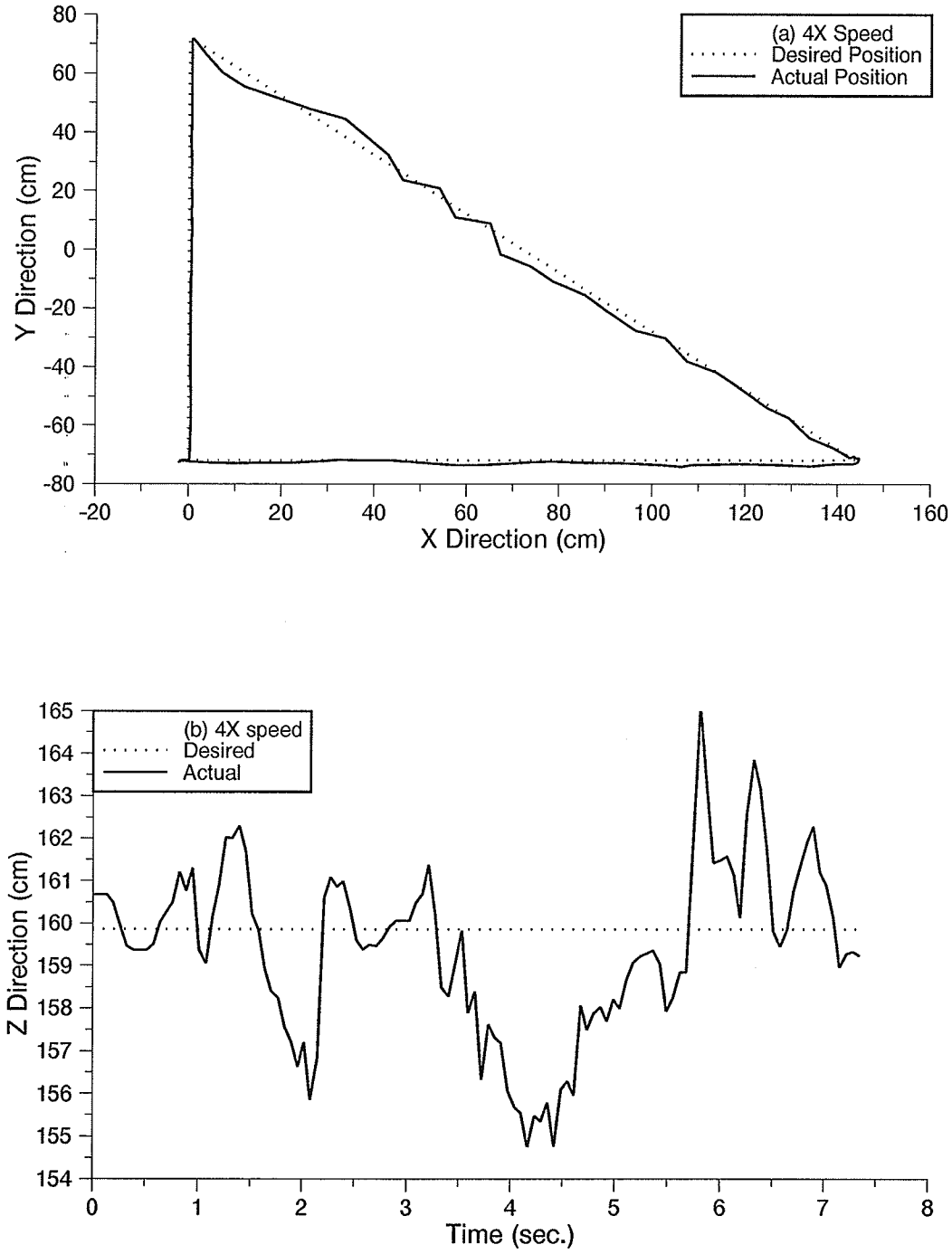

Figure 6.13: Effect of increased speed (4X): (a) XY direction; (b) Z direction

set integral method demonstrated a sufficient accuracy when applied to a trajectory tracking experiment.

6.2.5 Loading

Loads of 45lb, 85lb, and 85lb with extended arm, were applied to the Up/Down trajectory. The results are summarized in Figure 6.14. These can be compared with the unloaded response of Figure 6.10. With the load of 45lb and 85lb, no adverse effects were observed in the trajectory. The control values were stable with no increased oscillations about the desired position. With the 85lb weight and extended arm, there were some oscillations about the desired position. This was due to the higher inertia which was present. A zoomed in comparison between the the joint positions of the unloaded, loaded 85lb and loaded 85lb with arm extended is seen in Figure 6.15(a). The increased oscillations for the case of extended link were obvious. Both the unloaded and the 85lb extended velocity profile are compared in Figure 6.15(b). A decrease in gains could dampen these oscillations. The method was observed to oscillate about the desired position if the weight was excessive.

Total control values, of the PD-type fuzzy plus reset offset integral, are compared for the unloaded and loaded 85lb only in Figure 6.15(c). At the start of the ramp, the control values for the loaded case were higher to overcome the increased inertia. This was soon decreased when the proper speed was achieved. After this point there was no significant difference between the two. The loading showed larger oscillations in control during the decreased velocity section of the ramp at $t \approx 8sec.$

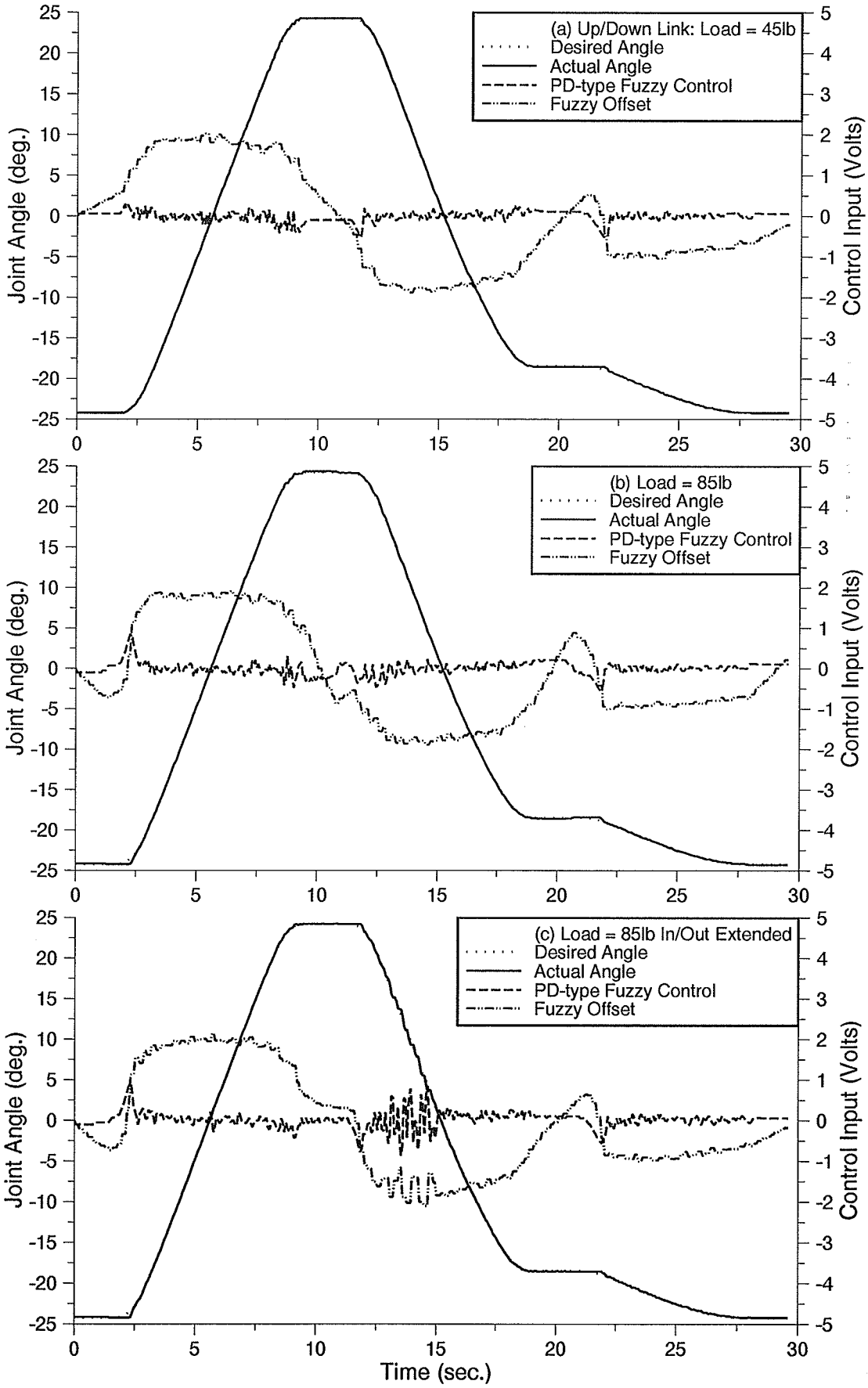

Figure 6.14: Up/Down response - loaded: (a) 45lb; (b) 85lb; (c) 85lb extended

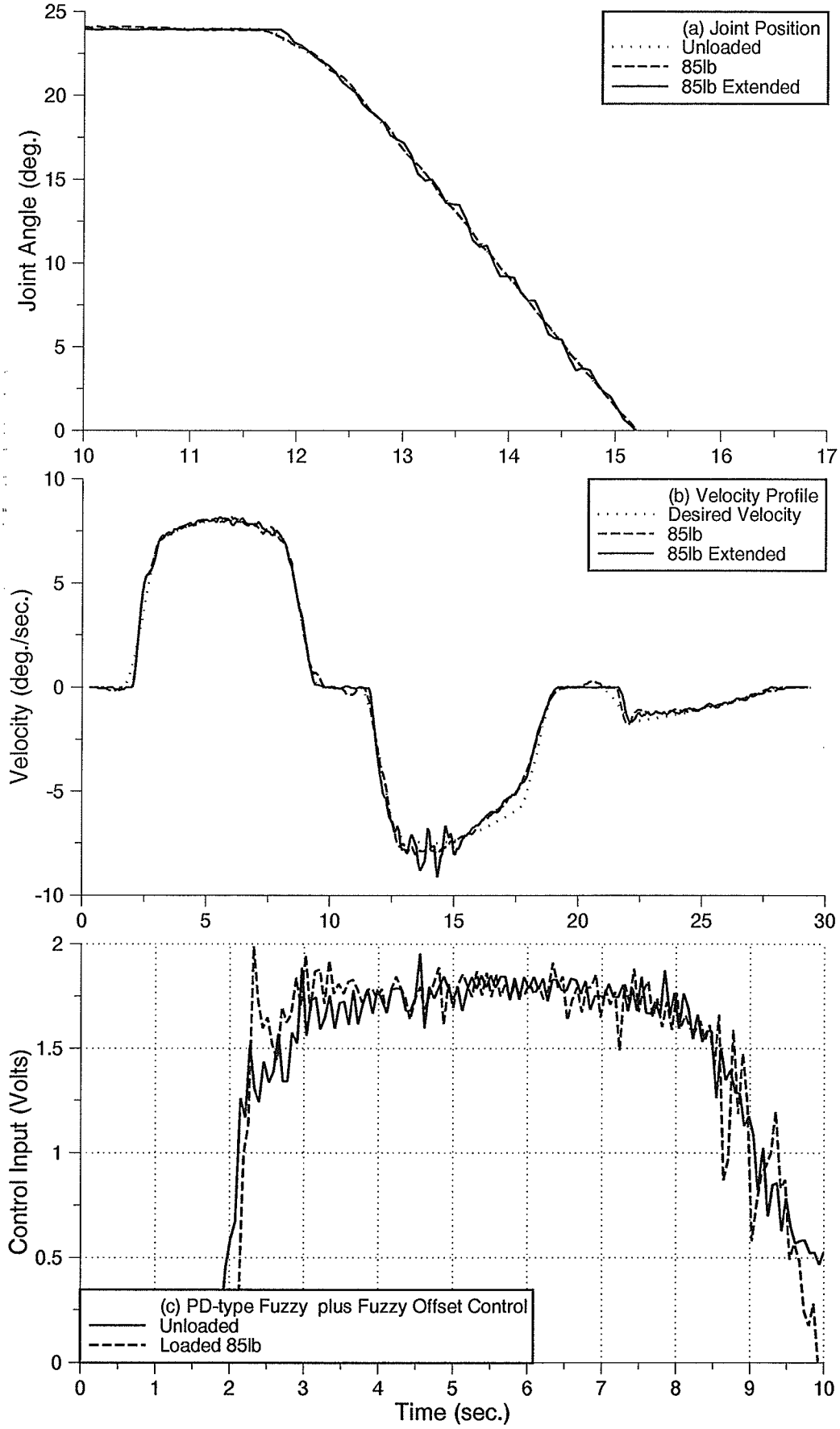

Figure 6.15: Up/Down response: (a) joint angle; (b) velocity profile; (c) control input

Chapter 7

Conclusions

7.1 Thesis Contributions

In this thesis a fuzzy logic controller was developed for a class of hydraulically actuated robots. In particular, it was addressed that hydraulically-actuated robots have different control requirements as compared to electrically-actuated robots. The control scheme consisted of simple yet effective rules which decided on the control inputs based on position and velocity errors. The fuzzy controller demonstrated robustness in the presence of load, variation of set points and nonideal hydraulic actuation.

A simulation model was first utilized, and using insight derived from the simulation studies, suitable fuzzy membership functions and rules were derived. The simulation model was found to be a very effective way of understanding what to expect from the experiment. The application of the conventional PD control to the simulation revealed some inherent problems such as the tradeoff between rise time and overshoot. The nonlinear characteristic of fuzzy logic control either reduced or eliminated these problems.

The fuzzy controller was then applied in experiment to control different links

of an instrumented Unimate MK-II hydraulic robot. Due to the slow dynamics of the servo valves, and other nonidealities such as friction and leakage, the responses were not as fast as they showed in the simulation for small spool displacements. As a result, the zero output voltage membership function was decreased to allow for higher control actions. The position and velocity related gains were tuned by an optimization technique based on the simplex method in an off-line manner.

An examination of the scaling factors, fuzzy logic parameters and rules was then performed. The results demonstrated how the control parameters affected the system performance. For example, changing the zero voltage output region altered stability in the form of oscillations at the set point, and any change in the small voltage output altered the responsiveness of the system. Control gains, in comparison, changed the entire response of the controller for all inputs. The rules designed for the hydraulic robot were found to improve the response rise time of a hydraulic robot as compared to the conventional rules normally used for motor control. With these experiments the true advantages of the fuzzy logic controller were observed.

The simple PD-type fuzzy controller performed well but did not eliminate the steady-state error. This was due to (along with the characteristics of the fuzzy PD-type controller) unavoidable nonlinearities such as valve deadbands. Two methods were developed and added in parallel with the PD-type fuzzy controller. The first method entitled 'reset error integral' was based on the integral of the position error. The second method entitled 'reset offset integral' produced an offset integral control based on a measure of the steady-state error obtained from the current PD-type fuzzy control action. Both methods were active only in the fuzzily described zero velocity error and were found to be easy to implement, conceptually simple in design and did not impose an increase in computation time.

The results of this study clearly show certain advantages of the application of fuzzy control to hydraulic robots. These advantages include a fast rise time while main-

taining a close to dampened response with simple rules and with only position and velocity feedback. The controller applied in this paper exhibited robustness in performance against loading and nonidealities inherent to any existing industrial robot. The automated gain setting algorithm applied here proved to be a time saving and reliable device to obtain the proper gains. The steady-state error elimination methods developed, particularly the reset offset integral controller, displayed accuracy, speed and stability. The use of these methods would be very beneficial to trajectory tracking systems requiring exact position and velocity control.

7.2 Future Work

Future work would include experimentation with the fuzzy PD-type controller to confirm that the method will universally possess the tuning capabilities which were observed in this work. These capabilities include the fuzzy logic parameters, rules and gains. Future study could also include the design of a fuzzy controller based on the experiments performed here, so that tuning the fuzzy logic parameters such as width and peak can be performed in an easier manner.

A series of studies could also be performed on the reset offset integral. One study could involve decreasing the time required to wind down the offset. To eliminate this problem the controller could be altered so that when position and velocity errors are close to zero, and the desired velocity changes direction, then the offset is set to zero. Other studies could include increasing/decreasing the update rate of the offset depending upon the degree of membership of velocity error input in fuzzy zero velocity error region.

Bibliography

[1] E. Cox, "Fuzzy Fundamentals", *IEEE Spectrum* (October), pp. 58-61, 1992.

[2] W.J.M. Kickert and E.H. Mamdani, "Analysis of a Fuzzy Logic Controller", *Fuzzy Sets and Systems* **1**, pp. 29-44, 1978.

[3] K. Kumbla, J. Moya, R. Baird, S. Rajagopalan and M. Jamshidi, "Fuzzy Control of Three Links of a Robotic Manipulator", *Robotics and Manufacturing; Proc. ISRAM'92* (M. Jamshidi et al., eds.), pp. 687-694, 1992.

[4] P.J. King and E.H. Mamdani, "The application of fuzzy control systems to industrial processes", *Automatica* **13**, pp. 235-242, 1977.

[5] J.A. Bernard, "Use of a Rule-Bases System for Process Control", *IEEE Control Systems Magazine* (October), pp. 3-13, 1988.

[6] C.C. Lee, "Fuzzy Logic in Control Systems: Fuzzy Logic Controller - Part I & II", *IEEE Transactions on Systems, Man and Cybernetics* **20**, pp. 404-433, 1990.

[7] J. Zhou and P. Coiffet, "Fuzzy Control of Robots", *1st IEEE International Conference on Fuzzy Systems*, San Diego, CA, pp. 1357-1364, 1992.

[8] L. Zheng, "A Practical Guide to Tune Proportional and Integral Like Fuzzy Controllers", *Proc. 1st IEEE International Conference on Fuzzy Systems*, San Diego, CA, pp. 633-640, 1992.

[9] W.C. Daugherity, "Performance Evaluation of a Self-Tuning Fuzzy Controller", *Proc. 1st IEEE International Conference on Fuzzy Systems*, San Diego, CA, pp. 389-397, 1992.

[10] C. Ken, L. Jinn-Ya and L.Y. Xiang, "Fuzzy Control of Robot Manipulator", *Proc. IEEE International Conference on Systems, Man, and Cybernetics* **2**, Beijing, China, pp. 1210-1212, 1988.

[11] S. Tzafestas and N.P. Papamikolopoulos, "Incremental Fuzzy Expert PID Control", *IEEE Trans. on Industrial Elect.* **37**, No.5, pp. 365-371, 1990.

[12] A. Boscolo, "Computer Aided Tuning Validation of Fuzzy Systems", *Proc. 1st IEEE International Conference on Fuzzy Systems*, San Diego, CA, pp. 605-614, 1992.

[13] S.M. Smith and D.J. Comer, "An Algorithm for Automated Fuzzy-Logic Controller Tuning", *Proc. 1st IEEE International Conference on Fuzzy Systems*, San Diego, CA, pp. 615-622, 1992.

[14] B.A.M. Wakileh and K.F. Gill, "Robot Control Using Self-Organizing Fuzzy-Logic", *Computers in Industry* **15**, pp. 175-186, 1990.

[15] T. Zhao and T. Virvalo, "Fuzzy Control of a Hydraulic Position Servo with Unknown Load", *2nd IEEE International Conference on Fuzzy Systems*, San Francisco, CA, pp. 785-788, 1993.

[16] C.H. Chou, H.C. Lu, "Design of a Real-time Fuzzy Controller for Hydraulic Servo Systems", *Computers in Industry* **15**, pp. 129-142, 1993.

[17] A. Kotzev, D.B. Cherchas, P.D. Lawrence and N. Sepehri, "Generalized Predictive Control of a Robotic Manipulator with Hydraulic Actuators", *Robotica* **10**, pp. 447-459, 1992.

[18] J. Lee, "On Methods for Improving Performance of PI-Type Fuzzy Logic Controller", *IEEE Transactions on Systems, Man and Cybernetics* **1**, pp. 298-301, 1993.

[19] Y.Y. Chen, and C.C. Yen, "PD-Type vs PID-Type Fuzzy Controllers", *Proc. 10th IEEE Regional Conference*, Melbourne, Australia, pp. 341-345, 1992.

[20] M. Mizumoto, "Realization of PID Controls by Fuzzy Control Methods", *Proc. 1st IEEE International Conference on Fuzzy Systems*, San Diego, CA, pp. 709-715, 1992.

[21] J.H. Kim, J.H. Park, S.W. Lee, and E.K.P. Chong, "Fuzzy Precompensation of PD Controllers for Systems with Deadzones", *Journal of Intelligent and Fuzzy Systems* **1**, pp. 125-133, 1993.

[22] H. Hanafusa, H. Asada and T. Mikoshi, "Design of Electrohydraulic Servo System for Articulated Robot Arm Control", *Proc. IFAC Symposium*, Warsaw, Poland, pp. 223-228, 1980.

[23] A. Al-Zaher, "*Study of Position Control in Two Classes of Hydraulically Actuated Manipulators*", M.Sc. Thesis, Department of Mechanical and Industrial Engineering, University of Manitoba, Winnipeg, Canada, 1994.

[24] H.E. Merritt, *"Hydraulic Control Systems"*, John Wiley and Sons, New York, 1967.

[25] N. Sepehri, G.A.M. Dumont, P.D. Lawrence and F. Sassani, "Cascade Control of Hydraulically Actuated Manipulators", *Robotica* **8**, pp. 207-216, 1990.

[26] H. Hanafusa and Z. Wang, "Pressure Feedback Compensation for Hydraulic Servomechanism which Derive Articulated Robots", *Proc. ISA Symposium* (Paper No. 0-87664-741-7/83/0909-8), pp. 909-915, 1983.

[27] W.H. Press, S.A. Teukolsky, W.T. Vetterling and B.P. Flannery, "*Numerical Recipes in C*", Cambridge University Press, New York, pp. 408-412, 1988.

[28] R.P. Adby and M.A.H. Dempster, *"Introduction to Optimization Methods"*, Chapman and Hall, London, pp. 42-48, 1974.

[29] K.J. Astrom and T. Hagglund, *Automatic Tuning of PID Controllers*, Published by the Instrument Society of America, Research Triangle Park, NC, 1994.